

**Role of USP48 and A20 on cell survival of gastric epithelium
during *Helicobacter pylori* infection**

Thesis

for the degree of

doctor rerum naturalium (Dr. rer. nat.)

approved by the Faculty of Natural Sciences of Otto von Guericke University Magdeburg

by M.Sc. Phatcharida Jantaree
born on 30 May 1990 in Chiangmai, Thailand

Examiner: Prof. Dr. rer. nat. Michael Naumann
Prof. Dr. rer. nat. Christine Josenhans

submitted on: 18 October 2022

defended on: 15 February 2023

Table of content

Summary	3
Zusammenfassung	5
List of publications	7
Chapter 1. Introduction	8
1.1 <i>Helicobacter pylori</i> infection	8
1.2 Gastric epithelial barrier	9
1.3 NF- κ B pathway	12
Chapter 2. Aims and outline of the dissertation	18
2.1 Research aims.....	18
2.2 Outline of the dissertation	18
Chapter 3. Publication I	19
Chapter 4. Publication II	39
Chapter 5. Publication III	50
Chapter 6. Discussion	61
6.1 USP48 counteracts UPS-dependent degradation of nuclear NF- κ B/RelA in gastric epithelial cells during <i>H. pylori</i> infection.	61
6.2 USP48 restrains apoptotic cell death of <i>H. pylori</i> -infected gastric epithelial cells in an A20-dependent mechanism.	62
6.3 Human gastric fibroblasts ameliorate <i>H. pylori</i> -induced A20 expression and suppress apoptotic cell death of gastric epithelial cells.	63
6.4 Analysis of drug-induced apoptotic cell death in polarised gastric epithelial cells on-a-chip	64
6.5 Conclusions	65
List of abbreviation	67
References	68
Declaration of honour	80

Summary

Helicobacter pylori is a human pathogen colonising the epithelium of gastric mucosa and is etiologically related to gastric diseases and cancer. *H. pylori*, via its effector ADP-L-glycero- β -D-manno-heptose (ADP-heptose), induces nuclear factor kappa-light-chain-enhancer of activated B cells (NF- κ B) signalling, which contributes to inflammation and resistance to apoptotic cell death. *H. pylori*-induced NF- κ B can support the long-term colonisation of the bacteria, increasing the risks of disease development. Therefore, understanding the regulation of *H. pylori*-induced NF- κ B, might pave the road for novel therapeutic approaches to gastric diseases including cancer.

NF- κ B signal transmission can be regulated by protein modifications, including ubiquitinylation. Deubiquitinylases (DUBs) counteract ubiquitin modification, thereby contributing to NF- κ B control. Herein, the nuclear DUB ubiquitin-specific peptidase 48 (USP48) stabilises the nuclear pool of NF- κ B/RelA and facilitates sustained NF- κ B activity. Mechanistically, the cullin-RING ubiquitin ligase (CRL) complex elongin-cullin-suppressor of cytokine signalling 1 (ECS^{SOCs1}) facilitates K48-ubiquitinylation and proteasomal degradation of NF- κ B/RelA in the nucleus, leading to the termination of nuclear RelA activity. I demonstrated that USP48 stabilises RelA by deubiquitinylation, thereby promoting the transcriptional activity of RelA to prolong *de novo* synthesis of the DUB A20 in *H. pylori* infection. Furthermore, USP48 enhances A20 expression, which suppresses caspase 8 activity and apoptotic cell death in *H. pylori*-infected gastric epithelial cells. Additionally, ubiquitin ligation of RelA by the CRL2 is inhibited by the multiprotein complex COP9 signalosome (CSN) that inactivates CRLs by deneddylation. Here, I have identified a mechanism by which CSN-associated USP48 and A20 synergistically regulate RelA and apoptotic cell death in *H. pylori* infection.

In the gastric mucosa, the epithelium is closely in contact with the surrounding stromal cells, involving fibroblasts which control proliferation, differentiation, and apoptosis of epithelial cells. Therefore, the analysis of the molecular crosstalk between gastric fibroblasts and epithelial cells is highly relevant for understanding the development of gastric diseases during *H. pylori* infection. In this thesis, I addressed the influence of fibroblasts on the apoptosis of gastric epithelial cells. Here, I showed the protective role of human gastric fibroblasts on *H. pylori*-induced apoptotic cell death of polarised gastric carcinoma cells and primary gastric mucosoids. Mechanistically, I identified that the fibroblast-dependent protection against apoptotic cell death in *H. pylori*-infected epithelial cells is in part supported by the upregulation of A20 expression.

The rise of microfluidic cell-on-a-chip technology provides an opportunity to recapitulate and miniaturise the *in vivo* situation for biomedical studies. The microfluidic chip established in this thesis contains two microfluidic channels separated by a porous membrane lined by polarised gastric epithelial (NCI-N87) cells. A dynamic environment was emulated with media flowing at a constantly low rate (0.5 μ l/min). Interestingly, results showed that the barrier integrity of gastric epithelial monolayer is enhanced with continuous media flow, compared to the static conditions. Furthermore, I experimentally analysed drug-induced apoptotic cell death in gastric epithelial cells by

integrating the cell-on-a-chip with the Incucyte® live-cell imaging system. In addition to this work, to better mimic *in vivo* situations, this microfluidic system could be used for *H. pylori*-induced apoptotic cell death in primary gastric mucosoids. This could be a valuable tool for studying the molecular crosstalk between cells of the microenvironment in response to infections.

Collectively, the thesis addressed the molecular interplay of USP48 and A20 in regulating NF- κ B transcriptional activity and apoptotic cell death in the *H. pylori*-infected gastric epithelium. Moreover, considerable insights were obtained into the impact of cells from the micromilieu on *H. pylori*-induced A20 expression and apoptotic cell death. By using cell-on-a-chip technologies these investigations provide opportunities to develop therapeutic strategies.

Zusammenfassung

Helicobacter pylori ist ein menschlicher Krankheitserreger, der das Epithel der Magenschleimhaut besiedelt und ätiologisch mit Magenerkrankungen und Krebs in Verbindung gebracht wird. *H. pylori* induziert über seinen Effektor ADP-L-Glycero- β -D-manno-Heptose (ADP-Heptose) die Signalübertragung durch den Nuklearfaktor Kappa-Lichtketten-Enhancer aktivierter B-Zellen (NF- κ B), der zur Entzündung und zur Resistenz gegenüber apoptotischem Zelltod beiträgt. Der durch *H. pylori* induzierte NF- κ B-Signalweg kann die langfristige Besiedlung durch das Bakterium begünstigen und das Risiko der Krankheitsentwicklung erhöhen. Daher könnte das Verständnis der Regulierung von *H. pylori*-induziertem NF- κ B den Weg zu neuen therapeutischen Ansätzen für Magenkrankheiten einschließlich Krebs ebnen.

Die NF- κ B-Signalübertragung kann durch Proteinmodifikationen, einschließlich Ubiquitylierung, reguliert werden. Deubiquitylasen (DUBs) wirken der Ubiquitinmodifikation entgegen und tragen so zur NF- κ B-Kontrolle bei. Die nukleäre DUB Ubiquitin-spezifische Peptidase 48 (USP48) stabilisiert den nukleären Pool von NF- κ B/RelA und ermöglicht eine anhaltende NF- κ B-Aktivität. Mechanistisch gesehen erleichtert der Cullin-RING-Ubiquitin-Ligase (CRL)-Komplex Elongin-Cullin-Suppressor of Cytokine Signalling 1 (ECS^{S^{OC}S¹}) die K48-Ubiquitylierung und den proteasomalen Abbau von NF- κ B/RelA im Zellkern, was zur Beendigung der nukleären RelA-Aktivität führt. Ich habe gezeigt, dass USP48 RelA durch Deubiquitylierung stabilisiert und dadurch die Transkriptionsaktivität von RelA fördert, um die De-novo-Synthese des DUB A20 bei einer *H. pylori*-Infektion zu verlängern. Darüber hinaus steigert USP48 die Expression von A20, was die Aktivität von Caspase 8 und den apoptotischen Zelltod in *H. pylori* infizierten Magenepithelzellen unterdrückt. Darüber hinaus wird die Ubiquitin-Ligation von RelA durch CRL2 durch den Multiproteinkomplex COP9-Signalosom (CSN) gehemmt, der CRLs durch Deneddylierung inaktiviert. Hier habe ich einen Mechanismus identifiziert, durch den CSN-assoziiertes USP48 und A20 RelA und den apoptotischen Zelltod bei einer *H. pylori*-Infektion synergistisch regulieren.

In der Magenschleimhaut steht das Epithel in engem Kontakt mit den umgebenden Stromazellen, an denen Fibroblasten beteiligt sind, die die Proliferation, Differenzierung und Apoptose der Epithelzellen kontrollieren. Daher ist die Analyse des molekularen Crosstalks zwischen Magenfibroblasten und Epithelzellen von großer Bedeutung für das Verständnis der Entwicklung von Magenerkrankungen während einer *H. pylori*-Infektion. In dieser Arbeit habe ich den Einfluss von Fibroblasten auf die Apoptose von Magenepithelzellen untersucht. Dabei konnte ich die schützende Rolle menschlicher Magenfibroblasten auf den *H. pylori*-induzierten apoptotischen Zelltod von polarisierten Magenkarzinomzellen und primären Magenschleimhäuten nachweisen. Mechanistisch gesehen habe ich festgestellt, dass der von Fibroblasten abhängige Schutz vor dem apoptotischen Zelltod in *H. pylori* infizierten Epithelzellen zum Teil durch die Hochregulierung der A20-Expression unterstützt wird.

Das Aufkommen der mikrofluidischen Cell-on-a-Chip-Technologie bietet die Möglichkeit, die *in vivo*-Situation für biomedizinische Studien zu rekapitulieren und zu miniaturisieren. Der in dieser Arbeit entwickelte mikrofluidische Chip enthält zwei

mikrofluidische Kanäle, die durch eine poröse Membran getrennt sind, die mit polarisierten Magenepithelzellen (NCI-N87) ausgekleidet ist. Es wurde eine dynamische Umgebung emuliert, in der die Medien mit einer konstant niedrigen Rate (0,5 $\mu\text{l}/\text{min}$) fließen. Interessanterweise zeigten die Ergebnisse, dass die Integrität der Barriere der Monoschicht des Magenepithels bei kontinuierlichem Medienfluss im Vergleich zu den statischen Bedingungen verbessert wird. Außerdem analysierte ich experimentell den medikamenteninduzierten apoptotischen Zelltod in Magenepithelzellen, indem ich den Cell-on-a-Chip mit dem Incucyte-Live-Cell-Imaging-System kombinierte. Zusätzlich zu dieser Arbeit könnte dieses mikrofluidische System zur besseren Nachahmung von In-vivo-Situationen für den von *H. pylori* ausgelösten apoptotischen Zelltod in primären Magenschleimhäuten verwendet werden. Dies könnte ein wertvolles Instrument zur Untersuchung des molekularen Zusammenspiels zwischen Zellen der Mikroumgebung als Reaktion auf Infektionen sein.

Insgesamt wurde in dieser Arbeit das molekulare Zusammenspiel von USP48 und A20 bei der Regulierung der NF- κ B-Transkriptionsaktivität und des apoptotischen Zelltods im *H. pylori*-infizierten Magenepithel untersucht. Darüber hinaus konnten wesentliche Erkenntnisse über den Einfluss von Zellen aus dem Mikromilieu auf die *H. pylori*-induzierte A20-Expression und den apoptotischen Zelltod gewonnen werden. Durch den Einsatz von Zell-on-a-Chip-Technologien bieten diese Untersuchungen die Möglichkeit, therapeutische Strategien zu entwickeln.

List of publications

Publications presented in this dissertation

Jantaree, P., Chaithongyot, S., Sokolova, O., & Naumann, M. (2022). USP48 and A20 synergistically promote cell survival in *Helicobacter pylori* infection. *Cell Mol Life Sci*, 79(8), 461. <https://doi.org/10.1007/s00018-022-04489-7>

Jantaree, P., Yu, Y., Chaithongyot, S., Täger, C., Sarabi, M. A., Meyer, T. F., Boccillato, F., Maubach, G., & Naumann, M. (2022). Human gastric fibroblasts ameliorate A20-dependent cell survival in co-cultured gastric epithelial cells infected by *Helicobacter pylori*. *Biochim Biophys Acta Mol Cell Res*, 1869(12), 119364. <https://doi.org/10.1016/j.bbamcr.2022.119364>

Bakhchova, L.†, **Jantaree, P.**†, Gupta, A., Isermann, B., Steinmann, U., & Naumann, M. (2021). On-a-chip-based sensitive detection of drug-induced apoptosis in polarized gastric epithelial cells. *ACS Biomater Sci Eng*, 7(12), 5474–5483. <https://doi.org/10.1021/acsbiomaterials.1c01094>

Related publications

Jantaree, P.†, Bakhchova, L.†, Steinmann, U., & Naumann, M. (2021). From 3D back to 2D monolayer stomach organoids-on-a-chip. *Trends Biotechnol*, 39(8), 745–748. <https://doi.org/10.1016/j.tibtech.2020.11.013>

Chaithongyot, S., **Jantaree, P.**, Sokolova, O., & Naumann, M. (2021). NF-κB in gastric cancer development and therapy. *Biomedicines*, 9(8), 870. <https://doi.org/10.3390/biomedicines9080870>

Noack, L., Bundkirchen, K., Xu, B., Gylstorff, S., Zhou, Y., Köhler, K., **Jantaree, P.**, Neunaber, C., Nowak, A. J., & Relja, B. (2022). Acute intoxication with alcohol reduces trauma-induced proinflammatory response and barrier breakdown in the lung via the Wnt/β-catenin signaling pathway. *Front Immunol*, 13, 866925. <https://doi.org/10.3389/fimmu.2022.866925>

†Both authors contributed equally to this work

Chapter 1. Introduction

1.1 *Helicobacter pylori* infection

The implication of gastric organisms with gastric diseases was recognised when Marshall and Warren (1984) identified the gastric bacterium, *Campylobacter pyloridis*, now known as *Helicobacter pylori*, in the biopsy specimens of patients with gastritis and peptic ulceration. *H. pylori* is a Gram-negative, microaerophilic bacterium, measuring approximately 2 to 4 μm in length and 0.5 to 1.0 μm in width (Kusters et al., 2006). The bacterium typically appears spiral or rod-shaped, while its coccoid form can occasionally be seen in a dormant state (Goodwin & Worsley, 1993). The natural reservoir of *H. pylori* is the human stomach and selectively the gastric epithelium (Ailloud et al., 2019). *H. pylori* localises to specific regions in the stomach, the corpus and the antrum (Rolig et al., 2012). *H. pylori* has 2-6 unipolar sheathed flagella, which enhance its mobility in the mucus layer overlying the gastric epithelial cells (O'Toole et al., 2000). In most cases, *H. pylori* infection begins during childhood and remains in the host's life without antimicrobial treatment. There is no explicit knowledge of the transmission route of *H. pylori*. However, person-to-person transmission, especially within the same family by the oral-oral or faecal-oral route, appears to be prevalent (Kayali et al., 2018). This transmission mode is also associated with environmental contamination, poor hygiene, and differences in geographical determinants. After transmitting, *H. pylori* stays for short duration within the lumen (pH \sim 2.0) and enters the mucus layer (pH \sim 4.5 - 6.5), which is the habitat of the *H. pylori*. It has been suggested that *H. pylori* has several mechanisms to overcome the gastric acidic pH, such as using urease to break down urea and produce ammonia that neutralises acidity (Ansari & Yamaoka, 2017).

The prevalence of *H. pylori* infection is 44.3% worldwide, ranging from 34.7% in developed countries to 50.8% in developing countries (Zamani et al., 2018). It was reported that Africa had the highest pooled prevalence (70.1%) whereas Oceania had the lowest prevalence (24.4%) (Hooi et al., 2017). Meanwhile, the majority of *H. pylori*-infected individuals never reported any related complications or symptoms (Reshetnyak et al., 2021). Chronic infection with *H. pylori* increases the risk of developing gastric diseases (Diaz et al., 2018). *H. pylori* infection can mediate clinical manifestations as follows: (1) chronic gastritis, which almost all infected individuals develop and mostly remain asymptomatic; (2) duodenal ulcer phenotype, which occurs in 10%-15% of infected individuals; (3) gastric ulcer/adenocarcinoma phenotype, which develops into gastric cancer in 1-3% of infected individuals; and (4) gastric mucosa-associated lymphoid tissue lymphoma, which develops in 0.1% of infected individuals (Ahn & Lee, 2015). The gastric adenocarcinoma phenotype, mainly occurring when there is proximal colonization of the stomach (pangastritis), damages gastric glands and causes atrophic gastritis. This phenotype eventually proceeds to a multistep process, including intestinal metaplasia, dysplasia, and adenocarcinoma, which could take up to seven or eight decades (Ahn & Lee, 2015). Accordingly, *H. pylori* is categorized as a Type I carcinogen for gastric cancer, involved in 90% of all gastric malignancies (Noto & Peek, 2012) and considered the most common etiologic agent of infection-related cancers (Bakhti et al., 2020).

Gastric cancer ranks as the fifth most common world malignancy. Although the incidence rate has decreased since the mid-20th century (Wu et al., 2019), it remains the fourth leading cause of cancer-related deaths worldwide (Sung et al., 2021). Due to late clinical signs, diagnosis is delayed resulting in a poor overall prognosis (Hunt et al., 2015). Endoscopic or surgical resection is the only curative option, often supported by interdisciplinary approaches such as perioperative chemotherapy. The most common conventional chemotherapeutic drugs used are fluoropyrimidines (5-fluorouracil, capecitabine, S-1), platinum compounds (cisplatin, oxaliplatin), docetaxel and epirubicin. The current approved targeted therapies include monoclonal antibodies against the human epidermal growth factor receptor 2 (HER2) (e.g. trastuzumab and pertuzumab) and the anti-vascular endothelial growth factor receptor (VEGFR) (e.g. ramucirumab) (Joshi & Badgwell, 2021).

1.2 Gastric epithelial barrier

The gastric mucosa is structured in narrow invaginations known as glands, which are made of a simple columnar epithelium (Figure 1). The interior part of the gland houses the gastric mucosa factory, including chief cells for digestive enzyme production, parietal cells for gastric acid production, endocrine cells for hormone production and stem cells for the generation of all cell types. The glands are supported by fibroblasts serving as a scaffold of mesenchymal-derived stromal tissue (lamina propria and muscularis mucosa). The upper part of the glands, known as pits or foveolae, is overlaid by abundant mucus produced by mucus-producing cells and is the contact surface to the stomach content (Traulsen et al., 2021). These epithelial cells are connected by tight junctions and play critical roles in preserving epithelial monolayer barrier integrity and function, cell polarity, and intercellular adhesion. Regarding a tight monolayer of epithelial cells, the gastric epithelium is the first significant barrier separating the luminal contents from the underlying tissue compartments. The gastric epithelial barrier prevents organisms in the lumen from accessing the gastric mucosa, while permitting flux of water, ions and solutes, including nutrients. Thus, epithelial cells lining the stomach represent the first line of defence against pathogens, including *H. pylori* (Wroblewski & Peek, 2011).

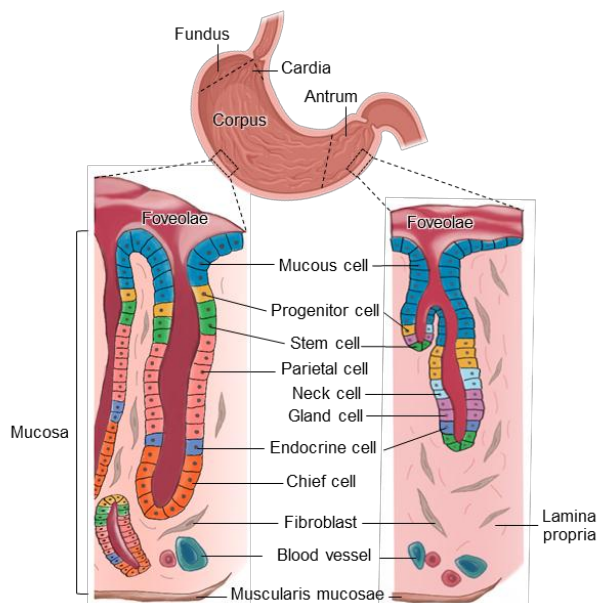


Figure 1. Schematic representation of human stomach and gastric epithelium organization. Human stomach is divided into different regions including cardia, fundus, corpus (body) and antrum. The gastric epithelium includes different cell types with different functions. The gastric glands are surrounded by stromal fibroblasts serving as a scaffold. The figure was modified with permission from Jantaree et al., 2021.

1.2.1 Crosstalk between stromal cells and epithelium

Mesenchymal stromal cells are heterogeneous cell populations, including fibroblast and myofibroblast populations and immunological stromal cells of the lymphoid tissue. In general, stromal cells are responsible for synthesising extracellular matrix (ECM) components such as fibronectin, laminin and collagen (type I, III, IV and V) and function to balance the ECM homeostasis and maintain tissue structure. Furthermore, stromal cells are involved in regulating epithelial differentiation and proliferation, inflammatory processes and wound repair (Gomes et al., 2021; Liu & Mak, 2022). Notably, different stimuli such as transforming growth factor β (TGF β), epidermal growth factor (EGF) and fibroblast growth factor 2 (FGF2) from damaged epithelial cells and infiltrating immune cells can activate fibroblasts. The activated fibroblasts, which are sometimes referred to as myofibroblasts, can release elevated amounts of matrix metalloproteinases (MMPs) and growth factors, e.g. EGF, FGF2 and hepatocyte growth factor (HGF), which in turn influences adjacent epithelial cells (Kalluri, 2016).

Gastric stromal cells, mainly fibroblasts, are part of the lamina propria in the gastric mucosa, surrounding the gastric glands. Although the general roles of stromal cells have been described, there is still limited knowledge regarding the distinct and precise function of gastric fibroblasts, in communication with the adjacent epithelium. Katano et al. (2015) studied *in vitro* co-culture of murine mesenchymal fibroblasts and epithelial cells and revealed a supporting role of fibroblasts on epithelial stem cell activity and proliferation. Furthermore, Sigal et al. (2017) found that murine gastric myofibroblasts proximal to the stem cell compartment produced R-spondin 3, which supported the self-renewal of the stem cell niche. They later reported that myofibroblastic R-spondin 3 induced differentiation of Lgr5⁺ stem cells into secretory phenotype secreting antimicrobial factors upon *H. pylori* infection (Sigal et al., 2019). Moreover, Boccellato et al. (2019) demonstrated that human gastric stromal cells of lamina propria reduced stemness capacity and induced partial differentiation of epithelial cells via secreted factors that inhibit the Wnt pathway. These studies emphasise the active communication between stroma and epithelium under pathological conditions and suggest the importance of gastric fibroblasts for maintaining the integrity and function of the gastric epithelium.

1.2.2 Gastric organoids

While experimental mice and human cell lines, mainly derived from cancer resections, are the common tools used for studying epithelial cells, the recent development of human gastric organoids presents a new possibility for the study of gastric pathogenesis. Organoids are stem cell-originated, self-organised 3D clusters of organ-specific cells that can preserve features of the originating organ's functioning as well as molecular and cellular heterogeneity (Pang et al., 2022). The formation of organoids from gastric epithelial cells depends on tissue-specific growth factors (Bartfeld et al., 2015; Schlaermann et al., 2016). Generally, human gastric organoids are generated by seeding gastric glands from human gastric resection tissue in a basement matrix (Matrigel™) and culturing in a medium containing several supplements including Wnt-3A, R-spondin-1, EGF, noggin, FGF10, gastrin, glutamax, B27, N2, 4-(2-hydroxyethyl)-1-piperazineethanesulfonic acid (HEPES), SB202190 (p38 MAPK inhibitor), A83-01 (an inhibitor of ALK5/4/7), N-acetyl-L-cysteine and Y-27632 (ROCK inhibitor) (Schlaermann et al., 2016). The activation of the Wnt/ β -catenin signalling pathway is

crucial for the maintenance of adult gastric stem cells during the generation of gastric organoids from adult tissue (Bartfeld et al., 2015; Schlaermann et al., 2016). Lack of Wnt signalling activation induces cell differentiation into mucus-producing cells at the pit of the gastric gland (Bartfeld et al., 2015; Boccellato et al., 2019; Schlaermann et al., 2016). In the other hand, gastric organoids can also be developed from pluripotent stem cells (PSCs) via simulating the sequential signalling interactions operating during *in vivo* development, which provides diverse populations of gastric epithelial cells and a surrounding layer of undifferentiated mesenchymal cells (Broda et al., 2019).

Human gastric organoid allows long-term cultivation of primary human cells in the supportive extracellular matrix (Matrigel™), providing a hollow cyst-like structure that can be up to 300 µm in diameter. The organoid is composed of a single layer of columnar epithelial cells with their apical side facing the lumen on the inside (Maubach et al., 2022). Therefore, infection of these gastric organoids can be accomplished by injecting the bacteria into their lumen, enabling the study of the epithelial host response to the pathogen following their natural apical route (Bartfeld, 2016; Bartfeld & Clevers, 2015). Interestingly, a culture system, namely gastric mucosoid, was established (Boccellato et al., 2019; Schlaermann et al., 2016). In this mucosoid culture, the freshly dissociated epithelial cells from explants or organoids were cultivated in an air-liquid interface in the collagen-coated polycarbonate filter of a transwell (Boyden chamber). The cells accessed the culture medium via the basal side. As a result, they formed a polarised monolayer involving various epithelial cell types and provided abundant mucus accumulation on the apical side, similar to the gastric mucosa *in vivo*. Moreover, the apical side of the gastric mucosoids was easier accessible, allowing infection of *H. pylori* directly into the mucous without injection. Therefore, gastric mucosoids provide an innovative tool for studying host-pathogen interaction.

1.2.3 Organ-on-a-chip

Human organ-on-a-chip, which implements human organoids or cell lines in microfluidic devices, provides an artificial bioengineered system to arrange cells to simulate tissue or organ physiology for biomedical studies. Human tissue from different origins has been reported to be implemented in a microfluidic chip for research in personalised medicine (Jodat et al., 2018; van den Berg et al., 2019). The most common used microfluidic chip model is a sandwich structure containing two microsize channels divided by a porous membrane. The channel size is in the range of 100 – 1000 µm in width, 50 – 200 µm in height and 1 cm in length (Figure 2). The chip can be microfabricated using soft lithography, injection molding, or 3D printing. The chip body is usually made of polymers, including polydimethylsiloxane (PDMS), which provides transparency, flexibility and gas permeability (Jantaree et al., 2021).

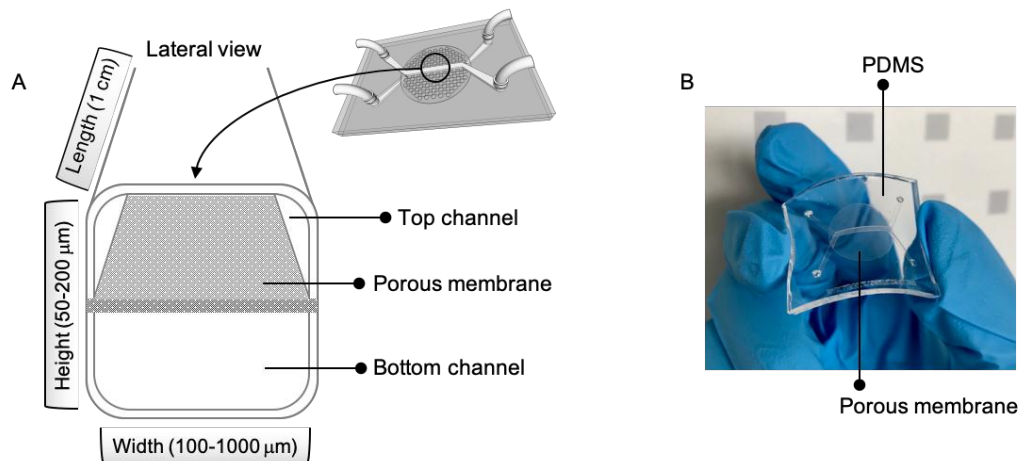


Figure 2. Schematic configuration of a microfluidic chip. (A) A sandwich structure containing two microsize channels (top and bottom) divided by a porous membrane. (B) A chip body made of PDMS provides transparency, flexibility and gas permeability.

Notably, the cells inside the microfluidic chips are exposed to media flow, creating shear stress on the cells (thus the term "dynamic"), which results in a better simulation of the *in vivo* micromilieu (Kim et al., 2012; Kim & Ingber, 2013). Previously, the so-called gut-on-a-chip was established in which the chip was lined by human intestinal epithelial (Caco-2) cells. Exposure to physiological peristalsis-like motions and liquid flow induced human Caco-2 cells to rapidly develop a polarised columnar epithelium, spontaneously grow into folds that recapitulate the structure of intestinal villi, and form a high integrity barrier to small molecules that better mimics the whole intestine than cells cultured in static Transwell models (Kim et al., 2012; Kim & Ingber, 2013). Interestingly, Workman et al. (2018) developed intestine-on-a-chip by dissociating the intestinal organoids into single cells before culturing them on the chip. They showed that the cells were polarised, had major intestinal epithelial subtypes, and were biologically responsive to exogenous stimuli. Nearly the same time, the first model of stomach-on-chip was developed, which is the implementation of the 3D gastric organoid embedded in Matrigel™ in a centre of microfluidic chamber (Lee et al., 2018). Luminal delivery of nutrients was done by injection via micropipettes connected to the peristaltic pump to recapitulate *in vivo* luminal flow. This model allows for robust 3D growth of gastric organoids with long-term time-course optical imaging capabilities. However, this system requires further development as the 3D organoid could deposit debris from dead cells and mucus in the lumen and inconvenient to access the apical side of the epithelium. Recently, Jeong et al. (2022) developed organoid-based human stomach micro-physiological system using microfluidic chip model of sandwich structure and showed that it could recapitulates the dynamic mucosal defence mechanism.

1.3 NF- κ B pathway

NF- κ B refers to a family of transcription factors which plays an essential role in regulating a wide variety of biological processes, including cell differentiation, proliferation, survival, and immune responses and inflammation (Taniguchi & Karin, 2018). Notably, NF- κ B is a master regulator of the inflammatory transcriptional response to bacterial molecules (Sokolova & Naumann, 2017). NF- κ B is frequently

dysregulated in gastric cancer, contributing to cell proliferation, tumour growth, metastasis and chemoresistance (Chaithongyot et al., 2021). The NF- κ B family involves five members: RelA, RelB, c-Rel, NF- κ B1 (p50), and NF- κ B2 (p52), which dimerise to form homodimers and heterodimers (Neumann & Naumann, 2007). Herein, the RelA/p50 is the prototypic dimeric transcription factor. The NF- κ B family members share a highly conserved 300-amino acid Rel Homology Domain (RHD), which is essential for dimerisation, binding to DNA and interaction with inhibitors of NF- κ B (I κ Bs). Without stimuli, NF- κ B dimers are sequestered in the cytosol by their interaction with I κ Bs. Upon stimulation, basically in the classical NF- κ B pathway, I κ B α is phosphorylated by a multi-subunit I κ B kinase (IKK) complex, consisting of two catalytic subunits (IKK α and IKK β) and NF- κ B essential modulator (NEMO). The phosphorylation of I κ B α triggers ubiquitin-dependent degradation of I κ B α by the 26S proteasome. Subsequently, the NF- κ B dimers RelA/p50 translocates into the nucleus, where it binds to the κ B enhancer sequences to induce the activation of target genes (Neumann & Naumann, 2007). Furthermore, another conserved pathway towards the activation of NF- κ B has also been identified and is referred to as the alternative pathway. This pathway requires the IKK α and NIK-dependent proteasomal processing of p100 to p52 and leads to the activation of NF- κ B dimers RelB/p52. The alternative pathway is activated by a relatively small number of TNF receptor superfamily members, e.g. CD40, lymphotoxin β receptor, and plays a crucial role in lymphoid organogenesis (Razani et al., 2011).

1.3.1 *H. pylori*-induced NF- κ B signalling

It was shown that *H. pylori* induced NF- κ B activation at an early time point in a type IV secretion system (T4SS)-dependent manner (Schweitzer & Naumann, 2010; Sokolova et al., 2013). Recently, it has been discovered that NF- κ B was activated in *H. pylori* infection by ADP-heptose, a key metabolic intermediate in LPS biosynthesis pathway of Gram-negative bacteria (Figure 3) (Maubach et al., 2021; Pfannkuch et al., 2019). ADP-heptose enters the cytosol and binds to alpha-protein kinase 1 (ALPK1), a serine/threonine kinase that belongs to the family of a typical protein kinase (Zhou et al., 2018). ALPK1 then phosphorylates the threonine residue T9 of tumour necrosis factor receptor-associated factor (TRAF)-interacting protein with forkhead-associated domain (TIFA) dimer, leading to TIFA oligomerisation (Milivojevic et al., 2017; Zimmermann et al., 2017). Upon *H. pylori* infection, TIFA can bind to different TRAF molecules to activate NF- κ B pathways (Maubach et al., 2021). Herein, TIFA-TRAF6 binding recruits the complex of transforming growth factor β -activated kinase 1 (TAK1) with TAK1-binding proteins (TABs) and activates IKK complex, and subsequently classical NF- κ B activation (Sokolova et al., 2018; Sokolova et al., 2014). Furthermore, TIFA can interact with TRAF2 in the NF- κ B-inducing kinase (NIK) complex, leading to destabilisation of cellular inhibitor of apoptosis 1 (cIAP1), allowing NIK accumulation and activation of alternative NF- κ B pathway (Maubach et al., 2021).

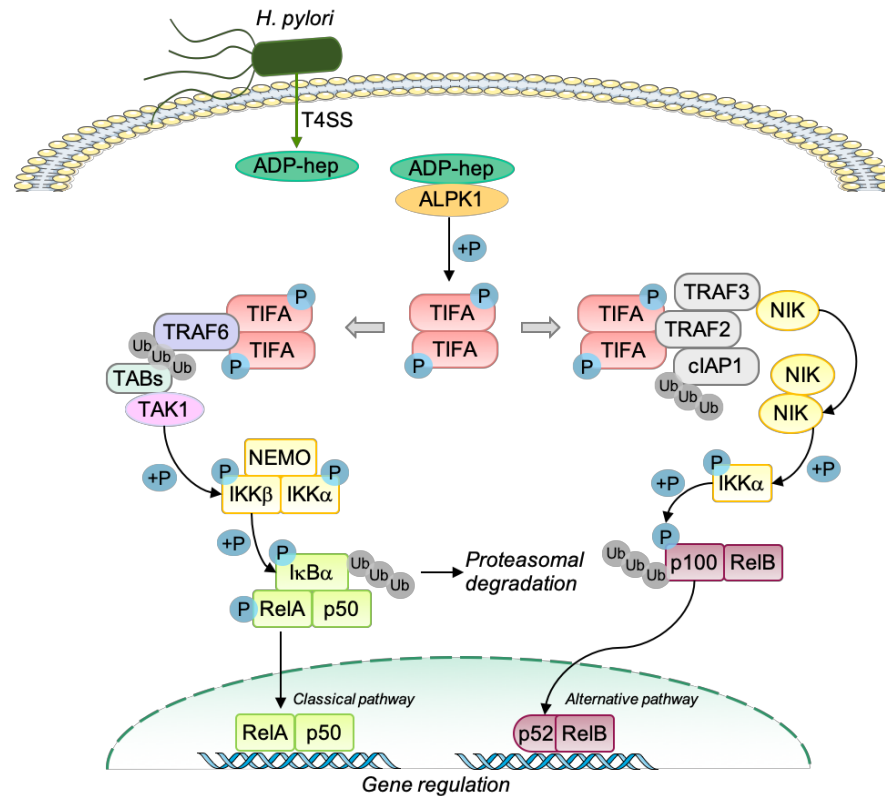


Figure 3. *H. pylori*-induced NF- κ B signalling. ADP-heptose of *H. pylori* binds and activates ALPK1, leading to phosphorylation of TIFA dimer. Interaction of TIFA dimers with the targets, TRAF6 or TRAF2, (called TIFAsomes) facilitates TRAF6 and cIAP1 ubiquitinylation and subsequently activates the classical or alternative NF- κ B, respectively. The figure was created based on the review articles by Maubach et al., 2022.

1.3.2 Regulation of NF- κ B

NF- κ B signalling can be controlled through several mechanisms. One major negative feedback control is the upregulation of NF- κ B target gene *NFKBIA* (encodes I κ B α), leading to a reaccumulation of I κ B α protein to sequester RelA/p50 in the cytosol and termination of NF- κ B activity. Moreover, protein degradation via the ubiquitin-proteasome system (UPS) is another important mechanism that contributes to the termination of NF- κ B molecules, including the degradation of RelA in the nucleus (Saccani et al., 2004). Ubiquitinylation is a protein modification in which the ubiquitin molecules covalent attach to a target protein. Ubiquitinylation is achieved by an enzymatic cascade composed of ubiquitin-activating enzymes (E1), ubiquitin-conjugating enzymes (E2) and ubiquitin ligases (E3) (Senft et al., 2018). It was reported that upon TNF stimulation, the nuclear RelA was ubiquitinylated by the CRL ECS^{SOCS1} composed of cullin-2, the adaptor proteins Elongin B and C, the substrate recognition molecule SOCS1 and the substrate adapter protein COMMD1 (Maine et al., 2007). The ubiquitinylated RelA was subsequently degraded by the 26S proteasome in subnuclear structures - promyelocytic leukemia (PML) bodies (Tanaka et al., 2007). Furthermore, a superpose regulation of ubiquitin ligation by CRLs is the multiprotein complex CSN. The CSN complex removes the CRL activating Ub-like molecule neural precursor cell expressed developmentally downregulated gene 8 (NEDD8) from cullin subunits (deneddylation), resulting in suppression of CRL ligation activity (Dubiel et al., 2020). The CSN complex composes of eight subunits (CSN1-8),

including six proteasome-COP9-initiation factor 3 (PCI) domain subunits and two Mov34-and-Pad1p N-terminal (MPN) domain subunits (CSN5, CSN6) situated on top of the helical bundle (Lingaraju et al., 2014). Of note, the JAB1/MPN/Mov34 metalloenzyme motif in CSN5 is responsible for the deneddylase activity of the CSN complex (Echalier et al., 2013).

1.3.3 NF- κ B control by DUBs

DUBs hydrolyse the isopeptide bond between ubiquitin and the targeted substrate or the peptide between individual ubiquitins to facilitate complete removal or modification of the ubiquitin signal (Pfoh et al., 2015). Approximately 100 DUBs encoded in the human genome can be divided into six different families according to their protease domain. The majority of DUBs are cysteine proteases and include the ubiquitin carboxy-terminal hydrolases (UCHs), ubiquitin-specific proteases (USPs), ovarian tumour proteases (OTUs), Machado-Joseph domain-containing proteases (MJDs) and the recently discovered motif interacting with Ub (MIU)-containing novel DUB family (MINDY) (Abdul Rehman et al., 2016). However, there is also a small group of zinc metalloproteases referred to as JAB1/MPN/Mov34 (JAMMs) (Pfoh et al., 2015). Some DUBs have been identified to regulate the NF- κ B transcriptional response in gastric epithelial cells. For example, the CSN-associated DUB USP15 removes stimulus-dependent K48-ubiquitin chains from the *de novo* synthesised I κ B α , resulting in stabilisation of I κ B α and suppression of NF- κ B signalling (Schweitzer et al., 2007). Furthermore, it was reported that DUB in the same family of USPs, USP47, could regulate NF- κ B activity by promoting RelA phosphorylation through stabilising β TrCP and subsequent degradation of I κ B α . USP47 also contributes to the chemoresistance and viability of gastric epithelial cells (Naghavi et al., 2018).

1.3.3.1 USP48

USP48 is a CSN-associated nuclear DUB (Schweitzer & Naumann, 2015). USP48 consists of a catalytic (USP) domain which is responsible for deubiquitylase activity, a DUSP domain which play a role in substrate recognition and a UBL domain which regulate USP catalytic activity (Tzimas et al., 2006). USP48 contains a carboxyl-terminal nuclear localizing signal, ⁹³⁸RHRK⁹⁴¹, which is responsible for its nuclear translocation (Liu et al., 2018). It was reported that USP48 removes K48-linked polyubiquitin chains from RelA in the nucleus, resulting in stabilisation of nuclear RelA and enhancing NF- κ B transcriptional activity upon TNF stimulation (Schweitzer & Naumann, 2015). Additionally, USP48 could antagonise BRCA1 E3 ligase functions which impact in genome stability and DNA repair (Velimezi et al. 2018; Uckelmann et al., 2018). It was suggested that phosphorylation of USP48 enhanced its DUB activity which could be mediated by casein-kinase 2 (Schweitzer & Naumann, 2015) or glycogen synthase kinase 3 β (GSK3 β) (Li et al., 2018). In addition, it was reported that USP48 could be upregulated via methyltransferase-like 14 (Mettl14)-induced m6A modification in USP48 mRNA, which maintains USP48 mRNA stability (Du et al., 2021).

1.3.3.2 A20

A20 is an NF- κ B inducible protein encoded by the NF- κ B target gene *TNFAIP3*. A20 contains an ovarian tumour domain at the N-terminus, which possesses a

deubiquitinylase activity, and seven zinc finger (ZnF) domains at the C-terminus, which involve ubiquitin-binding domains (ZnF4 and ZnF7) (Martens & van Loo, 2020). A20 down-regulates NF- κ B signalling in either catalytic or non-catalytic mechanisms (Bosanac et al., 2010; Chen & Chen, 2013; Skaug et al., 2011; Tokunaga et al., 2012; Verhelst et al., 2012; Wertz et al., 2015). For example, A20 interacts with linear polyubiquitin chain of NEMO, preventing activation of IKKs and thereby suppressing NF- κ B activation (Tokunaga et al., 2012). Notably, it has been shown that *H. pylori* infection induced *de novo* synthesis of A20, negatively suppressing classical NF- κ B activity in gastric epithelial cells (Lim et al., 2017). Furthermore, the DUB activity of A20 counteracted cullin3-mediated K63-linked ubiquitinylation of procaspase-8, thus suppressing the activity of caspase-8 and apoptotic cell death during *H. pylori* infection (Lim et al., 2017). Recently, it was shown that A20 suppressed alternative NF- κ B activity and anti-apoptotic genes involving baculoviral IAP repeat containing 2 (*BIRC2*), *BIRC3* and B-cell lymphoma 2-related protein A1 (*BCL2A1*) in gastric epithelial cells (Lim et al., 2022).

1.3.3.2.1 Other factors involved in *H. pylori*-associated apoptosis

During gastritis, *H. pylori* induces an increase in apoptosis in most infected epithelial cells, thus resulting in atrophy, phenotypic changes, and the development of an inflammatory response (Diaz et al., 2018). Several studies reported VacA as a bacteria virulence factor induced apoptotic cell death mainly via mitochondrial damage, allowing the release of cytochrome c (Akazawa et al., 2013; Boquet et al., 2003; Cho et al., 2003; Cover et al., 2003; Jain et al., 2011; Ki et al., 2008; Kuck et al., 2001; Lan et al., 2010). Moreover, it was reported that *H. pylori* infection could induce reactive oxygen species (ROS), leading to apoptotic cell death (Calvino Fernandez & Parra Cid, 2010; Chaithongyot & Naumann, 2022). Herein, bacterial factor GGT could contribute to the production of H₂O₂ (Gong et al., 2010; Ricci et al., 2014) and the induction of apoptotic cell death via a mitochondria-mediated pathway (Kim et al., 2007; Valenzuela et al., 2010). Furthermore, it was reported that other *H. pylori* factors involving glycine acid extract (GE), CagA, urease subunit A (UreA), and lipopolysaccharide (LPS) could also contribute to oxidative stress and apoptotic cell death (Gonciarz et al., 2019). Moreover, *H. pylori* could also trigger apoptotic cell death via extrinsic pathway through the upregulation of TNF-related apoptosis-inducing ligand (TRAIL) and Fas ligand (FasL) and their receptor subtypes (Domhan et al., 2004; Jones et al., 1999; Martin et al., 2004; Tsai & Hsu, 2017). Furthermore, analysis of apoptotic signalling proteins suggested that *H. pylori* induces apoptotic cell death through pathways involving the induction of the pro-apoptotic proteins (e.g. Bax, Bad and Bid) and the activation of caspase-8 or -9 and -3 (Maeda et al., 2002; Shibayama et al., 2001). Recently, it was suggested that *H. pylori* outer inflammatory protein A (OipA) could trigger an apoptotic cascade in host cells via an increase of Bax/Bcl-2 ratio and cleaved caspase-3 level (Teymournejad et al., 2017; Zhao et al., 2020) (Figure 4).

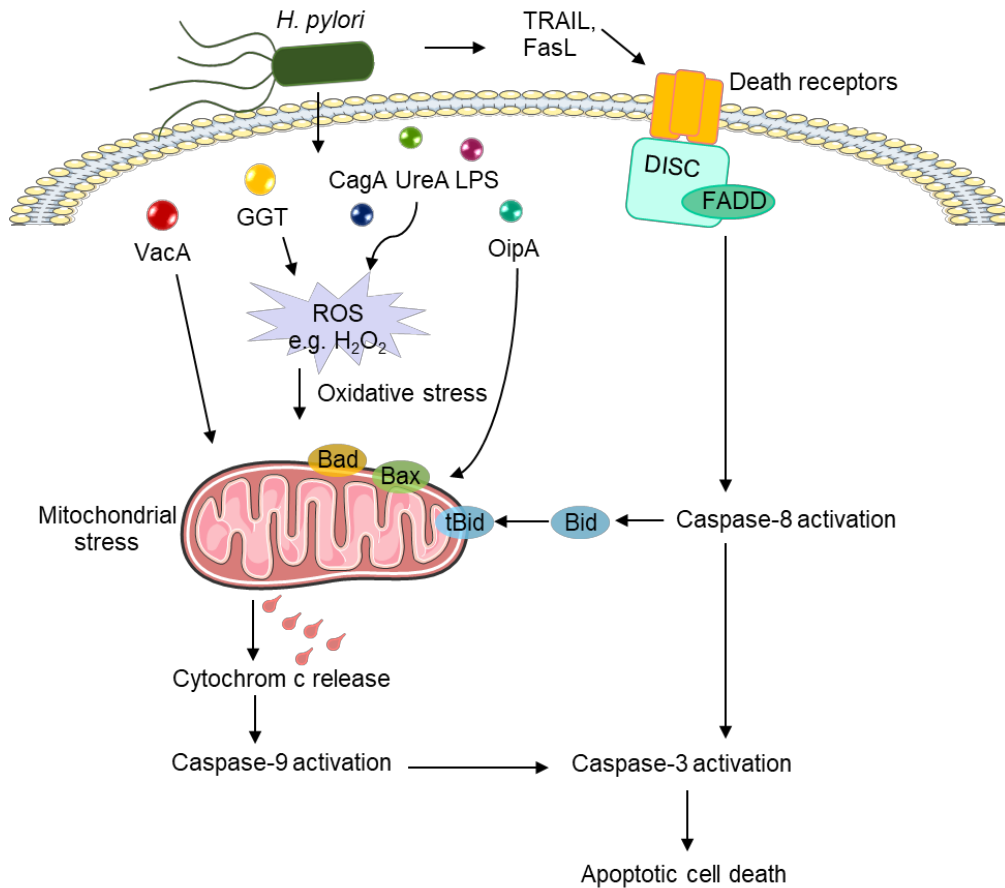


Figure 4. Mechanisms of *H. pylori*-induced apoptotic signalling. *H. pylori* virulence factor VacA targets mitochondria, while other bacteria factors (mainly GGT) could trigger oxidative stress, leading to the mitochondria-mediated apoptotic pathway. *H. pylori* could also induce pro-apoptotic proteins expression (e.g. Bax, Bad and Bid). The mitochondria stress leads to the release of cytochrome c into the cytosol. Cytochrome c then induces apoptosome formation, which activates caspase-9 and -3, provoking apoptotic cell death. Moreover, following activation of death receptors in *H. pylori* infection, caspase-8 is activated after being recruited into the death-inducing signalling complex (DISC) through FADD (Fas-associated death domain). The cascade then activates caspase-3 and eventually induces apoptosis. In addition, activated caspase-8 can also convey the death signal to mitochondria via cleavage of Bid, leading to activation of the mitochondrial pathway.

Chapter 2. Aims and outline of the dissertation

2.1 Research aims

The ultimate objective of this thesis work was to elucidate the molecular control of apoptotic cell death by DUBs, focusing on USP48 and A20, in the gastric epithelial cells during *H. pylori* infection. The following aims were addressed in this thesis:

- (1) To determine the role of USP48 in the turnover of *H. pylori*-induced NF- κ B in the gastric epithelium
- (2) To investigate the impact of USP48/A20 on apoptotic cell death during *H. pylori* infection
- (3) To analyse the impact of fibroblasts on the NF- κ B-dependent regulation of apoptotic cell death in the *H. pylori*-infected gastric epithelium
- (4) To establish a gastric epithelial monolayer on-a-chip as a tool for the study of drug- or *H. pylori*-induced apoptotic cell death

2.2 Outline of the dissertation

This thesis incorporates the following chapters in order to cover all aims.

- In **chapter 3 (publication I)**, we addressed the role of USP48 in the regulation of *H. pylori*-induced NF- κ B activity in gastric epithelial cells. Moreover, the mechanism by which USP48 and A20 regulate NF- κ B/RelA and apoptotic cell death in *H. pylori* infection was investigated.
- In **chapter 4 (publication II)**, we applied a co-culture system of gastric epithelial cells and fibroblasts to explore the cellular crosstalk. The impact of fibroblasts on NF- κ B-regulated A20 and the apoptotic cell death of gastric epithelial cells during *H. pylori* infection was investigated.
- In **chapter 5 (publication III)**, we established the gastric epithelial monolayer on-a-chip, which represents a powerful tool to study drug and *H. pylori*-induced apoptosis in gastric epithelial cells.
- In **chapter 6**, the main findings from all articles were summarised and discussed with regard to the research aims, limitations of the presented work, and prospective future work.

Chapter 3. Publication I

USP48 and A20 synergistically promote cell survival in *Helicobacter pylori* infection.

This study has been published in the journal Cellular and Molecular Life Sciences on 1st August 2022 and reprinted in this thesis with permission and is cited as follows:

Jantaree, P., Chaithongyot, S., Sokolova, O., & Naumann, M. (2022). USP48 and A20 synergistically promote cell survival in *Helicobacter pylori* infection. *Cell Mol Life Sci*, 79(8), 461. <https://doi.org/10.1007/s00018-022-04489-7>

Contribution to the publication

Jantaree, P.	Designed experiments Performed experiments Analysed and interpreted data Wrote the manuscript
Chaithongyot, S.	Performed experiments
Sokolova, O.	Performed experiments
Naumann, M.	Conceived the study Designed experiments Analysed and interpreted data Wrote the manuscript



USP48 and A20 synergistically promote cell survival in *Helicobacter pylori* infection

Phatcharida Jantaree¹ · Supattra Chaithongyot¹ · Olga Sokolova¹ · Michael Naumann¹

Received: 4 April 2022 / Revised: 24 June 2022 / Accepted: 11 July 2022
© The Author(s) 2022

Abstract

The human pathogen *Helicobacter pylori* represents a risk factor for the development of gastric diseases including cancer. The *H. pylori*-induced transcription factor nuclear factor kappa-light-chain-enhancer of activated B cells (NF- κ B) is involved in the pro-inflammatory response and cell survival in the gastric mucosa, and represents a trailblazer of gastric pathophysiology. Termination of nuclear NF- κ B heterodimer RelA/p50 activity is regulated by the ubiquitin-RING-ligase complex elongin-cullin-suppressor of cytokine signalling 1 (ECS^{SOC₁}), which leads to K48-ubiquitylation and degradation of RelA. We found that deubiquitylase (DUB) ubiquitin specific protease 48 (USP48), which interacts with the COP9 signalosome (CSN) subunit CSN1, stabilises RelA by deubiquitylation and thereby promotes the transcriptional activity of RelA to prolong de novo synthesis of DUB A20 in *H. pylori* infection. An important role of A20 is the suppression of caspase-8 activity and apoptotic cell death. USP48 thus enhances the activity of A20 to reduce apoptotic cell death in cells infected with *H. pylori*. Our results, therefore, define a synergistic mechanism by which USP48 and A20 regulate RelA and apoptotic cell death in *H. pylori* infection.

Keywords Apoptotic cell death · COP9 signalosome (CSN) · Deubiquitylase (DUB) · Nedd8 · RelA

Introduction

Infection of *H. pylori*, a Gram-negative microaerophilic spiral bacterium, has been observed in nearly half of the world population [1]. *H. pylori* specifically colonises the gastric mucosa and is a risk factor for chronic gastritis, initiating precancerous lesions, which may then progress to metaplasia [2]. At the cellular level, recent studies revealed that *H. pylori* ADP-glycero- β -D-manno-heptose (ADP heptose), as the activator of the proteins α -kinase 1 (ALPK1) and subsequently tumour necrosis factor receptor-associated factors (TRAF)-interacting protein with forkhead-associated domain (TIFA), induces classical and alternative NF- κ B in gastric epithelial cells [3, 4]. Activation of NF- κ B is strictly dependent on the type IV secretion system (T4SS) and independent of the cytotoxin A gene (CagA) [5].

Excessive and deregulated NF- κ B activation can cause massive damage to host tissues and contributes to the pathogenic processes of various inflammatory diseases [6]. A crucial mechanism for the timely termination of NF- κ B activity is controlled by the ubiquitin-proteasome system (UPS)-dependent degradation of RelA in the nucleus [7]. Ubiquitylation is regulated by an enzymatic cascade of E1 (activating enzymes), E2 (conjugating enzymes) and E3 (ligases) [8]. In TNF stimulation, the E3 cullin-RING-ubiquitin ligase (CRL) ECS^{SOC₁} ubiquitylates nuclear RelA [9], which is, in subnuclear structures (promyelocytic leukaemia protein nuclear bodies (PML bodies)), degraded by the 26S proteasome [10].

Ubiquitin ligation by CRLs is controlled by the protein complex CSN, which removes the CRL activating Ub-like molecule neural precursor cell expressed developmentally downregulated gene 8 (NEDD8) from cullin subunits [11]. The CSN composes of eight subunits, including six proteasome-COP9-initiation factor 3 (PCI) domain subunits and two Mov34-and-Pad1p N-terminal (MPN) domain subunits (CSN5, CSN6) situated on top of the helical bundle [12]. Of note, CSN5 possess the JAB1/MPN/Mov34 metalloenzyme (JAMM) motif of DUB families and is responsible for

✉ Michael Naumann
Naumann@med.ovgu.de

¹ Institute of Experimental Internal Medicine, Medical Faculty, Otto Von Guericke University, Leipziger Str. 44, 39120 Magdeburg, Germany

deneddylase activity [13]. Moreover, the CSN is associated with the DUBs USP15 [14], USP48 [15], CYLD [16] and STAMBPL1 [17], which control the activity of a variety of target molecules [11]. DUBs reverse ubiquitinylation by hydrolysis of the isopeptide bond between ubiquitin and the targeted substrate or the peptide between individual ubiquitins to facilitate complete removal or modification of the ubiquitin signal [18].

CSN-associated USP48 removes K48-linked polyubiquitin chains from nuclear RelA and promotes NF- κ B transcriptional activity of target genes, including tumour necrosis factor alpha-induced protein 3 (*TNFAIP3*), which encodes for the de novo synthesised DUB A20 upon TNF stimulation [15]. A20 is a zinc finger protein possessing an ovarian tumour (OTU) domain that serves via its DUB activity as a crucial negative regulator in NF- κ B signalling. A20 deficient cells are hypersensitive to NF- κ B activation by multiple stimuli, including TNF, interleukin 1 β (IL-1 β), toll like receptor (TLR) ligands and retinoic-acid-inducible protein 1 (RIG-1)-like receptor (RLR) ligands [19]. A20 interferes with the components of the NF- κ B signalling cascade and terminates NF- κ B activation, e.g. by interacting with the linear polyubiquitin chain of NF- κ B essential modulator (NEMO), thereby preventing activation of the I κ B kinases (IKKs) [20]. In addition, A20 enzymatically counteracts cullin3-mediated K63-linked ubiquitinylation of procaspase-8, suppressing caspase-8 activity and apoptotic cell death [21, 22]. On the other hand, A20 suppresses alternative NF- κ B activity and thus the anti-apoptotic genes baculoviral IAP repeat containing 2 (*BIRC2*), *BIRC3* and B-cell lymphoma 2-related protein A1 (*BCL2A1*), promoting apoptotic cell death [23].

Material and methods

Cell culture and *H. pylori* infection

AGS (ATCC, CRL-1739) and NCI-N87 (ATCC, CRL-5822) cells were cultured in RPMI 1640 medium (Gibco®/Life Technologies) supplemented with 10% foetal calf serum (FCS) (Biochrom) at 37 °C, 5% CO₂ in a humidified atmosphere. The culture medium was changed to fresh RPMI 1640 medium supplemented with 0.2% FCS overnight before infection with *H. pylori*.

H. pylori strain P1 [24] was grown on GC agar plates supplemented with 10% horse serum (Gibco®/Life Technologies), 5 μ g/ml trimethoprim (Sigma-Aldrich), 1 μ g/ml nystatin (Sigma-Aldrich) and 10 μ g/ml vancomycin (Sigma-Aldrich) at 37 °C under microaerophilic conditions for 48 h before infection. For infection, *H. pylori* were prepared in phosphate-buffered saline (PBS), and the cells were infected at a multiplicity of infection (MOI) of 100.

Transactivation assay

AGS cells were seeded in 24-well plate at a density of 60,000 cells/well. Firefly luciferase plasmid containing five copies of an NF- κ B response element (Promega) was mixed with *Renilla* Luciferase plasmid at a ratio of 50:1 and transfected using Attractene® transfection reagent (Qiagen) for 48 h. After 3.5 h of *H. pylori* infection or IL-1 β (10 ng/ml) stimulation, luciferase activity was estimated in cell lysates using a Dual-Luciferase Reporter Assay System (Promega) with a Lumat LB 9507 luminometer (Berthold Technologies). The inducible firefly luciferase activity was normalized relative to *Renilla* luciferase activity, and fold changes in stimulated samples were calculated compared to non-stimulated cells.

Transfection of siRNA and protein

Cells were seeded at 0.4×10^6 per 60-mm or 1.4×10^6 per 100-mm culture dish one day before transfection. Transfection of siRNA was performed using siLentFect™ (Bio-Rad, #1703362) following the manufacturer's instructions. Briefly, the cell culture medium was changed to Opti-MEM prior to transfection. siRNA against Elongin B, USP48, CSN2, and A20 were prepared at a final concentration of 40 nM. The following siRNAs were used: USP48^{si1} (s38642, ambion®/Life Technologies), USP48^{si5} (s38644, ambion®/Life Technologies), A20^{si9} (SI05018601, Qiagen), CSN2^{si} (AM16708, Thermo Fisher Scientific), Elongin B^{si} 5'-UGACCAACU CUUGGAUGAU-3' (Eurofins Genomics), Caspase-8^{si} (#SI02661946, Qiagen) and scrambled^{si} (#D-001810-10, Dharmacon). At 6 h after transfection, the medium was changed to fresh RPMI 1640 medium containing 10% FCS and the cells cultured for additional 42 h before infection. The transfection of His-tagged recombinant human USP48 protein (#E-614, Boston Biochem™) or recombinant human A20 protein (#80408, BPS Bioscience) was performed as follows: 1 μ g recombinant USP48 protein was mixed with 2 μ l Cas9 PLUS™ reagent (Thermo Fisher Scientific) in 125 μ l Opti-MEM and incubated for 5 min at room temperature (RT). 4 μ l CRISPRMAX transfection reagent (Thermo Fisher Scientific) was diluted in 125 μ l Opti-MEM. The USP48 protein/Cas9 PLUS™ solution was combined with the CRISPRMAX transfection solution, followed by incubation at RT for 20 min. The cell culture medium was changed to fresh RPMI 1640 medium containing 10% FCS before adding dropwise the transfection solution to the cells in the dish and the cells cultured for additional 1 h before infection.

Preparation of whole-cell lysates and subcellular fractionation

MG132 (20 μ M, Tocris) and Leptomycin B (LMB, 10 ng/ml, Calbiochem) were added to the culture medium 30 min after *H. pylori* infection when required, as indicated. For whole-cell lysates, the cells were washed twice with ice-cold PBS and lysed in RIPA lysis buffer (50 mM Tris (pH 7.5), 150 mM NaCl, 2 mM EDTA, 10 mM K_2HPO_4 , 10% glycerol, 1% Triton X-100, 0.05% SDS) supplemented with 1 mM Na_3VO_4 , 1 mM Na_2MoO_4 , 20 mM NaF, 10 mM $Na_4P_2O_7$, 1 mM AEBSF, 20 mM Glycerol-2-phosphate, and 1 \times EDTA-free protease inhibitor mix (PI) (cOmplete™, Mini, Roche). *N*-ethyl-maleimide (NEM) (7.5 mM, Fluka) and ortho-phenanthroline (OPT) (5 mM, Sigma-Aldrich) were added to the lysis buffer when preservation of ubiquitinated proteins was required. Lysates were obtained after centrifugation (13,000g, 4 °C, 10 min).

Subcellular fractionation was performed as previously described [15, 25] with some modifications. The cells were washed twice with ice-cold PBS and gently scraped in pre-chilled buffer A (20 mM Tris (pH 7.9), 10 mM NaCl, 1.5 mM $MgCl_2$, 10 mM K_2HPO_4 , and 10% Glycerol) supplemented with 1 \times PI, 1 mM Na_3VO_4 , 1 mM Na_2MoO_4 , 10 mM NaF, 0.5 mM AEBSF, 20 mM Glycerol-2-phosphate and 0.5 mM DTT. The cells were allowed to swell for 10 min on ice. Afterwards, 1 μ l of 12.5% NP-40 was added per 100 μ l cell suspension to burst the cytoplasmic membrane and incubated for 5 min on ice. Then, nuclei were separated from cytosolic supernatants by centrifugation (2000g, 4 °C, 10 min) and cytosolic fractions were cleared (13,000g, 4 °C, 10 min). Nuclear pellets (P1) were washed once with buffer A and then resuspended in buffer C (20 mM Tris (pH 7.9), 420 mM NaCl, 1.5 mM $MgCl_2$, 0.2 mM EDTA, 10 mM K_2HPO_4 , and 10% Glycerol), supplemented as described for buffer A, to extract soluble nuclear proteins (N1). The suspension was incubated for 30 min on ice with occasional vortexing. Afterwards, N1 fractions were cleared by centrifugation (13,000g, 4 °C, 10 min). The pellets (P2) with the subnuclear fractions were resuspended in buffer E (20 mM Tris (pH 7.9), 150 mM NaCl, 1.5 mM $MgCl_2$, 5 mM $CaCl_2$, 10% Glycerol and 2% SDS) supplemented as described for buffer A with additional Benzonase® Nuclease (25 U/ml, Novagen), DTT omitted. After incubating the suspension for 30 min on ice, the N2 fractions were cleared by centrifugation (13,000g, 4 °C, 10 min). NEM (7.5 mM) and OPT (5 mM) were added to the fractionation buffers when preservation of ubiquitinated protein was required. Protein concentration was determined using the Pierce™ BCA protein assay kit (Thermo Fisher Scientific), according to the manufacturer's instructions.

Immunoprecipitation and immunoblotting

For immunoprecipitation (IP) from cell lysates, equal amounts of protein were diluted with RIPA buffer supplemented with 1 mM Na_3VO_4 , 1 mM Na_2MoO_4 , 20 mM NaF, 10 mM $Na_4P_2O_7$, 1 mM AEBSF, 20 mM Glycerol-2-phosphate, and 1 \times PI. 1 μ g protein-specific antibody was added per IP and incubated overnight on a permanent rotator (7 rpm) at 4 °C. Pre-washed Pierce™ protein A/G magnetic beads (#88802, Thermo Fisher Scientific) were added and additionally rotated for 2 h at 4 °C. The beads were washed three times with RIPA buffer and twice with PBS, then eluted in 2 \times Laemmli sample buffer. For the analysis of ubiquitinated proteins, the buffer was additionally supplemented with NEM (7.5 mM), OPT (5 mM). For the IP under denaturing conditions, the cells were lysed in the buffer containing 1% SDS and the IP was performed with 0.1% SDS.

For SDS-PAGE and immunoblotting, samples were heated at 95 °C for 10 min, separated in Tris-Glycine gels and transferred onto PVDF membranes (Millipore). The membranes were blocked with 5% skim milk in TBS containing 0.1% Tween 20 (TBS-T) at RT for 1 h and incubated with primary antibodies in either 5% BSA or 5% skim milk in TBS-T at 4 °C overnight. The membranes were washed thrice with TBS-T before incubating with appropriate HRP-conjugated secondary antibody in 5% skim milk in TBS-T at RT for 1 h. The membranes were washed thrice with TBS-T and then developed using a chemiluminescent substrate (#WBKLS0500, Millipore). The band pattern was visualised using the ChemoCam Imager (Intas).

The following primary antibodies were used: A20 (sc-166692), C23 (sc-13057), CSN6 (sc-137153), Elongin B (sc-11447), Lamin B2 (sc-377379), RelA (sc-8008) and Ubiquitin (sc-8017) were purchased from Santa Cruz Biotechnology; Caspase 3 (#9662), Caspase 8 (#9746), Cleaved Caspase 3 (#9661), I κ B α (#4812), phospho-RelA (#3031) were purchased from Cell Signalling Technology; CSN2 (ab155774) and USP48 (ab72226) were purchased from Abcam; GAPDH (#MAB374) and Ubiquitin K63 linkage (05-1308) were purchased from Millipore; CSN1 (BML-PW8285-0100, ENZO); CSN5 (GTX70207, GeneTex); FLAG (#F3165, Sigma-Aldrich).

RNA isolation, reverse transcription and quantitative PCR

Total RNA was isolated from cultured cells using the Nucleospin® RNA Plus kit (Macherey-Nagel), following the manufacturer's protocol. RNA concentration was measured using the NanoDrop spectrophotometer. The isolated RNA was then reverse-transcribed into cDNA using RevertAid First Strand cDNA Synthesis Kit (Thermo Fisher Scientific). All steps were performed under nuclease-free conditions.

The SensiMix[®] Hi-ROX (Bioline) was used to analyse the gene transcripts. The quantitative PCR was performed using the StepOnePlus[™] Real-Time PCR system (Applied Biosystem, Thermo Fisher Scientific). The comparative C_T method ($\Delta\Delta C_T$) was used to quantify relative changes in the target mRNA by normalisation on a reference gene (*GAPDH*). The following primer pairs were used: *NFKBIA* (5'-GCAGACTCCACTCCACTTG-3' fw; 5'-CGTCCTCTGTGAAGTCCG-3' rev), *CXCL8* (5'-AGATGTCAGTGCATAAAGACA-3' fw; 5'-TATGAATTCTCAGCCCTCTTCAA-AA-3' rev), *TNFAIP3* (5'-CTGAAATCCGAGCTGTTCAC-3' fw; 5'-GAGATGAGTTGTGCCATGGTC-3' rev), *USP48* (5'-GGCAGGTGGCGAAGCCATT-3' fw; 5'-CAGTTTCGTCTGCACACGCCG-3' rev) and *GAPDH* (5'-CATCACCATCTTCCAGGAGC-3' fw; 5'-CATACTTCTCATGGTTCACACC-3' rev) were from Eurofins Genomics.

In vitro translation and binding assay

The CSN proteins were in-vitro translated using the PURExpress[®] In Vitro Protein Synthesis Kit (New England Biolabs), following the manufacturer's protocol. Each translated protein was incubated with 0.5 μ g recombinant human USP48 (E-614, Boston Biochem[™]) for 1 h at 37 °C followed by IP using an anti-USP48 antibody (ab72226, Abcam). IP buffer (20 mM Tris-HCl, 150 mM NaCl, 2 mM EDTA, 1% TritonX100, 0.1% SDS; pH 7.4) was supplemented with 2 mM Na₃VO₄, 20 mM NaF, 1 \times PI. The IPs were analysed by SDS-PAGE and IB.

In vitro DUB assay

RelA was immunoprecipitated from the total nuclear fraction of *H. pylori*-infected cells treated with MG132 using low-pH elution buffer (0.1 M glycine, pH 2.5). The eluted IP samples were immediately neutralised by 1 M Tris-HCl, pH 8.5 (1:10 of eluted volume).

Recombinant USP48 (0.5 μ M) was pre-incubated for 5 min at 30 °C with continuous shaking in DUB assay buffer (50 mM HEPES (pH 7.5) with 100 mM NaCl) supplemented with 1 mM DTT and 1 mM AEBSF. Next, ubiquitinated immunoprecipitated RelA was added and incubated in the presence or absence of NEM (10 mM) in a final reaction volume of 15 μ l at 30 °C with continuous shaking. Reactions were stopped after 2 h incubation by addition of 5 μ l 4 \times Laemmli sample buffer and 2 μ l β -ME and then boiled at 95 °C for 5 min. Samples were then separated by SDS-PAGE and analysed by IB.

Apoptotic cell death analysis

The cells were trypsinised and stained with an Annexin V-FITC/PI Kit (MabTag GmbH), according to the

manufacturer's instructions. Apoptotic cell death was determined using a flow cytometer (CyFlow space). Data were processed using Flowing Software 2.

Caspase 3/7 assay

After 24 h of siRNA transfection, cells were re-seeded into a 24-well plate at a density of 50,000 cells/well and allowed to adhere overnight. Transfection of recombinant human USP48 protein was performed as described before. The culture media were replaced by media containing *H. pylori* (MOI 100), Incucyte[®] Caspase 3/7 Green Dye (staining of apoptotic cells, dilution 1:1000, Sartorius) and Incucyte[®] NucLight Rapid Red Dye (staining of all cells, dilution 1:1000, Sartorius). The fluorescence signal was measured by the Incucyte[®] S3 Live-Cell Analysis System (Sartorius), and image sets of at least four pictures from distinct regions per well were captured with phase contrast and fluorescence channels at a magnification of 20 \times . The number of fluorescence-stained cells and fluorescence intensity were acquired using Incucyte[®] S3 Live-Cell Analysis System integrated software, and presented as percentages of apoptotic cells or fluorescence intensity (A.U.).

Caspase-Glo[™] 8 assay

Luminescence assay for caspase-8 activity was performed using Caspase-Glo[™] 8 Assay Kit (Promega). siRNA transfected cells were plated into a white-walled 96-well plate at a density of 10,000 cells/well. The cells were allowed to grow for 48 h. The culture media were changed to 100 μ l media containing *H. pylori* (MOI 100) and incubated for 24 h. Prior to starting the assay, the Caspase-Glo[®] 8 Reagent was prepared according to the manufacturer's instructions. Then, 100 μ l of Caspase-Glo[®] 8 Reagent was added to each well and gently mixed contents of the wells using a plate shaker at 300 rpm for 1 min. The plate was then incubated at room temperature for 1 h. After that, the luminescence of each sample was measured using a luminometer (SpectraMax M5, Molecular Devices), and caspase-8 activity (fold increase) was calculated.

Statistical analysis

Quantitative data from at least 3 independent experiments were presented as mean \pm SD (standard deviation). Statistical significance of data was analysed applying Student's T test. P values of ≤ 0.05 , 0.01, 0.001 were considered as significant (*, **, ***).

Results and discussion

UPS-dependent degradation of nuclear RelA in *H. pylori* infection

The recently discovered *H. pylori* effector molecule ADP heptose induces classical NF- κ B involving phosphorylation and subsequent proteasomal degradation of I κ B α [4]. This leads to phosphorylation of RelA in the cytosol and its nuclear translocation within 1 h after *H. pylori* infection (Fig. 1a). Nuclear RelA induces mRNA expression

of *NFKBIA* (Fig. 1b), and the de novo synthesised I κ B α re-accumulated in the cytoplasm within 2 h (Fig. 1a). In addition, NF- κ B transactivation activity was increased in cells infected with *H. pylori*, but to a lesser extent than in cells treated with IL-1 β (Fig. 1c). For stabilisation of the de novo synthesised I κ B α , it interacts with the CSN [26], which transmits the CSN-associated DUB USP15 [11] to the CRL-substrate I κ B α to prevent it from degradation [14]. In addition, we investigated the effects of *H. pylori* infection on the turnover of nuclear RelA. We observed that the abundance of nuclear RelA in the soluble nuclear fraction (N1) and the fraction with subnuclear structures

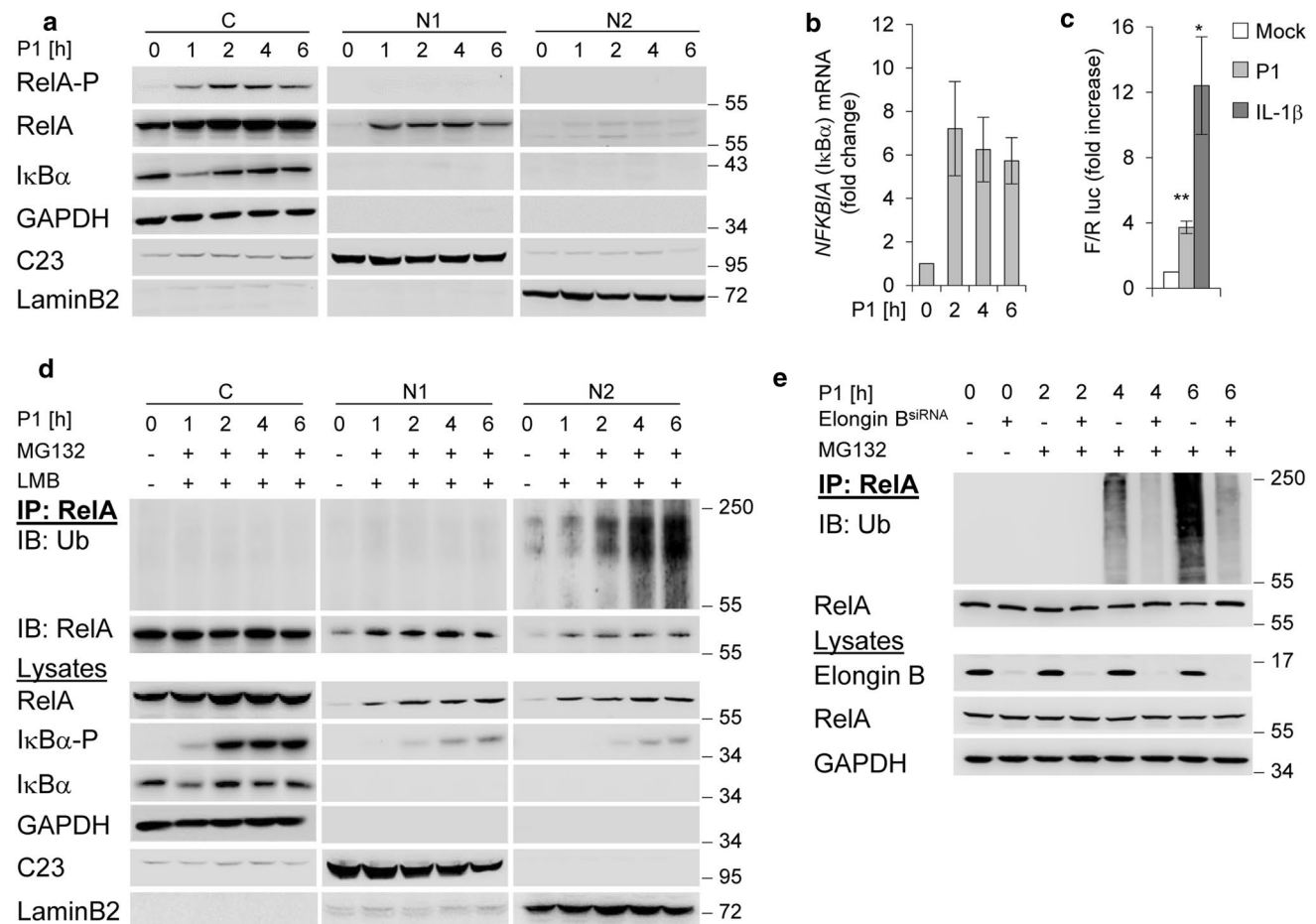


Fig. 1 NF- κ B/RelA turnover in *H. pylori* infection. **a** AGS cells were infected with *H. pylori* for the indicated times. Subcellular fractions were subjected to IB for analysis of the indicated proteins. **b** Total RNA was isolated from *H. pylori*-infected AGS cells and analysed using quantitative RT-PCR for the *NFKBIA* (the gene of I κ B α) transcript. Data shown depict the average of triplicate determinations normalized to *GAPDH* housekeeping gene. Error bars denote mean \pm SD. **c** AGS cells were transfected with luciferase reporters, treated with *H. pylori* or IL-1 β (10 ng/ml) and fold increase of NF- κ B transactivation activity (Firefly/Renilla luc) analysed after 3.5 h in a transactivation assay. **d** RelA-IP from subcellular fractions of *H. pylori*-infected AGS cells treated with MG132 and LMB 30 min after infection. The RelA-

IP was performed at the indicated times in the presence of NEM and OPT, followed by IB analysis of the indicated proteins. **e** AGS cells were transfected with siRNA against Elongin B and infected with *H. pylori* for the indicated times (MG132 was added 30 min after infection). IP with an anti-RelA or isotype-matched antibody (IgG) was performed at the indicated times in the presence of NEM and OPT, followed by IB analysis of the indicated proteins. Data information: Data shown in (a, d, e) are representative for at least two independent experiments. Data shown in (b, c) are from one experiment with three technical replicates. GAPDH, C23 and LaminB2 served as load controls and indicate the purity of the subcellular fractions

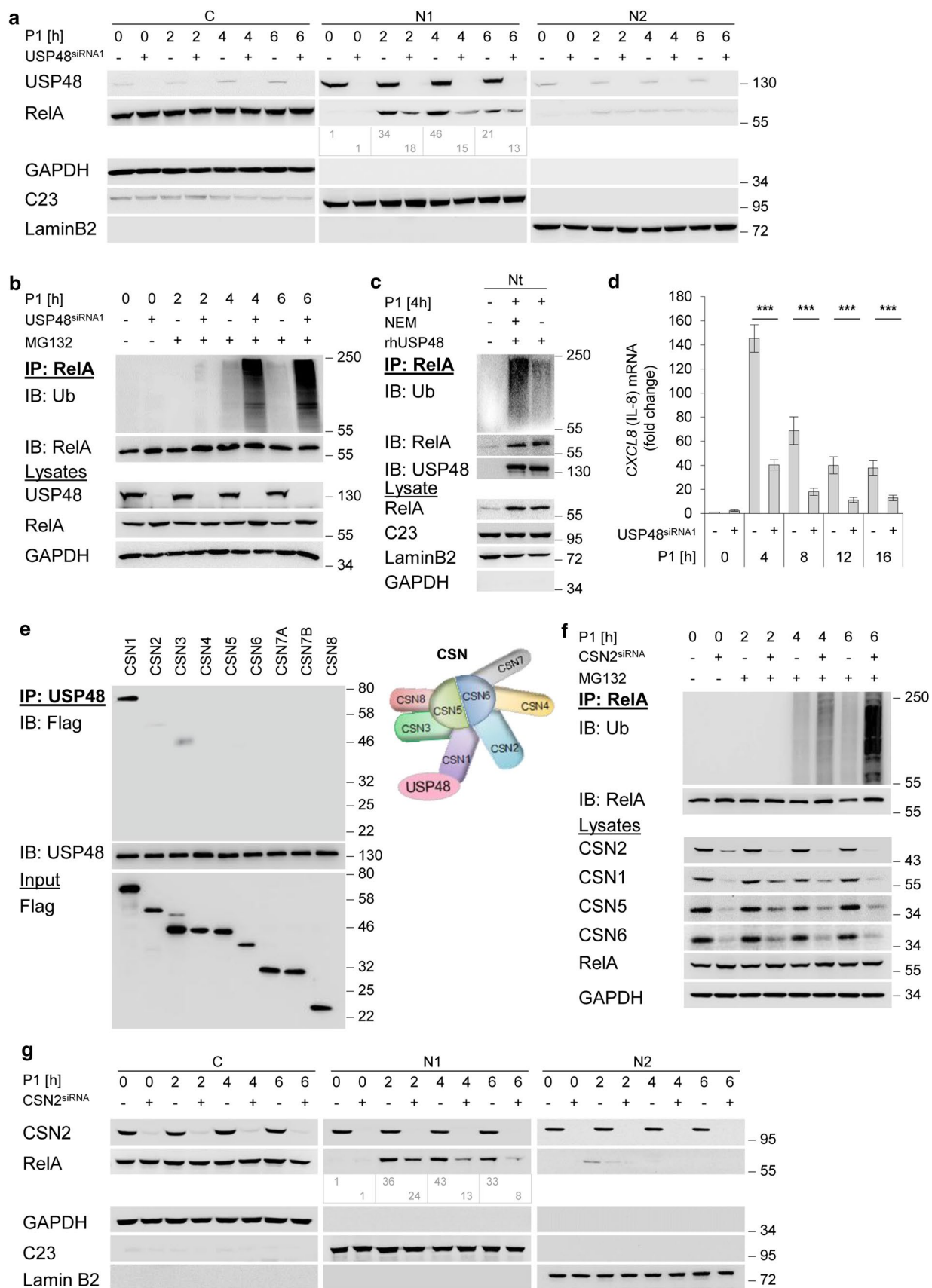


Fig. 2 CSN-associated USP48 deubiquitinylates nuclear RelA. **a** AGS cells were transfected with siRNA against USP48 and infected with *H. pylori* for indicated times. Subcellular fractions were subjected to IB analysis of the indicated proteins. **b** AGS cells were transfected with siRNA against USP48 and infected with *H. pylori* for the indicated times (MG132 was added 30 min after infection). IP with an anti-RelA antibody or isotype-matched antibody (IgG) was performed at the indicated times in the presence of NEM and OPT, followed by IB analysis of the indicated proteins. **c** RelA-IP from the total nuclear fraction of *H. pylori*-infected AGS cells was incubated with recombinant human USP48 in the presence or absence of NEM, followed by IB analysis of the indicated proteins. **d** AGS cells were transfected with siRNA against USP48 and infected with *H. pylori* for the indicated times. Total RNA was isolated at the indicated times and analysed using quantitative RT-PCR for the *CXCL8* transcript (the gene of IL-8). Data shown depict the average of triplicate determinations normalized to *GAPDH* housekeeping gene. Error bars denote mean \pm SD. **e** Equimolar amounts of in-vitro translated Flag-CSN subunits and 0.5 μ g of recombinant human USP48 were incubated at 37 °C for 1 h. IP with an anti-USP48 antibody was performed, followed by IB analysis with anti-Flag and anti-USP48 antibodies. **f** AGS cells were transfected with siRNA against CSN2 and infected with *H. pylori* for the indicated times (MG132 was added 30 min after infection). IP with an anti-RelA antibody was performed at the indicated times in the presence of NEM and OPT, followed by IB analysis of the indicated proteins. **g** AGS cells were transfected with siRNA against CSN2 and infected with *H. pylori* for indicated times. Subcellular fractions were subjected to IB analysis of the indicated proteins. Data information: Data shown in (a–c, e–g) are representative for at least two independent experiments. Data shown in (d) are from three independent experiments with three technical replicates. *** $P \leq 0.001$ (Student's *t*-test). The band intensities shown in (a, g) were quantified using ImageJ software (NIH). GAPDH, C23 and LaminB2 served as load controls and indicate the purity of the subcellular fractions

(N2) [10] decreases within 6 h of infection (Fig. 1a). Ubiquitylation and proteasomal degradation of RelA regulate its stability and abundance and actively promote transcription termination [7]. We determined *H. pylori*-induced ubiquitylation of RelA in subcellular fractions in the presence of MG132 and Leptomycin B (LMB) to prevent proteasomal degradation and nuclear export. Treatment of the cells with MG132 30 min after infection allowed phosphorylation and degradation of $\text{I}\kappa\text{B}\alpha$, and subsequently RelA translocation to the nucleus (Fig. 1d). Immunoprecipitation (IP) of RelA under denaturing conditions showed an enrichment of ubiquitylated RelA (RelA-Ub) in the subnuclear fraction (N2) with increasing time (Fig. 1d). Ubiquitylation of RelA is regulated by a multimeric ubiquitin-RING-ligase ECS^{SOCS1} containing cullin-2, the adaptor proteins elongin B and C, and substrate recognition molecule SOCS1 after TNF stimulation [9]. We therefore performed a transient knockdown of elongin B to investigate the effects of ECS^{SOCS1} on RelA ubiquitylation induced by *H. pylori*. The result was that RelA ubiquitylation induced by *H. pylori* infection was abolished in elongin B depleted cells (Fig. 1e), suggesting that ECS^{SOCS1} is the predominant E3 ligase for RelA

degradation in *H. pylori* infection. So far, our data suggest that nuclear RelA induced by *H. pylori* is promptly regulated by ubiquitylation and degradation through the proteasome.

USP48 deubiquitinylates and counteracts UPS-dependent degradation of nuclear RelA in *H. pylori* infected cells

We reported that the catalytic USP domain of USP48 interacts physically with the N-terminal region of the Rel homology domain (RHD) of RelA [27]. To analyse the impact of USP48 on nuclear RelA turnover in *H. pylori* infected cells, we performed a transient knockdown of USP48 in AGS and NCI-N87 cells. Our data show that the level of nuclear RelA decreased in USP48-depleted cells (Fig. 2a and Fig. S1), indicating a protective role of USP48 for nuclear RelA turnover in *H. pylori* infection. To detect ubiquitylated nuclear RelA during *H. pylori* infection, we treated cells with the proteasome inhibitor MG132 30 min after infection. We observed enhanced accumulation of RelA-Ub within 4 h of *H. pylori* infection in USP48-depleted cells in a RelA-IP under denaturing conditions (Fig. 2b). In addition, we transiently transfected USP48 protein before *H. pylori* infection and observed removal of ubiquitin from RelA immunoprecipitated from cell lysates (Fig. S2). To determine whether USP48 directly deubiquitinylates nuclear RelA, we performed an in vitro DUB assay in which we incubated ubiquitylated RelA immunoprecipitated from the nuclear fraction of cells infected with *H. pylori* together with recombinant USP48. We found that USP48 cleaved poly-Ub-chains bound to RelA. The presence of the DUB inhibitor N-ethylmaleimide (NEM) abolished the deubiquitylation of RelA (Fig. 2c), suggesting that USP48 deubiquitinylates nuclear RelA. Furthermore, we observed lower expression of the NF- κ B target gene *CXCL8* in *H. pylori* infection in USP48-depleted cells (Fig. 2d), consistent with increased degradation and lower nuclear accumulation of RelA (Fig. 2a). Accordingly, our data suggest that USP48 stabilises and prolongs the transcriptional activity of NF- κ B/RelA. Several reports have suggested a role of USP48 in protein stability in diverse cellular processes, e.g. glioma-associated oncogene 1 (Gli1) in glioblastoma [28], TRAF2 in epithelial barrier dysfunction [29] and antagonising Breast Cancer 1 (BRCA1) E3 ligase on histone H2A and genome stability [30]. Notably, USP48 could also promote the stability of oncoprotein mouse double minute 2 (Mdm2) in a deubiquitylation-independent manner [31]. Recently, USP48 was reported to stabilise SIRT6 by K48-linked deubiquitylation, which impedes metabolic reprogramming in hepatocellular carcinoma (HCC) [32], and control cell cycle progression by stabilising the Aurora B protein [33].

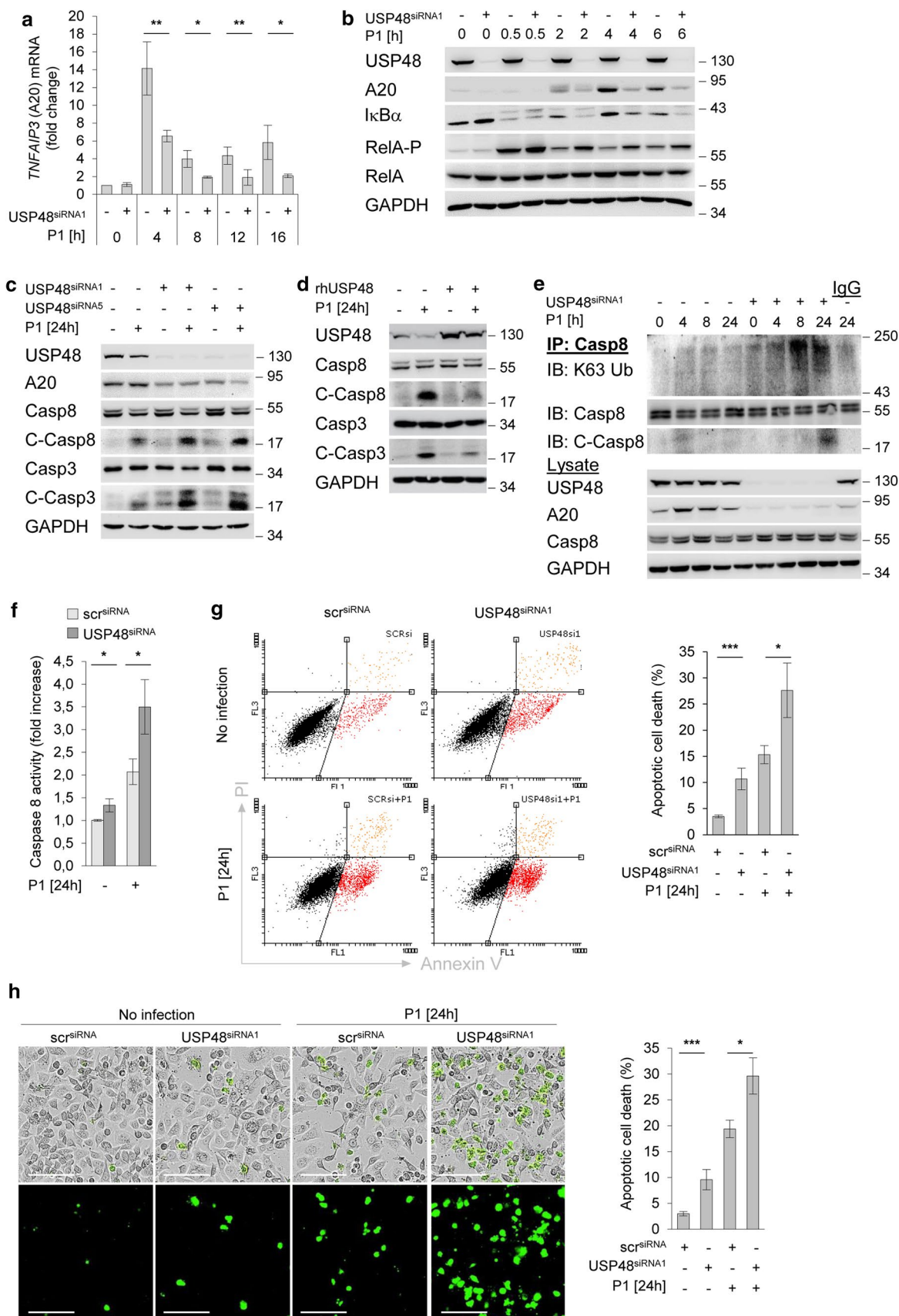


Fig. 3 USP48 controls A20 de novo synthesis and suppresses caspase cleavages. **a** AGS cells were transfected with siRNA against USP48 and infected with *H. pylori* for the indicated times. Total RNA was isolated at the indicated times and analysed using quantitative RT-PCR for the *TNFAIP3* transcript (gene of A20). Data shown depict the average of triplicate determinations normalized to *GAPDH* house-keeping gene. Error bars denote mean \pm SD. **b, c** AGS cells were transfected with siRNA against USP48 and infected with *H. pylori* for indicated times. Whole-cell lysates were subjected to IB for analysis of the indicated proteins. C-Casp8 or C-Casp3 = cleaved caspases. **d** AGS cells were transfected with recombinant human USP48 and infected with *H. pylori* for 24 h. Whole-cell lysates were subjected to IB analysis of the indicated proteins. **e** AGS cells were transfected with siRNA against USP48 and infected with *H. pylori* for the indicated times. IP with an anti-Caspase-8 antibody was performed at the indicated times in the presence of NEM and OPT, followed by IB analysis of the indicated proteins. **f** AGS cells transfected with siRNA were infected with *H. pylori* for 24 h before incubation with Caspase-Glo[®] 8 reagent for 1 h. Luminescence of caspase-8 activity was measured and calculated as a fold increase compared to the uninfected scramble control. **g** AGS cells were transfected with siRNA against USP48 and infected with *H. pylori* for 24 h, followed by staining with annexin V/PI. Apoptotic cell death was analysed by flow cytometry. Data shown depict the average of two independent experiments. Error bars denote mean \pm SD. **h** AGS cells were transfected with siRNA against USP48 and infected with *H. pylori* for 24 h. Cleaved caspase-3/7 expression was detected by the IncuCyte[®] S3 Live-Cell Analysis Image system. Scale bars = 100 μ m. Data shown depict the average of four pictures from distinct regions. Error bars denote mean \pm SD. Data information: Data shown in (a) are from three independent experiments with three technical replicates. Data shown in (b–e, g) are representative for at least two independent experiments. Data shown in (f) are from one experiment with three technical replicates. Data shown in (h) are from one experiment with four technical replicates. * $P \leq 0.05$, ** $P \leq 0.01$, *** $P \leq 0.001$ (Student's *t*-test)

Stabilisation of nuclear RelA in *H. pylori* infection is CSN-dependent

USP48 has been reported to interact with the CSN [15], which function as a signalling platform and integrates the activity of several proteins [11]. To identify the direct physical interaction partner within the CSN complex, we translated each CSN subunit in vitro and performed an IP with recombinant USP48. In this way, we identified CSN1 as the CSN subunit that interacts with USP48 (Fig. 2e). Interestingly, we previously observed that CSN1 also interacts with I κ B α [26]. The only other subunit interacting with I κ B α is CSN3, which showed also a weak interaction with USP48 suggesting that the juxtaposed CSN1 and CSN3 cooperate in recruiting USP48 [26]. Further, it was reported that CSN1 interacts with a number of other molecules, such as deneddylase 1 (DEN1), a cysteine protease in the Ubl-like protease (ULP) family possessing deneddylase activity. CSN1-DEN1 interaction initiates DEN1 degradation, thereby balancing cellular deneddylase activity [34]. In addition, it was reported that CSN1 interacts with inositol 1,3,4-trisphosphate 5/6-kinase [35], Ankyrin repeat and SOCS box containing protein 4 [6], SAP130/SF3b-3 [36],

and Tonsoku-associating protein 1 [37]. To determine the role of the CSN in nuclear RelA turnover, we performed a transient knockdown of the CSN2 subunit, which impairs the integrity of the CSN [38]. Downregulation of single CSN subunits by siRNA caused a significant and coordinated reduction of other CSN subunits suggesting a coordinated expression of the subunits tightly linked to the CSN complex assembly. As a common post-transcriptional regulator for CSN subunits, miRNAs of the let-7 family have been identified because a reduction or block of let-7 miRNAs induces the coordinated expression of CSN subunits [39]. Corresponding to USP48-depleted cells, we observed an increased accumulation of RelA-Ub (Fig. 2f) and a decrease of nuclear RelA in the CSN2 depleted cells (Fig. 2g).

USP48 controls A20 de novo synthesis and suppresses caspase cleavages

We previously reported NF- κ B-dependent upregulation of A20 in *H. pylori* infection [21]. As expected we found in *H. pylori* infection that induction of NF- κ B-dependent A20 de novo synthesis was suppressed in USP48-depleted cells, in both mRNA (Fig. 3a) and protein levels (Fig. 3b and Fig. S3a). In addition, we show that *H. pylori* strain (P12) similarly regulates USP48-dependent control of A20 in AGS cells (Fig. S3b). Notably, we reported that A20 inhibits apoptotic cell death by deubiquitinating caspase-8, interfering with the caspase-8 activation [21]. The K63-linked polyubiquitinylation of caspase-8 mediates its processing into a fully activated cleaved form that subsequently mediates cleavage of the critical exogenous apoptotic substrates, including caspase-3 and -7 [40]. To investigate the relationship between caspase cleavage and apoptotic cell death in *H. pylori*-infected cells, we analysed cells in which caspase-8 was knocked down and showed suppression of caspase-3 cleavage (Fig. S4a) and apoptotic cell death (Fig. S4b). Similar results were observed when *H. pylori*-infected cells were treated with the caspase-8 specific inhibitor Z-IETD-FMK [21]. We investigated the effects of USP48 on the activation of apoptotic caspases in *H. pylori* infection. An increase in activated cleaved caspase-8 and -3 was observed in USP48-depleted cells (Fig. 3c). Conversely, transient transfection of USP48 protein before *H. pylori* infection suppressed cleavage of caspases (Fig. 3d). Therefore, we hypothesised that USP48 counteracts the ubiquitinylation of caspase-8 in an A20-dependent manner. IP of caspase-8 under denaturing conditions showed an increase in K63-linked polyubiquitinylation of caspase-8 in USP48-depleted cells, corresponding to an accumulation of cleaved caspase-8 (Fig. 3e). Moreover, we performed Caspase-Glo8 Assay and observed that caspase-8 activity was increased in USP48 knockdown cells (Fig. 3f). These data suggest that USP48 can promote deubiquitinylation of caspase-8 and impair caspase-8

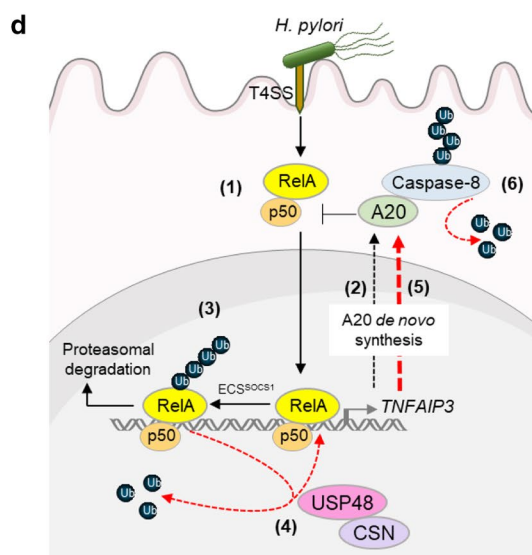
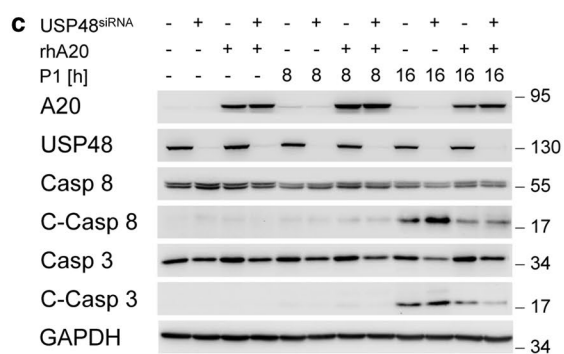
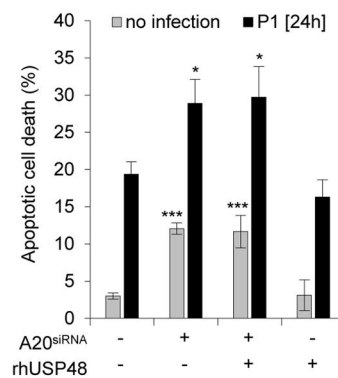
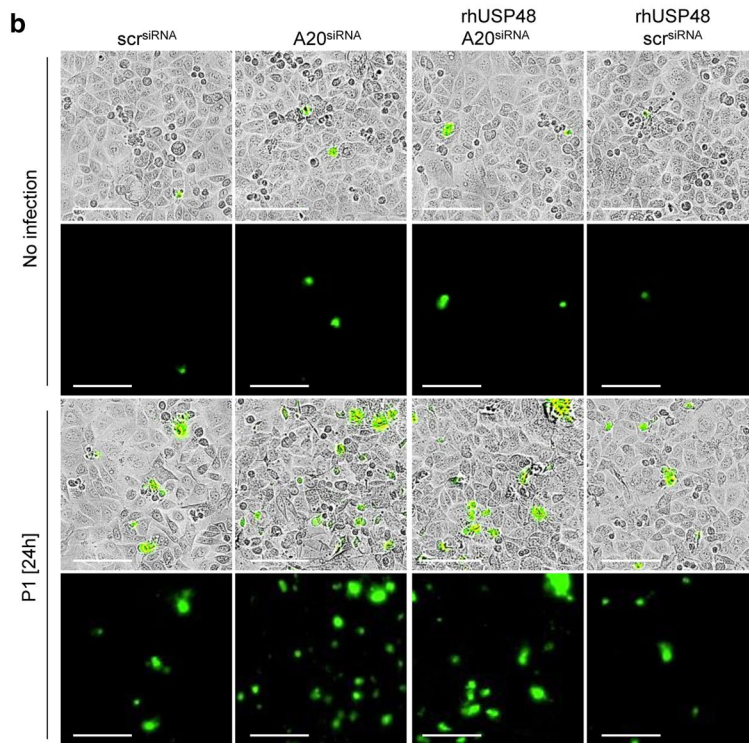
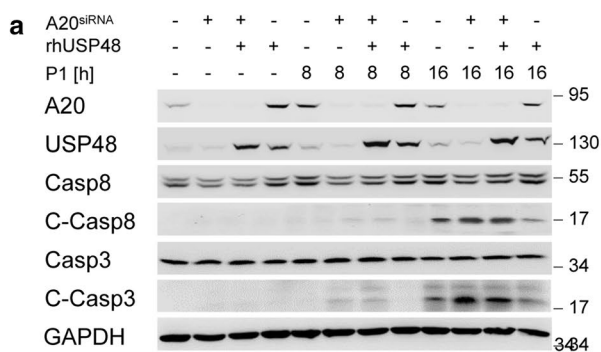


Fig. 4 USP48-suppressed caspase cleavage is A20-dependent. **a** AGS cells were transfected with siRNA against A20, and subsequently transfected with recombinant human USP48. One hour after transfection, the cells were infected with *H. pylori* for indicated times. Whole-cell lysates were subjected to IB for analysis of the indicated proteins. **b** AGS cells were transfected with siRNA against A20, and subsequently transfected with recombinant human USP48. One hour after transfection, the cells were infected with *H. pylori* for 24 h. Cleaved caspase-3/7 expression was detected by the IncuCyte® S3 Live-Cell Analysis Image system. Scale bars = 100 µm. Data shown depict the average of four pictures from distinct regions. Error bars denote mean ± SD. **c** AGS cells were transfected with siRNA against USP48 and then transfected with recombinant human A20 protein. One hour after protein transfection, cells were infected with *H. pylori* for the indicated times. Total cell lysates were subjected to IB analysis of the indicated proteins. **d** Schematic representation of the findings in this study. Infection of *H. pylori* induces fast activation of NF-κB, leading to nuclear translocation of RelA (1) and expression of the target gene *TNFAIP3* (encodes for A20) (2). Termination of RelA activity by ECS^{soes1}-dependent ubiquitinylation and degradation (3). CSN-associated USP48 deubiquitinylates RelA-Ub resulting in RelA stabilisation (4) and prolonged A20 de novo synthesis (5). USP48 and A20 synergistically suppresses caspase-8 activity and apoptotic cell death (6). Data information: Data shown in (a, c) are representative for at least two independent experiments. Data shown in (b) are from one experiments with four technical replicates. * $P \leq 0.05$, *** $P \leq 0.001$ (Student's *t*-test)

activity. We also investigated the effects of USP48 on *H. pylori* induced apoptotic cell death in gastric epithelial cells. Analysis of annexin V/PI stained cells showed increased apoptotic cell death after deletion of USP48 (Fig. 3g and Fig. S5). Accordingly, *H. pylori* infection induces apoptotic cell death in various cell lines via a pathway that involves sequential induction of caspase activity. In addition, we studied *H. pylori* associated apoptotic cell death by detection of caspase-3/7-stained cells using IncuCyte® Live-Cell Imaging analysis and showed more apoptotic cell death in USP48-depleted cells (Fig. 3h).

USP48-suppressed apoptotic cell death is A20-dependent

The effects of USP48 on A20 expression and caspase-8 cleavage and apoptotic cell death in cells infected with *H. pylori* strongly suggest that the effect is dependent on A20. To test this hypothesis, we transiently transfected recombinant USP48 protein into A20 knockdown cells and found that USP48 rescued *H. pylori*-induced caspase cleavages in parental cells but not in A20-depleted cells (Fig. 4a). A similar result was obtained when we analysed apoptotic cells stained for caspase-3/7 by IncuCyte® Live-Cell Imaging (Fig. 4b). Furthermore, transfection of A20 protein in USP48-depleted cells before *H. pylori* infection suppressed caspase cleavage and apoptotic cell death (Fig. 4c), indicating that the protective effect on apoptotic cell death is dependent on the expression of A20. On the other hand, *H. pylori* infection induces reactive oxygen species (ROS)

leading to apoptotic cell death, independent of the T4SS [17]. Gamma-glutamyl transpeptidase (GGT) is an effector that contributes to the production of H₂O₂ by glutathione (GSH) hydrolysis [41]. Future studies focussed on elucidating the *H. pylori*-associated pathogenesis of gastric disease will uncover the importance of apoptotic cell death for the mucosal microenvironment to better understand how this might contribute to gastric diseases.

Our study has shown that CSN-associated USP48 stabilises nuclear RelA through deubiquitinylation, thereby promoting the transcriptional activity of RelA to prolong A20 de novo synthesis. Furthermore, USP48 promotes cell survival during *H. pylori* infection through A20-dependent suppression of caspases activity and apoptotic cell death. We highlight the interplay of USP48 and A20 in regulating NF-κB and cell death in the gastric epithelium. This may contribute to the control of immune responses and gastric cancer development and represent an attractive target for future therapeutic intervention strategies.

Supplementary Information The online version contains supplementary material available at <https://doi.org/10.1007/s00018-022-04489-7>.

Author contributions MN conceived the study; MN, PJ designed experiments; PJ, SC, OS performed experiments; MN, PJ analysed and interpreted data; MN, PJ wrote the manuscript.

Funding Open Access funding enabled and organized by Projekt DEAL. The work was supported by Grants of the German Research Foundation (RTG 2408-361210922) and (CRC 854-97850925 (A04)) to M.N., and by a stipend from the Medical Faculty of the Otto von Guericke University to S.C.

Data availability No data were deposited in a public database. Inquiries for reagents used in this study should be addressed to M. Naumann (naumann@med.ovgu.de).

Declarations

Conflict of interest All authors declare that they have no conflict of interest.

Ethics approval and consent to participate Not applicable.

Consent for publication All the authors have approved and agreed to publish this manuscript.

Open Access This article is licensed under a Creative Commons Attribution 4.0 International License, which permits use, sharing, adaptation, distribution and reproduction in any medium or format, as long as you give appropriate credit to the original author(s) and the source, provide a link to the Creative Commons licence, and indicate if changes were made. The images or other third party material in this article are included in the article's Creative Commons licence, unless indicated otherwise in a credit line to the material. If material is not included in the article's Creative Commons licence and your intended use is not permitted by statutory regulation or exceeds the permitted use, you will need to obtain permission directly from the copyright holder. To view a copy of this licence, visit <http://creativecommons.org/licenses/by/4.0/>.

References

- Zamani M, Ebrahimitabar F, Zamani V, Miller WH, Alizadeh-Navaei R, Shokri-Shirvani J, Derakhshan MH (2018) Systematic review with meta-analysis: the worldwide prevalence of *Helicobacter pylori* infection. *Aliment Pharmacol Ther* 47(7):868–876. <https://doi.org/10.1111/apt.14561>
- Ahn HJ, Lee DS (2015) *Helicobacter pylori* in gastric carcinogenesis. *World J Gastrointest Oncol* 7(12):455–465. <https://doi.org/10.4251/wjgo.v7.i12.455>
- Pfannkuch L, Hurwitz R, Traulsen J, Sigulla J, Poeschke M, Matzner L, Kosma P, Schmid M, Meyer TF (2019) ADP heptose, a novel pathogen-associated molecular pattern identified in *Helicobacter pylori*. *FASEB J* 33(8):9087–9099. <https://doi.org/10.1096/fj.201802555R>
- Maubach G, Lim MCC, Sokolova O, Backert S, Meyer TF, Naumann M (2021) TIFA has dual functions in *Helicobacter pylori*-induced classical and alternative NF- κ B pathways. *EMBO Rep* 22(9):e52878. <https://doi.org/10.15252/embr.202152878>
- Schweitzer K, Sokolova O, Bozko PM, Naumann M (2010) *Helicobacter pylori* induces NF- κ B independent of CagA. *EMBO Rep* 11(1):10–11. <https://doi.org/10.1038/embor.2009.263> (author reply 11–12)
- Li JY, Chai BX, Zhang W, Liu YQ, Ammori JB, Mulholland MW (2007) Ankyrin repeat and SOCS box containing protein 4 (Asb-4) interacts with GPS1 (CSN1) and inhibits c-Jun NH2-terminal kinase activity. *Cell Signal* 19(6):1185–1192. <https://doi.org/10.1016/j.cellsig.2006.12.010>
- Saccani S, Marazzi I, Beg AA, Natoli G (2004) Degradation of promoter-bound p65/RelA is essential for the prompt termination of the nuclear factor κ B response. *J Exp Med* 200(1):107–113. <https://doi.org/10.1084/jem.20040196>
- Senft D, Qi J, Ronai ZA (2018) Ubiquitin ligases in oncogenic transformation and cancer therapy. *Nat Rev Cancer* 18(2):69–88. <https://doi.org/10.1038/nrc.2017.105>
- Maine GN, Mao X, Komarck CM, Burstein E (2007) COMMD1 promotes the ubiquitination of NF- κ B subunits through a cullin-containing ubiquitin ligase. *EMBO J* 26(2):436–447. <https://doi.org/10.1038/sj.emboj.7601489>
- Tanaka T, Grusby MJ, Kaisho T (2007) PDLIM2-mediated termination of transcription factor NF- κ B activation by intranuclear sequestration and degradation of the p65 subunit. *Nat Immunol* 8(6):584–591. <https://doi.org/10.1038/ni1464>
- Dubiel W, Chaithongyot S, Dubiel D, Naumann M (2020) The COP9 signalosome: a multi-DUB complex. *Biomolecules* 10(7):1082. <https://doi.org/10.3390/biom10071082>
- Lingaraju GM, Bunker RD, Cavadini S, Hess D, Hassiepen U, Renatus M, Fischer ES, Thoma NH (2014) Crystal structure of the human COP9 signalosome. *Nature* 512(7513):161–165. <https://doi.org/10.1038/nature13566>
- Echalier A, Pan Y, Birol M, Tavernier N, Pintard L, Hoh F, Ebel C, Galophe N, Claret FX, Dumas C (2013) Insights into the regulation of the human COP9 signalosome catalytic subunit, CSN5/Jab1. *Proc Natl Acad Sci USA* 110(4):1273–1278. <https://doi.org/10.1073/pnas.1209345110>
- Schweitzer K, Bozko PM, Dubiel W, Naumann M (2007) CSN controls NF- κ B by deubiquitylation of IkappaBalpha. *EMBO J* 26(6):1532–1541. <https://doi.org/10.1038/sj.emboj.7601600>
- Schweitzer K, Naumann M (2015) CSN-associated USP48 confers stability to nuclear NF- κ B/RelA by trimming K48-linked Ub-chains. *Biochim Biophys Acta* 1853(2):453–469. <https://doi.org/10.1016/j.bbamer.2014.11.028>
- Huang X, Dubiel D, Dubiel W (2021) The COP9 signalosome variant CSNCSN7A stabilizes the deubiquitylating enzyme CYLD impeding hepatic steatosis. *Livers* 1(3):116–131
- Chaithongyot S, Naumann M (2022) *Helicobacter pylori*-induced reactive oxygen species direct turnover of CSN-associated STAMBPL1 and augment apoptotic cell death. *Cell Mol Life Sci* 79(2):86. <https://doi.org/10.1007/s00018-022-04135-2>
- Pföh R, Lacadao IK, Saridakis V (2015) Deubiquitinases and the new therapeutic opportunities offered to cancer. *Endocr Relat Cancer* 22(1):T35–54. <https://doi.org/10.1530/ERC-14-0516>
- Chen J, Chen ZJ (2013) Regulation of NF- κ B by ubiquitination. *Curr Opin Immunol* 25(1):4–12. <https://doi.org/10.1016/j.coi.2012.12.005>
- Tokunaga F, Nishimasu H, Ishitani R, Goto E, Noguchi T, Mio K, Kamei K, Ma A, Iwai K, Nureki O (2012) Specific recognition of linear polyubiquitin by A20 zinc finger 7 is involved in NF- κ B regulation. *EMBO J* 31(19):3856–3870. <https://doi.org/10.1038/emboj.2012.241>
- Lim MCC, Maubach G, Sokolova O, Feige MH, Diezko R, Buchbinder J, Backert S, Schluter D, Lavrik IN, Naumann M (2017) Pathogen-induced ubiquitin-editing enzyme A20 bifunctionally shuts off NF- κ B and caspase-8-dependent apoptotic cell death. *Cell Death Differ* 24(9):1621–1631. <https://doi.org/10.1038/cdd.2017.89>
- Lim MCC, Maubach G, Naumann M (2018) NF- κ B-regulated ubiquitin-editing enzyme A20 paves the way for infection persistency. *Cell Cycle* 17(1):3–4. <https://doi.org/10.1080/15384101.2017.1387435>
- Lim MCC, Maubach G, Birkl-Toegelhofer AM, Haybaeck J, Vieth M, Naumann M (2022) A20 undermines alternative NF- κ B activity and expression of anti-apoptotic genes in *Helicobacter pylori* infection. *Cell Mol Life Sci* 79(2):102. <https://doi.org/10.1007/s00018-022-04139-y>
- Backert S, Ziska E, Brinkmann V, Zimny-Arndt U, Fauconnier A, Jungblut PR, Naumann M, Meyer TF (2000) Translocation of the *Helicobacter pylori* CagA protein in gastric epithelial cells by a type IV secretion apparatus. *Cell Microbiol* 2(2):155–164. <https://doi.org/10.1046/j.1462-5822.2000.00043.x>
- Studencka-Turski M, Maubach G, Feige MH, Naumann M (2018) Constitutive activation of nuclear factor κ B-inducing kinase counteracts apoptosis in cells with rearranged mixed lineage leukemia gene. *Leukemia* 32(11):2498–2501. <https://doi.org/10.1038/s41375-018-0128-7>
- Lee JH, Yi L, Li J, Schweitzer K, Borgmann M, Naumann M, Wu H (2013) Crystal structure and versatile functional roles of the COP9 signalosome subunit 1. *Proc Natl Acad Sci USA* 110(29):11845–11850. <https://doi.org/10.1073/pnas.1302418110>
- Ghanem A, Schweitzer K, Naumann M (2019) Catalytic domain of deubiquitylase USP48 directs interaction with Rel homology domain of nuclear factor κ B transcription factor RelA. *Mol Biol Rep* 46(1):1369–1375. <https://doi.org/10.1007/s11033-019-04587-z>
- Zhou A, Lin K, Zhang S, Ma L, Xue J, Morris SA, Aldape KD, Huang S (2017) Gli1-induced deubiquitinase USP48 aids glioblastoma tumorigenesis by stabilizing Gli1. *EMBO Rep* 18(8):1318–1330. <https://doi.org/10.15252/embr.201643124>
- Li S, Wang D, Zhao J, Weathington NM, Shang D, Zhao Y (2018) The deubiquitinating enzyme USP48 stabilizes TRAF2 and reduces E-cadherin-mediated adherens junctions. *FASEB J* 32(1):230–242. <https://doi.org/10.1096/fj.201700415RR>
- Uckelmann M, Densham RM, Baas R, Winterwerp HHK, Fish A, Sixma TK, Morris JR (2018) USP48 restrains resection by site-specific cleavage of the BRCA1 ubiquitin mark from H2A. *Nat Commun* 9(1):229. <https://doi.org/10.1038/s41467-017-02653-3>
- Cetkowska K, Sustova H, Uldrijan S (2017) Ubiquitin-specific peptidase 48 regulates Mdm2 protein levels independent of its deubiquitinase activity. *Sci Rep* 7:43180. <https://doi.org/10.1038/srep43180>

32. Du L, Li Y, Kang M, Feng M, Ren Y, Dai H, Wang Y, Wang Y, Tang B (2021) USP48 is upregulated by Mettl14 to attenuate hepatocellular carcinoma via regulating SIRT6 stabilization. *Cancer Res* 81(14):3822–3834. <https://doi.org/10.1158/0008-5472.CAN-20-4163>
33. Antao AM, Kaushal K, Das S, Singh V, Suresh B, Kim KS, Ramakrishna S (2021) USP48 governs cell cycle progression by regulating the protein level of aurora B. *Int J Mol Sci* 22(16):8508. <https://doi.org/10.3390/ijms22168508>
34. Christmann M, Schmalzer T, Gordon C, Huang X, Bayram O, Schinke J, Stumpf S, Dubiel W, Braus GH (2013) Control of multicellular development by the physically interacting deneddylases DEN1/DenA and COP9 signalosome. *PLoS Genet* 9(2):e1003275. <https://doi.org/10.1371/journal.pgen.1003275>
35. Sun Y, Wilson MP, Majerus PW (2002) Inositol 1,3,4-trisphosphate 5/6-kinase associates with the COP9 signalosome by binding to CSN1. *J Biol Chem* 277(48):45759–45764. <https://doi.org/10.1074/jbc.M208709200>
36. Menon S, Tsuge T, Dohmae N, Takio K, Wei N (2008) Association of SAP130/SF3b-3 with Cullin-RING ubiquitin ligase complexes and its regulation by the COP9 signalosome. *BMC Biochem* 9:1. <https://doi.org/10.1186/1471-2091-9-1>
37. Li W, Zang B, Liu C, Lu L, Wei N, Cao K, Deng XW, Wang X (2011) TSA1 interacts with CSN1/CSN and may be functionally involved in Arabidopsis seedling development in darkness. *J Genet Genomics* 38(11):539–546. <https://doi.org/10.1016/j.jgg.2011.08.007>
38. Naumann M, Bech-Otschir D, Huang X, Ferrell K, Dubiel W (1999) COP9 signalosome-directed c-Jun activation/stabilization is independent of JNK. *J Biol Chem* 274(50):35297–35300
39. Leppert U, Henke W, Huang X, Muller JM, Dubiel W (2011) Post-transcriptional fine-tuning of COP9 signalosome subunit biosynthesis is regulated by the c-Myc/Lin28B/let-7 pathway. *J Mol Biol* 409(5):710–721. <https://doi.org/10.1016/j.jmb.2011.04.041>
40. Jin Z, Li Y, Pitti R, Lawrence D, Pham VC, Lill JR, Ashkenazi A (2009) Cullin3-based polyubiquitination and p62-dependent aggregation of caspase-8 mediate extrinsic apoptosis signaling. *Cell* 137(4):721–735. <https://doi.org/10.1016/j.cell.2009.03.015>
41. Gong M, Ling SS, Lui SY, Yeoh KG, Ho B (2010) *Helicobacter pylori* gamma-glutamyl transpeptidase is a pathogenic factor in the development of peptic ulcer disease. *Gastroenterology* 139(2):564–573. <https://doi.org/10.1053/j.gastro.2010.03.050>

Publisher's Note Springer Nature remains neutral with regard to jurisdictional claims in published maps and institutional affiliations.

Supplementary material

USP48 and A20 synergistically promote cell survival in *Helicobacter pylori*-infection

Phatcharida Jantaree¹, Supattra Chaithongyot¹, Olga Sokolova¹, Michael Naumann^{1*}

¹Otto von Guericke University, Institute of Experimental Internal Medicine, Medical Faculty, Leipziger Str. 44, 39120 Magdeburg, Germany

Figure legends

Figure S1. USP48 stabilises nuclear RelA in *H. pylori* infection

a NCI-N87 cells were transfected with siRNA¹, or **b** siRNA⁵ against USP48 and infected with *H. pylori* for indicated times. Subcellular fractions were subjected to IB for analysis of the indicated proteins. Data information: Data shown are representative for at least two independent experiments. The band intensity was quantified using ImageJ software (NIH). GAPDH, C23 served as load controls and indicate for the purity of the subcellular fractions.

Figure S2. USP48 deubiquitinylates RelA

AGS cells were transfected with recombinant human USP48 (rhUSP48) and infected with *H. pylori* for the indicated times. MG132 was added 30 min after infection. IP with an anti-RelA antibody was performed at the indicated times in the presence of NEM and OPT, followed by IB analysis of the indicated proteins. Data information: Data shown are representative of at least two independent experiments.

Figure S3. USP48 prolongs A20 *de novo* synthesis

a NCI-N87 cells were transfected with siRNA against USP48 and infected with *H. pylori* for indicated times. **b** AGS cells were transfected with siRNA against USP48 and infected with *H. pylori* strain P12 for indicated times. Whole-cell lysates were subjected to IB for analysis of the indicated proteins. Data information: Data shown are representative for at least two independent experiments.

Figure S4. Caspase-8 cleavage contributes to *H. pylori* associated apoptotic cell death

a AGS cells were transfected with siRNA against caspase-8 and infected with *H. pylori* for indicated times. Whole-cell lysates were subjected to IB for analysis of the indicated proteins. **b** AGS cells were transfected with siRNA against caspase-8 and infected with *H. pylori* for 24 h. Cleaved caspase-3/7 expression was detected by the IncuCyte® S3 Live-Cell Analysis System. Scale bars = 100 μ m. Data shown depict the average of nine pictures from distinct regions. Error bars denote mean \pm SD. Data information: Data shown in (a) are representative for at least two independent experiments. Data shown in (b) are from two independent experiments. *P \leq 0.05 (Student's t-test).

Figure S5. USP48 suppresses apoptotic cell death

AGS cells were transfected with siRNA against USP48 (siRNA⁵) and infected with *H. pylori* for 24 h, followed by staining with annexin V/PI. Apoptotic cell death was analysed by flow cytometry. Data shown depict the average of two independent experiments. Error bars denote mean \pm SD. Data information: Data shown are representative for at least two independent experiments. *P \leq 0.05, **P \leq 0.01 (Student's t-test).

Figure S1

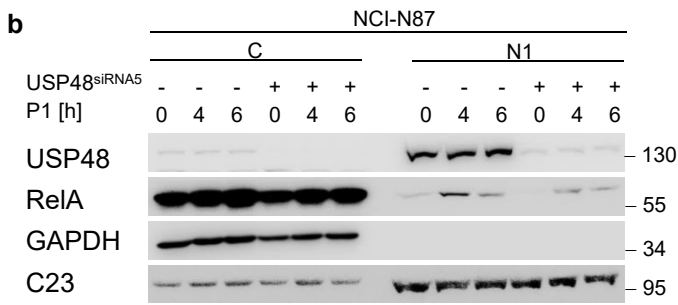
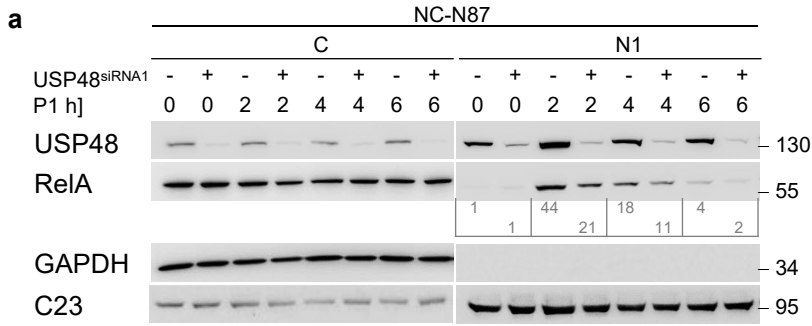


Figure S2

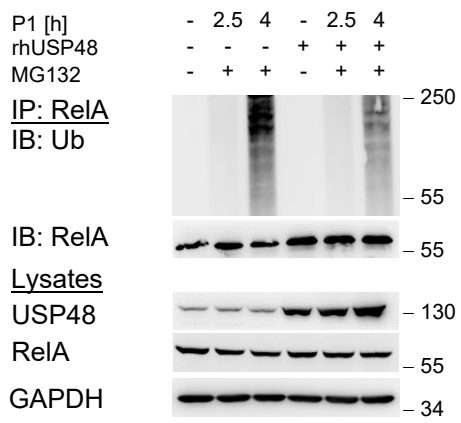


Figure S3

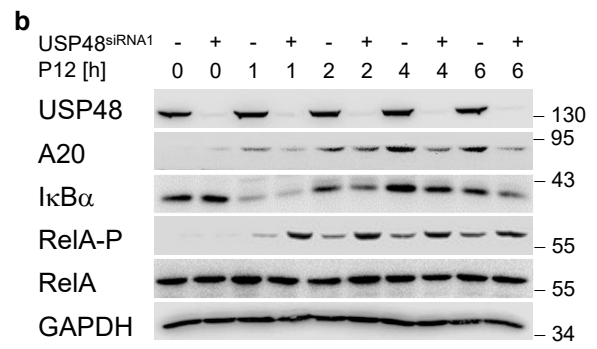
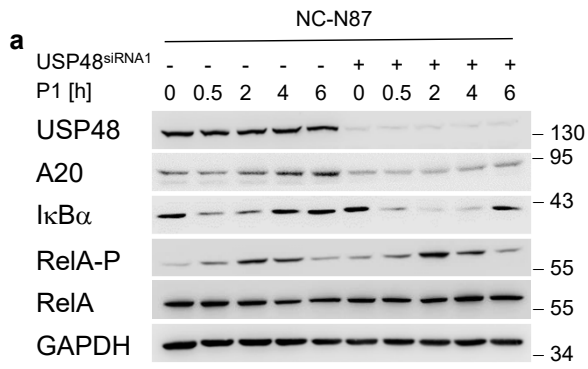


Figure S4

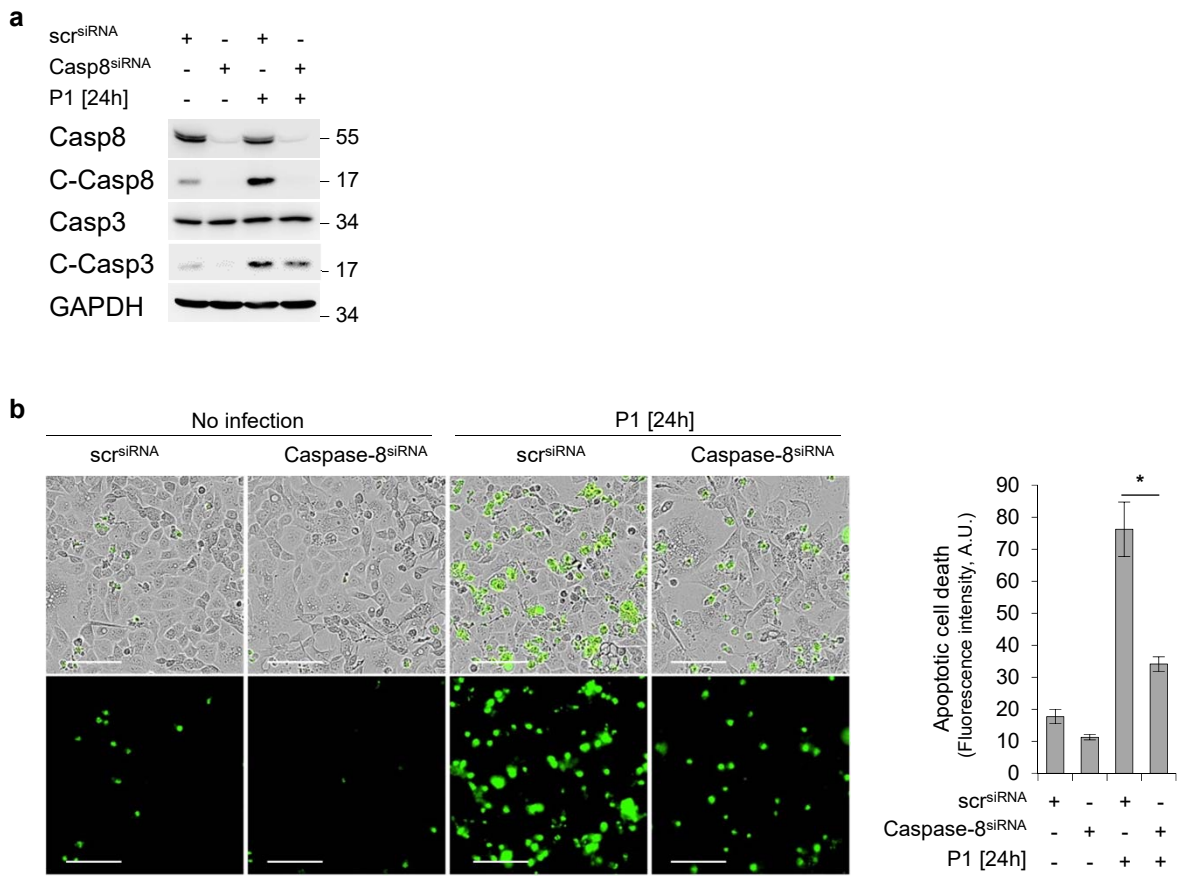
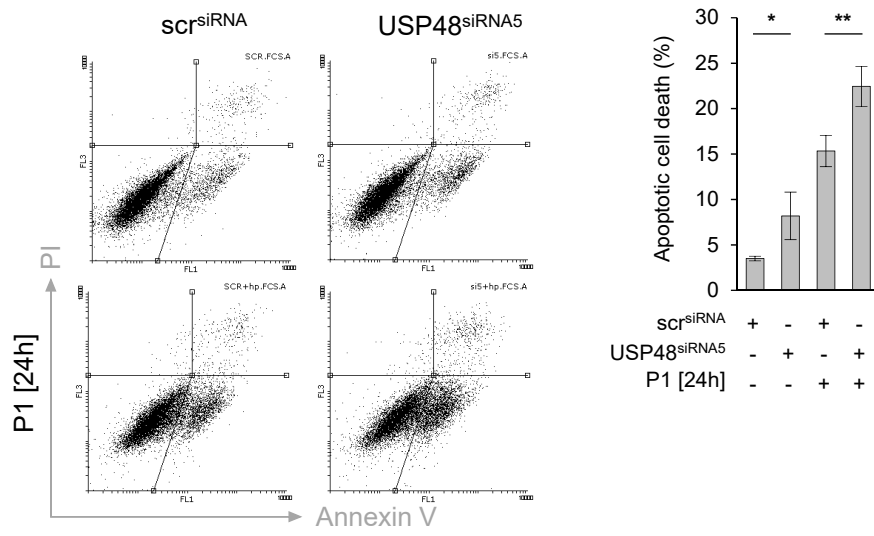


Figure S5



Chapter 4. Publication II

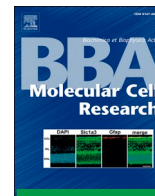
Human gastric fibroblasts ameliorate A20-dependent cell survival in co-cultured gastric epithelial cells infected by *Helicobacter pylori*

This study has been published in the journal *Biochimica et Biophysica Acta (BBA) - Molecular Cell Research* on 23th September 2022 and reprinted in this thesis with permission and is cited as follows:

Jantaree, P., Yu, Y., Chaithongyot, S., Täger, C., Sarabi, M. A., Meyer, T. F., Boccellato, F., Maubach, G., & Naumann, M. (2022). Human gastric fibroblasts ameliorate A20-dependent cell survival in co-cultured gastric epithelial cells infected by *Helicobacter pylori*. *Biochim Biophys Acta Mol Cell Res*, 1869(12), 119364. <https://doi.org/10.1016/j.bbamcr.2022.119364>

Contribution to the publication

Jantaree, P.	Investigation Methodology Writing-Original draft
Yu, Y.	Investigation
Chaithongyot, S.	Investigation
Täger, C.	Investigation
Sarabi, M. A.	Investigation
Mayer, T. F.	Methodology
Boccellato, F.	Methodology
Maubach, G.	Investigation Writing-Review & Editing
Naumann, M.	Conceptualization Methodology Writing & Editing Supervision Funding acquisition



Research paper

Human gastric fibroblasts ameliorate A20-dependent cell survival in co-cultured gastric epithelial cells infected by *Helicobacter pylori*

Phatcharida Jantaree^a, Yanfei Yu^a, Supattra Chaithongyot^a, Christian Täger^a,
Mohsen Abdi Sarabi^b, Thomas F. Meyer^c, Francesco Boccellato^d, Gunter Maubach^a,
Michael Naumann^{a,*}

^a Institute of Experimental Internal Medicine, Otto von Guericke University, 39120 Magdeburg, Germany

^b Department of Internal Medicine, Division of Cardiology and Angiology, Otto von Guericke University, 39120 Magdeburg, Germany

^c Laboratory of Infection Oncology, Institute of Clinical Molecular Biology, Christian Albrechts University and University Hospital Schleswig Holstein, 24105 Kiel, Germany

^d Ludwig Institute for Cancer Research, Nuffield Department of Medicine, University of Oxford, Oxford OX3 7DQ, United Kingdom



ARTICLE INFO

Keywords:

Caspase-8
Gastric cancer
Gastric mucosoids
Gastric organoids
NF-κB
Stromal fibroblasts

ABSTRACT

Crosstalk within the gastric epithelium, which is closely in contact with stromal fibroblasts in the gastric mucosa, has a pivotal impact in proliferation, differentiation and transformation of the gastric epithelium. The human pathogen *Helicobacter pylori* colonises the gastric epithelium and represents a risk factor for gastric pathophysiology. Infection of *H. pylori* induces the activation of the transcription factor nuclear factor kappa-light-chain-enhancer of activated B cells (NF-κB), which is involved in the pro-inflammatory response but also in cell survival. In co-cultures with human gastric fibroblasts (HGF), we found that apoptotic cell death is reduced in the polarised human gastric cancer cell line NCI-N87 or in gastric mucosoids during *H. pylori* infection. Interestingly, suppression of apoptotic cell death in NCI-N87 cells involved an enhanced A20 expression regulated by NF-κB activity in response to *H. pylori* infection. Moreover, A20 acts as an important negative regulator of caspase-8 activity, which was suppressed in NCI-N87 cells during co-culture with gastric fibroblasts. Our results provide evidence for NF-κB-dependent regulation of apoptotic cell death in cellular crosstalk and highlight the protective role of gastric fibroblasts in gastric epithelial cell death during *H. pylori* infection.

1. Introduction

The epithelium of the gastric mucosa contains different cell types with distinct functions, including mucus-producing cells, acid-secreting parietal cells and pepsinogen-secreting chief cells [1]. The lamina propria, a loose connective tissue under the gastric epithelium, contains various surrounding stromal cells, including fibroblasts and vascular endothelial, and immune cells in case of inflammation [2]. Remarkably, emerging evidence suggests critical functions of fibroblasts that go beyond their fundamental role as structural scaffolds, including the control of cell survival, differentiation, and migration [3]. However, the effect of fibroblasts on epithelial cell survival remains a controversy. It has been suggested that different types of fibroblasts may release diverse factors that influence proliferation, regeneration, differentiation, apoptosis, and drug response of epithelial cells [4–7]. Thus, fibroblasts may function as either positive or negative regulators of epithelial cell

growth depending on the type of fibroblast. Interestingly, the co-culture of murine glandular stomach cells and gastric mesenchymal fibroblasts revealed that the gastric fibroblasts contribute to the long-term maintenance of stem cell activity and increase the differentiation and proliferation of the gastric epithelium [8]. This finding suggests the importance of gastric fibroblasts for maintaining the functional integrity of the gastric epithelium in the gastric mucosa.

The gastric epithelium represents a barrier protecting the stomach from external agents, including pathogens. However, a colonising of *H. pylori* bacterium exists in nearly half of the world's population [9]. *H. pylori* is also a risk factor for stomach diseases such as peptic ulcers, chronic gastritis, and gastric cancer [10]. Furthermore, infection with *H. pylori* is associated with significant gastric epithelial cell damage, including apoptotic cell death [11–19]. Herein, the *H. pylori*-induced NF-κB pathways and their target genes encoding cell survival factors (cIAP1, cIAP, A20) play a crucial role [20].

* Corresponding author at: Institute of Experimental Internal Medicine, Otto von Guericke University, Leipziger Str. 44, 39120 Magdeburg, Germany.
E-mail address: Naumann@med.ovgu.de (M. Naumann).

Although the fibroblasts below the human gastric epithelium are important for the homeodynamics of the gastric mucosa, their interaction with the overlying epithelium is still not well characterised. In particular, it is unclear if the fibroblasts affect survival of gastric epithelial cells during *H. pylori* infection. Here, we studied the effect of gastric fibroblasts on the survival of polarised gastric epithelial cancer cells and primary gastric mucosoids. We found a protective role of the fibroblasts in epithelial cell death during *H. pylori* infection and suggest that NF- κ B-regulated A20 contributes to this process.

2. Materials and methods

2.1. Cell culture and *H. pylori* infection

The human NCI-N87 gastric carcinoma cell line (CRL-5822, ATCC) was cultured as polarised cell monolayer. 2×10^5 cells were seeded on a porous membrane (pore size 1 μ M) of 12-well ThinCert™ inserts (Greiner Bio-One). The cells were further cultivated for 4 days in RPMI 1640 medium (Gibco®/Life Technologies) supplemented with 10 % fetal calf serum (FCS; Biochrom) at 37 °C in a humidified 5 % CO₂ atmosphere to obtain a confluent polarised cell monolayer. Human gastric fibroblasts (HGF; #2830, ScienceCell™ Research Laboratory) were seeded at 2×10^5 cells per well in 12-well plate and cultured in RPMI 1640 medium supplemented with 10 % FCS at 37 °C in a humidified 5 % CO₂ atmosphere for 4 days. The culture medium was replaced with fresh RPMI 1640 medium supplemented with 10 % FCS overnight before starting the co-culture experiment and infection.

Human gastric organoids (GAT23) were derived from gastric tissue samples [7] and obtained prior approval from the ethics committee of the Charite University Medicine, Berlin (EA1/129/12). For gastric mucosoid cultures, 4×10^5 cells derived from gastric organoids [7] were seeded onto a collagen-coated (15 μ g/cm², A10644-01, Gibco®) membrane of a 12-well ThinCert™ insert. The cells were cultivated in a mucosoid culture medium (advance DMEM/F12 ++ (12634-010, Thermo Fisher Scientific) and 25 % (v/v) R-Spondin conditioned medium supplemented with 25 ng/ml Wnt Surrogate-Fc Fusion Protein (N001, U-Protein Express B.V.), 2 % (v/v) B-27™ Supplement (50 \times) (17504-044, Thermo Fisher Scientific), 10 mM Nicotinamide (N0636-100G, Sigma Aldrich), 1 % (v/v) Penicillin-Streptomycin (100 \times) (15140-122, Thermo Fisher Scientific), 1 % (v/v) N-2 Supplement (100 \times) (17502-048, Thermo Fisher Scientific), 20 ng/ml Human EGF (PHG0311, Thermo Fisher Scientific), 1 μ M TGF- β RI Kinase Inhibitor IV (Alk-I) (616454, Calbiochem), 150 ng/ml Human FGF-10 (100-26, PeproTech), 150 ng/ml Human Noggin (120-10C, PeproTech), 10 nM Human [Leu¹⁵]-Gastrin I (G9145, Sigma-Aldrich) and 7.5 μ M ROCK inhibitor (Y-27632) (Y0503, Sigma Aldrich) at 37 °C in a humidified 5 % CO₂ atmosphere.

The medium over the cells was removed on day 4 after seeding to create an air-liquid interface (ALI). The medium at the basolateral side was then replaced with a mucosoid culture medium supplemented with 1.5 μ M ROCK inhibitor twice a week. Under ALI culture conditions, the mucosoids produce and accumulate mucous on the apical side, which was removed twice a week. The gastric mucosoids were cultivated for 18 days to form a monolayer with complete barrier integrity [7]. The mucous was removed and the mucosoids were washed twice with PBS containing calcium and magnesium before starting the co-culture experiment and infection.

For the co-culture experiment, the ThinCert™ inserts containing confluent polarised NCI-N87 cells or gastric mucosoids were hung in the 12-well plate on top of the HGF cells.

For collecting the conditioned media, the NCI-N87 and HGF cells were seeded on a membrane of ThinCert™ inserts and in a 12-well plate, respectively. The cells were cultured in three different conditions as follows: (1) HGF mono-culture, (2) HGF in co-culture with polarised NCI-N87 cells and (3) HGF in co-culture with *H. pylori*-infected polarised NCI-N87 cells. After 12 or 18 h, the culture medium of HGF in the

basolateral compartment (conditioned medium) was collected, centrifuged at 600 g for 10 min, and filtered through 0.2- μ m filters.

H. pylori strain P1 [21] and *H. pylori* P1 variant expressing the green fluorescent protein (GFP) [22] were grown on GC agar plates supplemented with 10 % horse serum (Gibco®/Life Technologies), 5 μ g/ml trimethoprim (Sigma-Aldrich), 1 μ g/ml nystatin (Sigma-Aldrich), 10 μ g/ml vancomycin (Sigma-Aldrich) under microaerophilic conditions at 37 °C for 48 h prior infection. Cells were infected with *H. pylori* at MOI 100.

2.2. Assessment of cell monolayer integrity

2.2.1. TEER measurement

Measurement of transepithelial electrical resistance (TEER) was performed using a Millicell electrical resistance system (Millipore) according to the manufacturer's instruction. TEER values were calculated as kOhm (k Ω) \times cm². The cell monolayers reaching TEER values above 0.5 k Ω \times cm² were considered to have an appropriate barrier function and used for further study.

2.2.2. FITC dextran measurement

The paracellular permeability of the cell monolayer was evaluated by measuring the diffusion of fluorescein isothiocyanate (FITC)-labelled dextran (molecular mass 4 kDa, Sigma) from the apical to the basolateral medium compartment. The apical culture medium was replaced by a medium containing FITC-dextran (1 mg/ml), whereas the basolateral medium was changed to a fresh medium without FITC-dextran. After incubation at 37 °C for 4 h, aliquots were collected from apical and basolateral compartments. The fluorescence intensity of the collected media was measured using a multi-mode plate reader (SpectraMax M5, Molecular Devices) with an excitation wavelength of 492 nm and an emission wavelength of 520 nm. The cell monolayer's permeability was presented as a percentage of FITC-dextran transported across the gastric monolayer compared to control (blank membrane).

TEER and FITC-dextran measurements of polarised NCI-N87 cells in co-culture conditions were performed after *H. pylori* infection for 24 h. The results were presented as a percentage of TEER or FITC-dextran transport compared to control (uninfected polarised NCI-N87 cells).

2.3. siRNA transfection

Cells were seeded at 2×10^5 cells on the porous membrane of the 12-well ThinCert™ inserts 1 day before transfection. Transfection of siRNA was performed using siLentFect™ (Bio-Rad, #1703362). Briefly, the cell culture media in both apical and basolateral compartments were changed to Opti-MEM (Gibco®/Life Technologies) before transfection. siRNA against A20 (SI05018601, Qiagen) and scrambled siRNA (#D-001810-10, Dharmacon) were prepared at a final concentration of 50 nM and added onto the apical side. At 6 h after transfection, the medium was changed to a fresh RPMI 1640 medium containing 10 % FCS. The cells were cultured for an additional 42 h before starting the co-culture experiment and infection.

2.4. Apoptotic cell death analysis

The cells were harvested using trypsin and stained with an Annexin V-FITC/PI Kit (MabTag GmbH), according to the manufacturer's instructions. Annexin V/PI stained cells were determined by flow cytometry using the CyFlow space (Sysmex). Ten thousand gated single cells were acquired and the data were processed and analysed using Flowing Software 2.5.1. The Annexin V-positive cells (early apoptotic cells) and Annexin V/PI double-positive cells (late apoptotic cells) were summed up to give the percentage of total apoptotic cells.

Caspase-8 Inhibitor (20 μ M Z-IETD-FMK, TNB-1004-M001, Tonbo Biosciences) was used to treat the cells 15 min before *H. pylori* infection.

2.5. Preparation of cell lysates and immunoblotting

The cells on porous membrane were washed with ice-cold PBS, followed by lysis in RIPA lysis buffer (50 mM Tris (pH 7.5), 150 mM NaCl, 2 mM EDTA, 10 mM K₂HPO₄, 10 % glycerol, 1 % Triton X-100, 0.05 % SDS) supplemented with 1 mM Na₃VO₄, 1 mM Na₂MoO₄, 20 mM NaF, 10 mM Na₄P₂O₇, 1 mM AEBBSF, 20 mM Glycerol-2-phosphate, and 1× EDTA-free protease inhibitor mix (PI) (cOmplete™, Mini, Roche). Lysates were obtained after centrifugation (13,000g, 4 °C, 10 min). The total protein amount in the lysates was measured by the bicinchoninic acid (BCA) method using Pierce™ BCA Protein Assay Kit (23225, ThermoFisher Scientific). Then, 20–40 µg of the lysates were mixed with Laemmli buffer, heated at 95 °C for 10 min, separated in SDS containing Tris-Glycine gels, and transferred onto PVDF membranes (Millipore). The membranes were blocked with 5 % skim milk in TBS containing 0.1 % Tween 20 (TBS-T) at room temperature (RT) for 1 h. The membranes were incubated with primary antibodies in either 5 % BSA or 5 % skim milk in TBS-T at 4 °C overnight and subsequently with appropriate HRP-conjugated secondary antibody in 5 % skim milk in TBS-T at RT for 1 h. The immunoblot was then developed using a chemiluminescent substrate (#WBKLS0500, Millipore) and visualised using the ChemoCam Imager (Intas).

The following primary antibodies were used: A20 (sc-166692) was purchased from Santa Cruz Biotechnology; Caspase 3 (#9662), Caspase 8 (#9746), Cleaved Caspase 3 (#9661), Cleaved caspase 8 (#9496) and phospho-IκBα (#9246) were purchased from Cell Signaling Technology, and GAPDH (#MAB374) was purchased from Millipore.

Protein bands were quantified (normalised to the respective band intensities of GAPDH) in infected cells relative to uninfected control by Image J software (National Institutes of Health).

2.6. Caspase-3/7 assay

The apical culture medium was replaced by a medium containing *H. pylori* (MOI 100) and Incucyte® Caspase-3/7 Green Dye (dilution 1:1000, Sartorius). At 24 h after *H. pylori* infection, the hanging arms of ThinCert™ insert were cut off and the insert was placed into a 12-well plate well. The plate was then placed into the Incucyte® S3 Live-Cell Analysis System (Sartorius) for measuring the fluorescence signal using the phase contrast and green fluorescence channel at a magnification of 20× (36 images per membrane). To exclude the fluorescence signal from the edge of the ThinCert™ membrane, a set of nine images were selected randomly from the central region of the membrane. The selected images were exported from Incucyte® software and then imported to Image J software (National Institutes of Health) for quantification of fluorescence intensity (A.U.).

2.7. Immunofluorescence

The mucosoid cultures on the porous membrane of the ThinCert™ inserts were fixed with 4 % paraformaldehyde for 15 min, followed by three washes with PBS. The specimens were then blocked and permeabilised in PBS containing 1 % BSA (w/v), 2 % FCS (v/v) and 0.25 % (v/v) Triton-X-100 for 30 min at RT. The inserts were washed thrice with PBS, incubated with a primary antibody against E-cadherin (ab1416, Abcam) or occludin (611090, BD Biosciences) in 10× diluted blocking buffer at RT for 30 min. Afterwards washed thrice with PBS and incubated with the secondary antibody (AlexaFluor 488 or AlexaFluor 555, ThermoFisher Scientific) in 10× diluted blocking buffer at RT for 30 min, followed by three washes with PBS containing 0.1 % (v/v) Tween-20. DAPI (100 µg/ml, Sigma-Aldrich) diluted 1:60 in MilliQ water was added to stain the nuclei. In order to perform histology (H&E staining) and immunofluorescence on filter sections the filters were fixed overnight in 4 % paraformaldehyde at 4 °C, washed with PBS twice and embedded in Histogel (HG-4000-144) inside a cryomold (Tissue-Tek®). Further, the sample were processed overnight, paraffin embedded and 5

µm sections were cut with a rotation microtome (Leica) and mounted onto frosted slides. Deparaffinization, rehydration and H&E staining was performed according to standard protocols. Antigen was retrieved after rehydration by boiling the slides in citrate buffer pH 6.0 for 25 min. The immunofluorescence protocol was used as above. Images were acquired on an AxioObserver 7 equipped with the Colibri 5 RGB-UV, a camera AxioCam 305 colour and a 40× objective (Zeiss Plan-Apochromat, NA 1.4, Oil a = 0.13 mm) using the software ZEN 3.0 pro (Carl Zeiss microscopy). The filter sets used were as follows: DAPI, 96 HE BFP; AlexaFluor 488, 38 HE GFP; and AlexaFluor 555, 43 HE DsRed.

2.8. Statistical analysis

Quantitative data were presented as mean ± SD (standard deviation) of at least two independent experiments. The statistical significance of data was analysed by applying Student's *t*-test. *P*-values ≤ 0.05, 0.01, 0.001 were considered significant (*, **, ***, respectively).

3. Results

3.1. Co-culture with fibroblasts protects the monolayer integrity of NCI-N87 cells during *H. pylori* infection

Gastric epithelial NCI-N87 cells were grown on the porous membrane of the ThinCert™ inserts to obtain a polarised cell monolayer. The cell monolayer's integrity was determined by measuring the trans-epithelial electrical resistance (TEER) and the amount of fluorescein isothiocyanate (FITC)-labelled dextran transported from the apical to the basolateral sides of the cell monolayer over time. An increase in TEER (Fig. 1A) and a decrease of FITC-dextran transport (Fig. 1B) was observed over time, in which the cells reached the state of the fully polarised monolayer with completed barrier integrity after 4 days of cell culture. Therefore, the polarised NCI-N87 cells at this time point were used for further experiments.

The interaction between epithelial cells and fibroblasts is closely linked to the gastric pathophysiology of bacterial infection [23]. Therefore, we established a co-culture system of polarised gastric epithelial NCI-N87 cells and human gastric fibroblasts (HGF) to simulate in part the gastric microenvironment (Fig. 1C), in which the polarised NCI-N87 cells were infected with *H. pylori* at the apical side and could communicate with HGF at the basolateral side. We then investigated the impact of HGF on the monolayer integrity of NCI-N87 cells upon *H. pylori* infection. We found a significant decrease in TEER (Fig. 1D) and an increase in FITC-dextran transport (Fig. 1E) in polarised NCI-N87 cells after *H. pylori* infection, suggesting that *H. pylori* impairs the monolayer integrity of polarised NCI-N87 cells. Interestingly, the loss of TEER and increase in FITC-dextran passage was attenuated in the presence of HGF co-culture, but not if co-cultivated with NCI-N87 cells (Fig. 1D and E). Our results suggest a protective role of HGF on the monolayer integrity of the polarised NCI-N87 cells.

3.2. Co-culture with fibroblasts suppresses apoptotic cell death of NCI-N87 cells during *H. pylori* infection

It is known that growth factors and cytokines released by fibroblasts can affect the integrity of the epithelial barrier by influencing membrane morphology, proliferation, differentiation or apoptotic cell death [4–7]. Based on our previous observations on *H. pylori*-associated apoptotic cell death [20] we investigated the effects of HGF on apoptotic cell death of polarised NCI-N87 cells. Apoptotic cell death was determined by Annexin V/PI staining in polarised NCI-N87 cells infected with *H. pylori*. We observed an increase in apoptotic cell death upon *H. pylori* infection for 24 and 48 h (Fig. 2). Quantitative analysis revealed that the apoptosis in polarised NCI-N87 cells in co-culture with HGF prominently decreased upon *H. pylori* infection. However, this effect was not

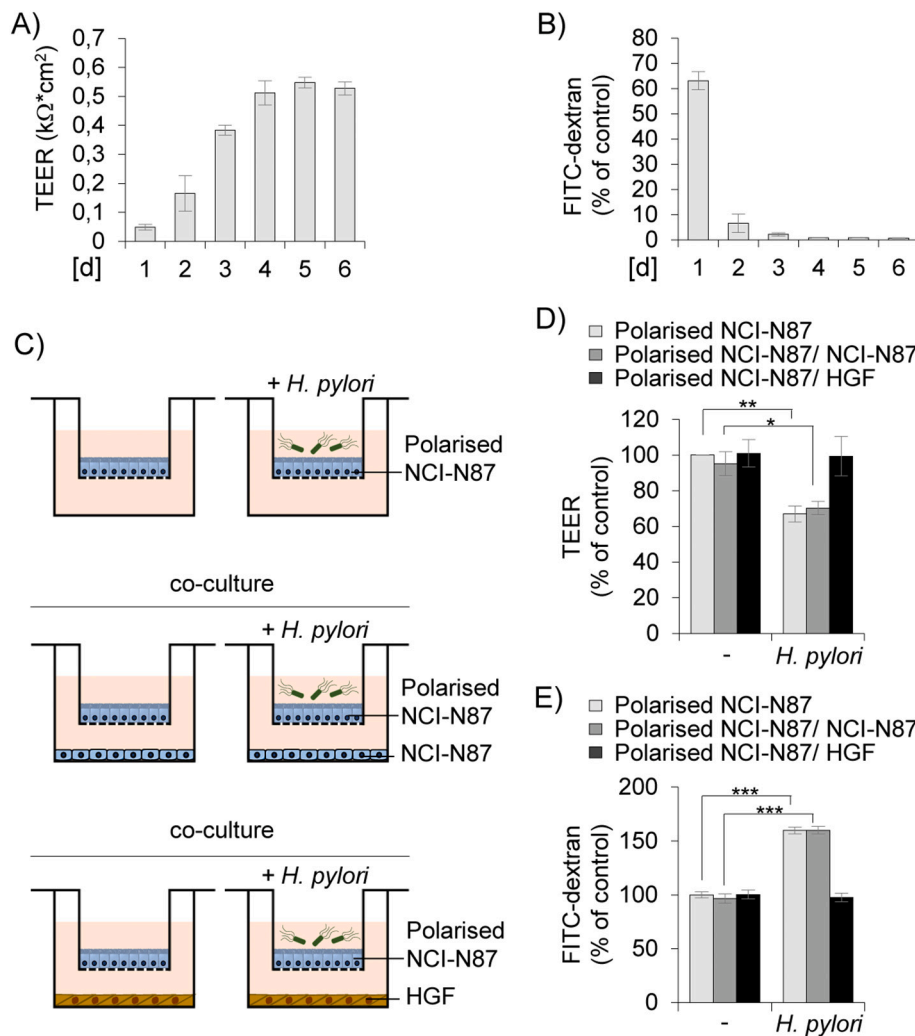


Fig. 1. Co-culture with fibroblasts protects the monolayer integrity of *H. pylori*-infected NCI-N87 cells. NCI-N87 cells were grown as a polarised cell monolayer on a porous membrane of ThinCert™ insert. (A) TEER values were measured at the indicated time. (B) FITC-dextran was measured as percentage compared to the membrane without cells for the indicated time. (C) Schematic illustration of the mono- and co-culture system of polarised gastric epithelial cells (NCI-N87) and human gastric fibroblasts (HGF). *H. pylori* were added to the apical side of the polarised NCI-N87 cells. (D, E) Polarised NCI-N87 cells were infected with *H. pylori* in the absence or presence of either NCI-N87 cells or HGF for 24 h, followed by measurement of (D) TEER and (E) FITC dextran. Polarised NCI-N87 cells were set as 100 % (control). Data information: Data shown in (A and B) and (D and E) are from two independent experiments with three technical replicates each and represent mean \pm SD. * $P \leq 0.05$, *** $P \leq 0.001$ (Student's *t*-test).

observed when NCI-N87 cells and NCI-N87 cells were co-cultured, indicating that co-culture specifically with HGF could suppress *H. pylori*-induced cell death in NCI-N87 cells.

3.3. Conditioned media from fibroblasts suppresses apoptotic cell death of NCI-N87 cells during *H. pylori* infection

Our co-culture system provides a platform where fibroblasts and polarised NCI-N87 cells can communicate through secreted factors in the medium. Therefore, we hypothesised that the HGF communicate with polarised NCI-N87 cells through secreted factors and thus protected NCI-N87 cells from death during *H. pylori* infection. We determined the impact of different conditioned media (CM) from HGF on *H. pylori*-induced cell death in polarised NCI-N87 cells. Briefly, three different conditioned media of HGF (CM of HGF mono-culture (yellow), CM of HGF in co-culture with non-infected polarised NCI-N87 cells (blue), and CM of HGF in co-culture with infected polarised NCI-N87 cells (green)) were collected at 12 and 18 h and added to the basolateral side of the polarised NCI-N87 cells (Fig. 3). The polarised NCI-N87 cells were then infected with *H. pylori* for 24 h, after which apoptotic cell death of polarised NCI-N87 cells was analysed. We found that only the conditioned medium from HGF in co-culture with infected polarised NCI-N87 cells (green) was capable of decreasing *H. pylori*-induced apoptotic cell death in NCI-N87 cells, while the others had little or no effect. This result indicates that HGF contributes to the suppression of apoptotic cell death of polarised NCI-N87 cells via factors secreted in response to the

presence of infected NCI-N87 cells.

3.4. Co-culture with fibroblasts ameliorates *H. pylori*-induced A20 expression and cell survival of NCI-N87 cells

We have previously reported that *H. pylori* infection leads to activation of NF- κ B signalling, which subsequently upregulates the NF- κ B target gene *TNFAIP3*, encoding A20 [24]. A20 is a deubiquitylase that interferes with the enhanced activation of caspase-8 via cullin-3 [25], leading to the inhibition of caspase-8 activation and suppression of apoptotic cell death [24]. Therefore, we hypothesised that the co-cultivation of HGF cells might affect regulation of A20 and thereby cell survival in NCI-N87 cells. Indeed, we observed a further increase in *H. pylori*-induced A20 expression via NF- κ B activation, and a corresponding stronger decrease in caspase-8 cleavage in NCI-N87 cells when co-cultured with HGF compared to NCI-N87 cells without HGF (Fig. 4A). Furthermore, depletion of A20 led to increased cleavage of caspase-8 in NCI-N87 cells without HGF exemplifying the role of A20 on caspase-8 activity (Fig. 4A). The effects on caspase-8 cleavage were also observed for caspase-3 (Fig. 4A). Consistently, the IncuCyte® live-cell imaging analysis of the activated caspase-3/7 after 24 h of *H. pylori* infection showed a decrease in fluorescence intensity in NCI-N87 cells when co-cultured with HGF compared to NCI-N87 without HGF, exemplary for a decrease in caspase-3/7 activity (Fig. 4B). Moreover, the fluorescence intensity increased in both conditions upon A20 depletion (Fig. 4B). Here again we observed a stronger increase for NCI-N87 cells

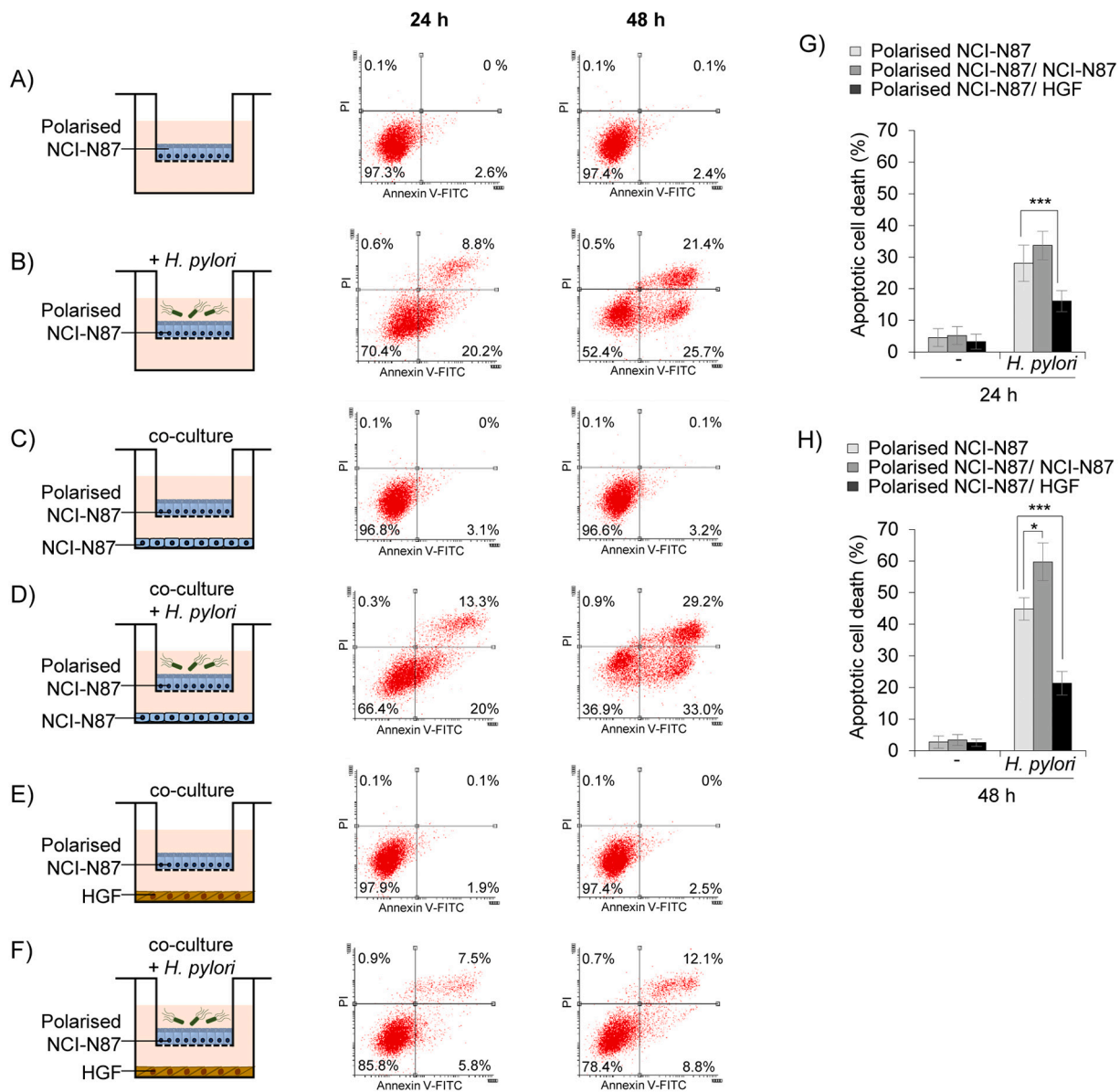


Fig. 2. Co-culture with fibroblasts suppresses apoptotic cell death of polarised NCI-N87 cells during *H. pylori* infection. (A, C, E) Polarised NCI-N87 cells in the absence (A) or presence of either NCI-N87 cells (C) or HGF (E) co-culture. (B, D, F) Polarised NCI-N87 cells were infected with *H. pylori* for 24 or 48 h in the absence (B) or presence of either NCI-N87 cells (D) or HGF (F) co-culture. Polarised NCI-N87 cells were stained with Annexin V/PI, and the apoptotic cell death was analysed by flow cytometry. (G and H) Quantitative analysis of apoptotic cell death. Data information: Data shown are representative of three independent experiments with two technical replicates each, and the graph represents mean \pm SD. *** $P \leq 0.001$ (Student's *t*-test).

cultured without HGF.

So far, our results suggest the involvement of A20 in the suppression of apoptotic cell death in *H. pylori*-infected NCI-N87 cells during co-culture with HGF. A20 exerts its inhibitory effect via caspase-8, thus, we further examined whether inhibition of caspase-8 affects apoptotic cell death in *H. pylori*-infected NCI-N87 cells co-cultured with HGF. Treatment with the caspase-8 inhibitor (Z-IETD-FMK) 15 min prior to *H. pylori* infection diminished apoptotic cell death of NCI-N87 cells (Fig. 5). However, the co-culture of NCI-N87 cells (with or without Z-IETD-FMK treatment) with HGF led to a more prominent reduction of apoptotic cell death. This suggests that apoptotic cell death in NCI-N87 cells co-cultured with HGF is caused in part by regulation of caspase-8 activity (Fig. 5).

3.5. Co-culture with fibroblasts suppresses apoptotic cell death of gastric mucosoids during *H. pylori* infection

To further corroborate our data, we used primary tissue and employed gastric mucosoid cultures [7]. Gastric mucosoids grown on a collagen-coated membrane as a highly polarised columnar epithelial layer with nuclei located on the basal side (Fig. 6A, left panel) were IF labelled for occludin to show the apical tight junction of the mucosoids, giving rise to a closed monolayer (Fig. 6A, middle panel). The infection of gastric mucosoids with GFP-labelled *H. pylori* was shown in Fig. 6A (right panel). Consistent with polarised NCI-N87 cells, we found that co-culture with HGF promoted *H. pylori*-induced I κ B α phosphorylation and enhanced A20 expression in gastric mucosoids (Fig. 6B). Further, we also observed a decrease in caspase-8 cleavage in gastric mucosoids when co-cultured with HGF (Fig. 6B). Consistently, the IncuCyte® live-cell imaging analysis of the activated caspase-3/7 after 24 h of *H. pylori*

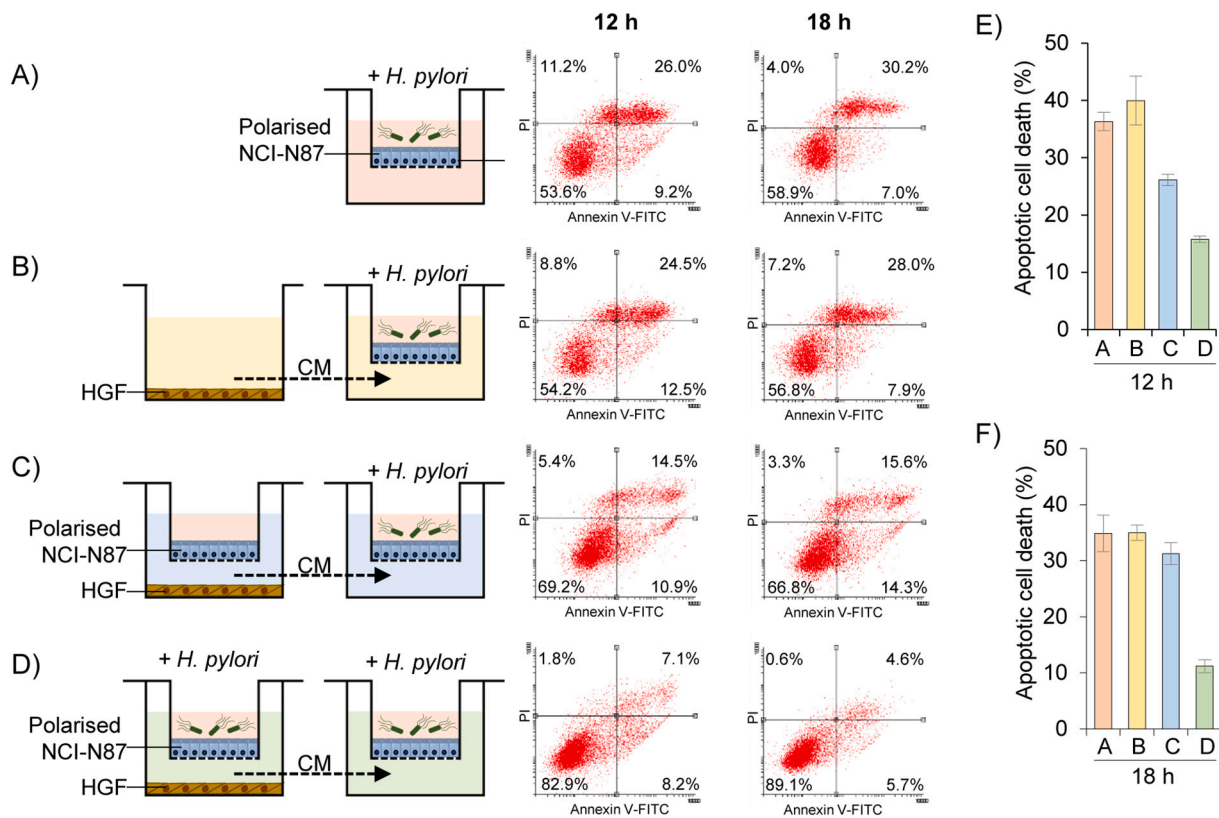


Fig. 3. Effect of fibroblast conditioned media on *H. pylori*-induced apoptotic cell death of polarised NCI-N87 cells. (A-D) Different conditioned media (CM) were collected including RPMI medium as control (A; pink), CM of HGF mono-culture (B; yellow), CM of HGF co-cultured with non-infected NCI-N87 cells (C; blue), and CM of HGF co-cultured with infected NCI-N87 cells (D; green), for 12 or 18 h. The conditioned medium was added to the basolateral side of the polarised NCI-N87 cells and the apical side of polarised NCI-N87 cells were infected with *H. pylori* for 24 h prior to staining with Annexin V/PI. The apoptotic cell death was analysed by flow cytometry. (E and F) Quantitative analysis of apoptotic cell death. Data information: Data shown are representative of two independent experiments, and the graph represents mean \pm SD from two independent experiments. (For interpretation of the references to colour in this figure legend, the reader is referred to the web version of this article.)

infection showed a decrease in fluorescence intensity in gastric mucosoids when co-cultured with HGF (Fig. 6C).

4. Discussion

Fibroblasts are the major stromal cells as part of the lamina propria of the gastric mucosa, that are closely in contact with the gastric epithelium and could affect gastric epithelial differentiation and proliferation [8]. Crosstalk between the stromal fibroblasts and epithelium is considered to act as a functional driver of gastric cancer development [26,27]. However, little is known about the crosstalk between fibroblasts and gastric epithelium and its impact on epithelial cell survival. In this study, we performed experiments with co-culture systems by using either polarised human gastric cancer cell line NCI-N87 or gastric mucosoids in co-culture with HGF upon *H. pylori* infection. We showed that co-culture with HGF could suppress apoptotic cell death in polarised NCI-N87 cells during *H. pylori* infection. Co-culture of polarised NCI-N87 cells with non-polarised NCI-N87 cells representative of epithelial tissue served as a control. In contrast to HGF, we found that the non-polarised NCI-N87 cells did not affect the apoptotic cell death induced by *H. pylori* in polarised NCI-N87 cells (Fig. 2). These data highlight the important role of gastric fibroblasts in suppressing apoptotic cell death in *H. pylori*-infected epithelial cells. The non-contact co-culture system used in this study indicated that the effect of co-cultivation of polarised NCI-N87 cells with HGF was directed through factors secreted by HGF.

Cells of the gastric epithelium interactively communicate with cells of the microenvironment such as fibroblasts via soluble factors,

including low molecular weight metabolites, and probably also via exosomes [28]. Factors secreted by fibroblasts can influence the cellular responses of epithelial cells, such as proliferation and apoptotic cell death [28]. Here, keratinocyte growth factor (KGF) had been identified as the growth-stimulating factor from human gastric fibroblasts to human scirrhous gastric carcinoma cells [29]. Furthermore, Sun et al. [30] reported that fibroblast growth factor 9 (FGF9) is a novel growth factor overexpressed in cancer-associated fibroblasts and a possible secreted mediator that promotes the survival and invasive capability of gastric cancer cells. Possibly factors such as cytokines secreted by *H. pylori*-infected gastric epithelial cells [31] induce the expression of FGFs and their release from fibroblasts. Specifically, we observed that the conditioned HGF medium protected against apoptotic cell death after co-culturing with *H. pylori*-infected polarised NCI-N87 cells (Fig. 3). Therefore, this suggests that the HGF respond to a component secreted basolaterally by polarised NCI-N87 cells after *H. pylori* infection.

Infection of *H. pylori* induces early and transient activation of NF- κ B in gastric epithelial cells [32–34]. Dysregulation of NF- κ B impacts on gastric inflammation and carcinogenesis due to the regulation of growth factors, anti-apoptotic factors and cytokine/chemokine production [35]. Our results showed a transient increase in phospho-I κ B α , indicating NF- κ B activity, and a stronger increase in the expression of the NF- κ B regulated molecule A20 in NCI-N87 cells infected with *H. pylori*, when co-cultured with HGF as compared to NCI-N87 cells without co-culture (Fig. 4A). Therefore, the crosstalk between the gastric epithelial cells and HGF suggest NF- κ B dependency. A factor secreted from gastric epithelial cells, which induces a response in HGF, intensify the NF- κ B

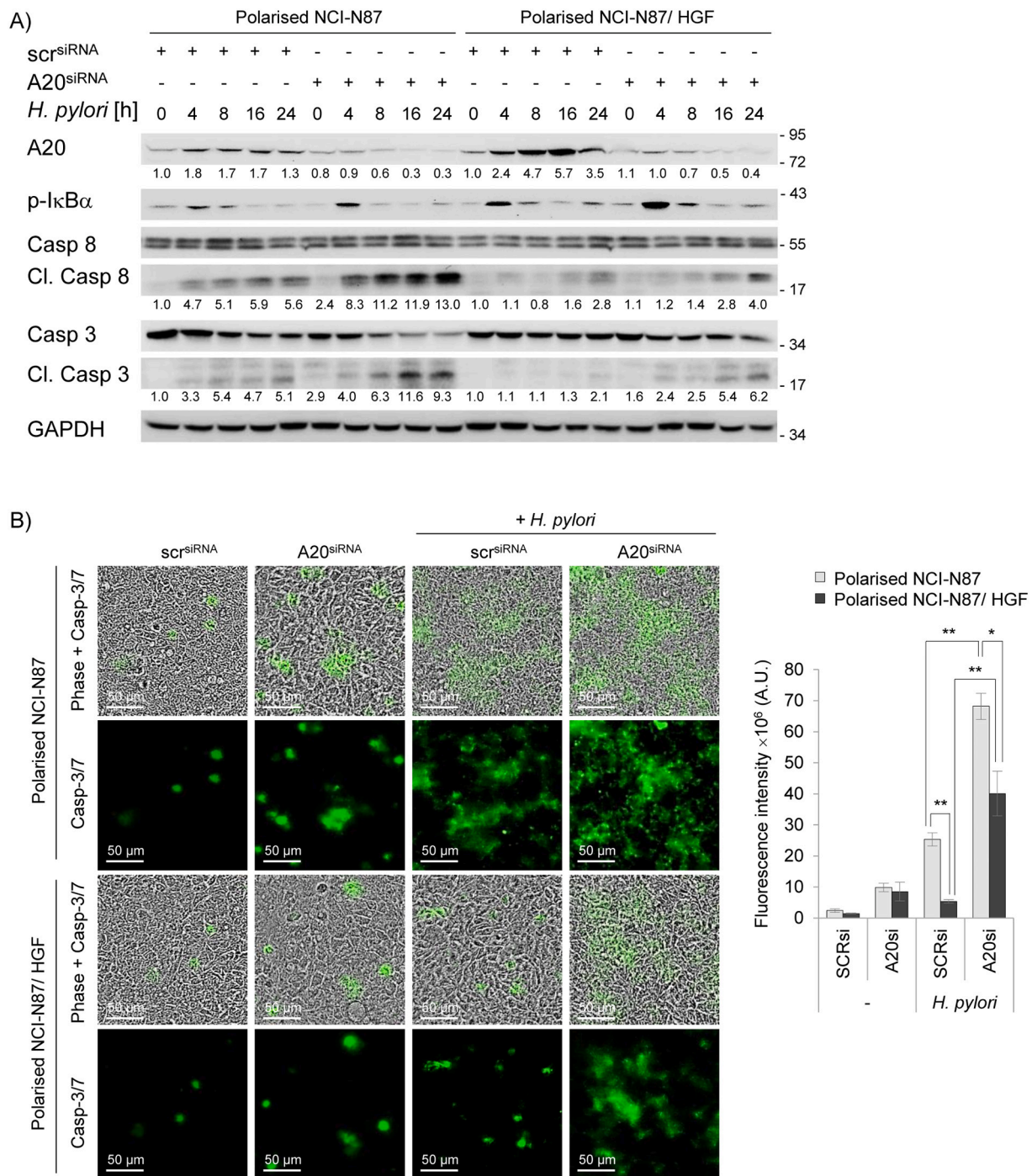


Fig. 4. Co-culture with fibroblasts ameliorates *H. pylori*-induced A20 expression and cell survival of NCI-N87 cells. (A) Polarised NCI-N87 cells were transfected with siRNA against A20 and infected with *H. pylori* in the absence or presence of HGF for the indicated time. Whole-cell lysates were subjected to IB analysis of the indicated proteins. (B) Polarised NCI-N87 cells were transfected with siRNA against A20 and infected with *H. pylori* in the absence or presence of HGF for 24 h. Cleaved caspase-3/7 (green) in polarised NCI-N87 cells was detected by the InCuCyte® S3 Live-Cell imaging analysis system. Scale bars = 50 μm. Data information: Data shown in (A and B) are representative of two independent experiments. Fluorescence intensity in (B) depicts mean ± SD from two independent experiments. **P* ≤ 0.05, ***P* ≤ 0.01 (Student's *t*-test). The numbers indicate the band intensities of the given proteins (normalised to the respective band intensities of GAPDH) in infected cells relative to uninfected control. Similar data were obtained from two independent experiments. (For interpretation of the references to colour in this figure legend, the reader is referred to the web version of this article.)

activation in the gastric epithelial cells and subsequently promote cell survival. An impact of *H. pylori* infected-epithelial cells on stroma cells has been reported by Ferrand et al. [36]. Here, it was shown that *H. pylori*-infected gastrointestinal epithelial cells secrete multiple cytokines, with a major role of TNF, mainly via the NF-κB-dependent pathway, which induces the migration of bone marrow-derived

mesenchymal stromal cells to the site of infection [36]. In another study, the secretome of activated gastric fibroblasts induced a cancer stem cell-related differentiation program in gastric epithelial cells, partially by TGFβ signalling [37]. Furthermore, the reciprocal interaction between gastric tumor cells and activated fibroblasts through TNF/IL-33/ST2L signalling has been reported, leading to a malignant

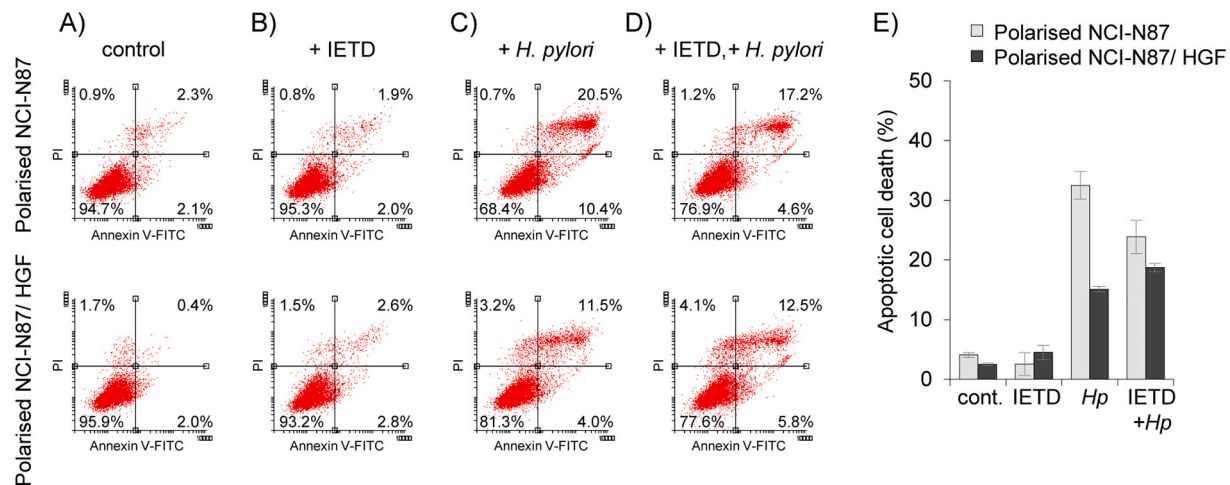


Fig. 5. Co-culture with fibroblasts suppresses caspase-8-dependent apoptotic cell death in polarised NCI-N87 cells during *H. pylori* infection. (A) Polarised NCI-N87 cells in mono-culture, or co-culture with HGF and (B) treatment with Z-IETD-FMK. (C) Polarised NCI-N87 cells in mono-culture, or co-culture with HGF and *H. pylori* infection for 24 h or (D) *H. pylori* infection with pre-treatment with Z-IETD-FMK for 15 min. The cells were stained with Annexin V/PI, and apoptotic cell death was analysed by flow cytometry. (E) Quantitative analysis of apoptotic cell death. Data information: Data shown are representative of two independent experiments, and the graph represents mean \pm SD from two independent experiments.

phenotype [27].

Infection of *H. pylori* in gastric epithelial cells initiates moderate apoptotic cell death. The bacterial virulence factors such as vacuolating cytotoxin (VacA) and gamma-glutamyltranspeptidase (GGT) can trigger the intrinsic/mitochondria-dependent apoptotic pathway, while upregulation of TRAIL and FasL and their corresponding receptors upon *H. pylori* infection are implicated in triggering the extrinsic apoptotic pathway [11–19]. Caspase-8 is a master regulator of the extrinsic cell death pathway [38]. We previously reported that A20 deubiquitinylates caspase-8, suppressing efficient caspase-8 cleavage and apoptotic cell death [24]. We found that co-culture with HGF enhanced the expression of A20 in *H. pylori*-infected NCI-N87 cells and suppressed the extent of caspase-8 cleavage in polarised NCI-N87 cells during *H. pylori* infection (Fig. 4A), suggesting that the enhanced expression of A20 mediates the suppressive effect of HGF via intensified NF- κ B activation. This effect of A20 was antagonised by depletion of A20, resulting in an increase in caspase-8 and caspase-3 cleavage compared with the scrambled control in polarised NCI-N87 cells co-cultured with HGF. The extent of cleaved caspase-8 and caspase-3 in NCI-N87 cells co-cultured with HGF treated with siRNA against A20 was not as much as that in siRNA treated NCI-N87 cells without HGF (Fig. 4A). The treatment with a caspase-8 inhibitor suppressed caspase-8-dependent apoptotic cell death induced by *H. pylori* infection to a similar extent as the HGF co-culture (Fig. 5) and demonstrates that the suppressive effect of HGF on apoptotic cell death of polarised NCI-N87 cells is caspase-8 sensitive. Taken together, it suggests that in addition to A20 also other factors affect caspase-8 cleavage. Mechanistically we propose the following: a soluble factor secreted from infected polarised NCI-N87 cells induces a response in HGF that intensifies the NF- κ B activation in NCI-N87 cells and subsequently promotes cell survival via a strong upregulation of A20 and its restraining activity towards caspase-8.

Moreover, we used human primary epithelial mucosoids, which recapitulate most of the functions of the human gastric epithelium [7]. In an air-liquid interface culture, the gastric mucosoids developed a continuous cell monolayer with columnar epithelial morphology of the gastric epithelium (Fig. 6A). The apical mucus secretion indicates for the gastric epithelial phenotype and constitutes a protective shield for the gastric mucosoids. Co-culture of gastric mucosoids and HGF represents a model of gastric epithelium-stroma communication. Using this model, we confirmed the effect of HGF co-culture on the protection of gastric mucosoid from apoptotic cell death by enhanced A20 expression during *H. pylori* infection (Fig. 6B and C).

A complex network of anti- and pro-apoptotic signalling pathways in gastric epithelial cells is influenced by factors secreted by fibroblasts that promote cell survival. This promotion of cell survival could overcome gastric epithelial cell self-renewal and foster genomic alterations such as somatic mutations, copy number variations and gene fusions that favour the development of gastric cancer and cancer metastases. Enhanced cell survival could also contribute to persistent *H. pylori* infection.

5. Conclusion

Our data demonstrate the protective role of human gastric fibroblasts on apoptotic cell death of gastric epithelial cells. We identified enhanced expression of A20 regulated by NF- κ B activity in response to *H. pylori* infection in gastric epithelial cells as an underlying mechanism for suppression of apoptotic cell death in gastric epithelial cells by HGF in co-culture. This can be attributed to a complex crosstalk via secreted factors between HGF and gastric epithelial cells. However, the identity of the secreted factor(s) involved in this crosstalk will need further investigation. Finally, our finding highlights the impact of cell-cell communication on cell survival in the gastric mucosa during *H. pylori* infection and might suggest potential therapeutic strategy by interfering with the interaction between fibroblasts and epithelial cells.

CRedit authorship contribution statement

Phatcharida Jantaree: Investigation, Methodology, Writing-Original draft. **Yanfei Yu:** Investigation. **Supattra Chaithongyot:** Investigation. **Christian Täger:** Investigation. **Mohsen Abdi Sarabi:** Investigation. **Thomas F Meyer:** Methodology. **Francesco Boccellato:** Methodology. **Gunter Maubach:** Investigation, Writing-Review & Editing. **Michael Naumann:** Conceptualization, Methodology, Writing & Editing, Supervision, Funding acquisition.

Declaration of competing interest

The authors declare the following financial interests/personal relationships which may be considered as potential competing interests: Michael Naumann reports financial support was provided by German Research Foundation. Michael Naumann reports financial support was provided by European Union.

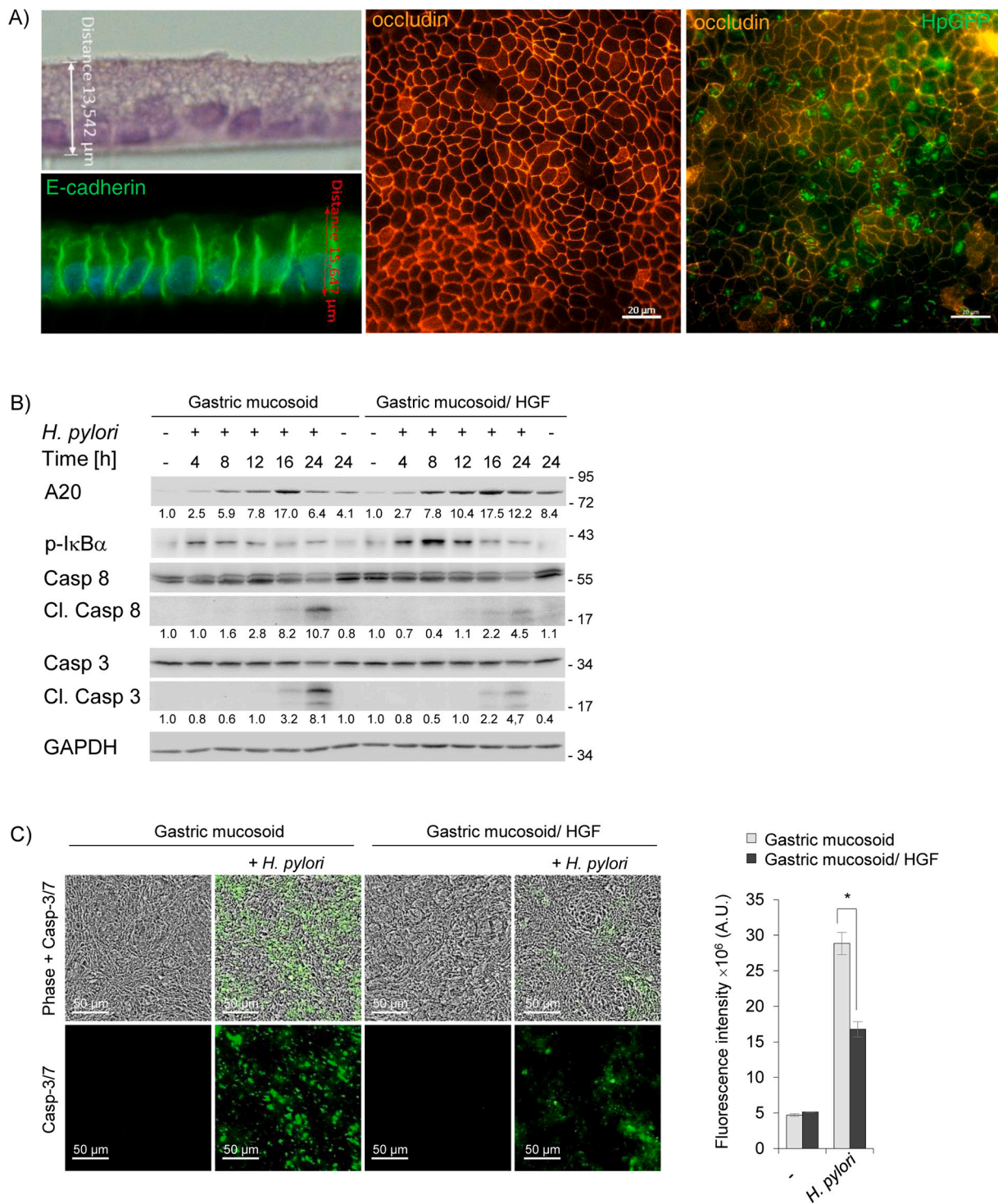


Fig. 6. Co-culture of gastric mucosoids with fibroblasts suppresses apoptotic death during *H. pylori* infection. (A) Gastric mucosoids grown on filter inserts were fixed, paraffin-embedded, cut into 5 μm sections and stained for H&E or E-cadherin by immunofluorescence (left). Whole mount filter inserts either uninfected or infected for 2 h with GFP-labelled *H. pylori* were IF stained for occludin (pseudo-coloured for the uninfected sample). Scale bars = 20 μm (right). (B) Gastric mucosoids were infected with *H. pylori* in the absence or presence of HGF for the indicated time. Whole-cell lysates were subjected to IB analysis of the indicated proteins. (C) Gastric mucosoids were infected with *H. pylori* in the absence or presence of HGF for 24 h. Cleaved caspase-3/7 (green) in the gastric mucosoids was detected by the IncuCyte® S3 Live-Cell imaging analysis system. Scale bars = 50 μm. Data information: Data shown in (B) are representative of three independent experiments. Data shown in (C) are representative of two independent experiments. Fluorescence intensity in (C) depicts mean ± SD from two independent experiments. **P* ≤ 0.05 (Student's *t*-test). The numbers indicate the band intensities of the given proteins (normalised to the respective band intensities of GAPDH) in infected cells relative to uninfected control. Similar data were obtained from two independent experiments. (For interpretation of the references to colour in this figure legend, the reader is referred to the web version of this article.)

Data availability

All data generated and analysed during the current study are included in this article and its additional files.

Acknowledgements

We would like to thank K. Herrmanns (Institute of Pathology, Medical Faculty, Otto von Guericke University) for the preparation of the paraffin sections. This work was supported in part by grants of the European Union Program European Regional Development Fund of the Ministry of Economy, Science and Digitalisation in Saxony Anhalt within the Center of Dynamic Systems (ZS/2016/04/78155) to M.N. and by the German Research Foundation from RTG 2408 (361210922) to M. N.

References

- [1] T.H. Kim, R.A. Shivdasani, Stomach development, stem cells and disease, *Development* 143 (2016) 554–565, <https://doi.org/10.1242/dev.124891>.
- [2] B. Hunyady, E. Mezey, M. Palkovits, Gastrointestinal immunology: cell types in the lamina propria—a morphological review, *Acta Physiol. Hung.* 87 (2000) 305–328.
- [3] C. Liu, M. Mak, Fibroblast-mediated uncaging of cancer cells and dynamic evolution of the physical microenvironment, *Sci. Rep.* 12 (2022) 791, <https://doi.org/10.1038/s41598-021-03134-w>.
- [4] R.N. Gomes, F. Manuel, D.S. Nascimento, The bright side of fibroblasts: molecular signature and regenerative cues in major organs, *NPJ Regen. Med.* 6 (2021) 43, <https://doi.org/10.1038/s41536-021-00153-z>.
- [5] B. Koh, H. Jeon, D. Kim, D. Kang, K.R. Kim, Effect of fibroblast co-culture on the proliferation, viability and drug response of colon cancer cells, *Oncol. Lett.* 17 (2019) 2409–2417, <https://doi.org/10.3892/ol.2018.9836>.
- [6] M. Sigal, M.D.M. Reines, S. Mullerke, C. Fischer, M. Kapalczynska, H. Berger, E.R. M. Bakker, H.J. Mollenkopf, M.E. Rothenberg, B. Wiedenmann, S. Sauer, T. F. Meyer, R-spondin-3 induces secretory, antimicrobial Lgr5(+) cells in the stomach, *Nat. Cell Biol.* 21 (2019) 812–823, <https://doi.org/10.1038/s41556-019-0339-9>.
- [7] F. Boccellato, S. Woelffling, A. Imai-Matsushima, G. Sanchez, C. Goosmann, M. Schmid, H. Berger, P. Morey, C. Denecke, J. Ordemann, T.F. Meyer, Polarised epithelial monolayers of the gastric mucosa reveal insights into mucosal homeostasis and defence against infection, *Gut* 68 (2019) 400–413, <https://doi.org/10.1136/gutjnl-2017-314540>.
- [8] T. Katano, A. Ootani, T. Mizoshita, S. Tanida, H. Tsukamoto, K. Ozeki, H. Kataoka, T. Joh, Gastric mesenchymal myofibroblasts maintain stem cell activity and proliferation of murine gastric epithelium in vitro, *Am. J. Pathol.* 185 (2015) 798–807, <https://doi.org/10.1016/j.ajpath.2014.11.007>.
- [9] M. Zamani, F. Ebrahimitabar, V. Zamani, W.H. Miller, R. Alizadeh-Navaei, J. Shokri-Shirvani, M.H. Derakhshan, Systematic review with meta-analysis: the worldwide prevalence of *Helicobacter pylori* infection, *Aliment. Pharmacol. Ther.* 47 (2018) 868–876, <https://doi.org/10.1111/apt.14561>.
- [10] H.J. Ahn, D.S. Lee, *Helicobacter pylori* in gastric carcinogenesis, *World J. Gastrointest. Oncol.* 7 (2015) 455–465, <https://doi.org/10.4251/wjgo.v7.i12.455>.
- [11] V. Ricci, M. Giannouli, M. Romano, R. Zarrilli, *Helicobacter pylori* gamma-glutamyl transpeptidase and its pathogenic role, *World J. Gastroenterol.* 20 (2014) 630–638, <https://doi.org/10.3748/wjg.v20.i3.630>.
- [12] P. Jain, Z.Q. Luo, S.R. Blanke, *Helicobacter pylori* vacuolating cytotoxin A (VacA) engages the mitochondrial fission machinery to induce host cell death, *Proc. Natl. Acad. Sci. U. S. A.* 108 (2011) 16032–16037, <https://doi.org/10.1073/pnas.1105175108>.
- [13] J.H. Martin, A. Potthoff, S. Ledig, M. Cornberg, O. Jandl, M.P. Manns, S. Kubicka, P. Flemming, C. Athmann, W. Beil, S. Wagner, Effect of *H. pylori* on the expression of TRAIL, FasL and their receptor subtypes in human gastric epithelial cells and their role in apoptosis, *Helicobacter* 9 (2004) 371–386, <https://doi.org/10.1111/j.1083-4389.2004.00269.x>.
- [14] N.L. Jones, A.S. Day, H.A. Jennings, P.M. Sherman, *Helicobacter pylori* induces gastric epithelial cell apoptosis in association with increased Fas receptor expression, *Infect. Immun.* 67 (1999) 4237–4242, <https://doi.org/10.1128/IAI.67.8.4237-4242.1999>.
- [15] K. Shibayama, Y. Doi, N. Shibata, T. Yagi, T. Nada, Y. Iinuma, Y. Arakawa, Apoptotic signaling pathway activated by *Helicobacter pylori* infection and increase of apoptosis-inducing activity under serum-starved conditions, *Infect. Immun.* 69 (2001) 3181–3189, <https://doi.org/10.1128/IAI.69.5.3181-3189.2001>.
- [16] S. Maeda, H. Yoshida, Y. Mitsuno, Y. Hirata, K. Ogura, Y. Shiratori, M. Omata, Analysis of apoptotic and antiapoptotic signalling pathways induced by *Helicobacter pylori*, *Gut* 50 (2002) 771–778, <https://doi.org/10.1136/gut.50.6.771>.
- [17] T.L. Cover, U.S. Krishna, D.A. Israel, R.M. Peek Jr., Induction of gastric epithelial cell apoptosis by *Helicobacter pylori* vacuolating cytotoxin, *Cancer Res.* 63 (2003) 951–957.
- [18] K.M. Kim, S.G. Lee, M.G. Park, J.Y. Song, H.L. Kang, W.K. Lee, M.J. Cho, K.H. Rhee, H.S. Youn, S.C. Baik, Gamma-glutamyltranspeptidase of *Helicobacter pylori* induces mitochondria-mediated apoptosis in AGS cells, *Biochem. Biophys. Res. Commun.* 355 (2007) 562–567, <https://doi.org/10.1016/j.bbrc.2007.02.021>.
- [19] H. Ashktorab, R.H. Dashwood, M.M. Dashwood, S.I. Zaidi, S.M. Hewitt, W. R. Green, E.L. Lee, M. Darempouran, M. Nouriaie, R. Malekzadeh, D.T. Smoot, *H. pylori*-induced apoptosis in human gastric cancer cells mediated via the release of apoptosis-inducing factor from mitochondria, *Helicobacter* 13 (2008) 506–517, <https://doi.org/10.1111/j.1523-5378.2008.00646.x>.
- [20] M.C.C. Lim, G. Maubach, A.M. Birkl-Toegelhofer, J. Haybaeck, M. Vieth, M. Naumann, A20 undermines alternative NF-kappaB activity and expression of anti-apoptotic genes in *Helicobacter pylori* infection, *Cell. Mol. Life Sci.* 79 (2022) 102, <https://doi.org/10.1007/s00018-022-04139-y>.
- [21] W. Schmitt, R. Haas, Genetic analysis of the *Helicobacter pylori* vacuolating cytotoxin: structural similarities with the IgA protease type of exported protein, *Mol. Microbiol.* 12 (1994) 307–319, <https://doi.org/10.1111/j.1365-2958.1994.tb01019.x>.
- [22] S. Backert, T. Kwok, W. Konig, Conjugative plasmid DNA transfer in *Helicobacter pylori* mediated by chromosomally encoded relaxase and TraG-like proteins, *Microbiology* 151 (2005) 3493–3503, <https://doi.org/10.1099/mic.0.28250-0> (Reading).
- [23] J. Traulsen, C. Zagami, A.A. Daddi, F. Boccellato, Molecular modelling of the gastric barrier response, from infection to carcinogenesis, *Best Pract. Res. Clin. Gastroenterol.* 50–51 (2021), 101737, <https://doi.org/10.1016/j.bpg.2021.101737>.
- [24] M.C.C. Lim, G. Maubach, O. Sokolova, M.H. Feige, R. Diezko, J. Buchbinder, S. Backert, D. Schluter, I.N. Lavrik, M. Naumann, Pathogen-induced ubiquitin-editing enzyme A20 bifunctionally shuts off NF-kappaB and caspase-8-dependent apoptotic cell death, *Cell Death Differ.* 24 (2017) 1621–1631, <https://doi.org/10.1038/cdd.2017.89>.
- [25] Z. Jin, Y. Li, R. Pitti, D. Lawrence, V.C. Pham, J.R. Lill, A. Ashkenazi, Cullin3-based polyubiquitination and p62-dependent aggregation of caspase-8 mediate extrinsic apoptosis signaling, *Cell* 137 (2009) 721–735, <https://doi.org/10.1016/j.cell.2009.03.015>.
- [26] L. Zhu, X. Cheng, J. Shi, L. Jiacheng, G. Chen, H. Jin, A.B. Liu, H. Pyo, J. Ye, Y. Zhu, H. Wang, H. Chen, J. Fang, L. Cai, T.C. Wang, C.S. Yang, S.P. Tu, Crosstalk between bone marrow-derived myofibroblasts and gastric cancer cells regulates cancer stemness and promotes tumorigenesis, *Oncogene* 35 (2016) 5388–5399, <https://doi.org/10.1038/ncr.2016.76>.
- [27] Q. Zhou, X. Wu, X. Wang, Z. Yu, T. Pan, Z. Li, X. Chang, Z. Jin, J. Li, Z. Zhu, B. Liu, L. Su, The reciprocal interaction between tumor cells and activated fibroblasts mediated by TNF-alpha/IL-33/ST2L signaling promotes gastric cancer metastasis, *Oncogene* 39 (2020) 1414–1428, <https://doi.org/10.1038/s41388-019-1078-x>.
- [28] Y. Miki, M. Yashiro, L. Moyano-Galceran, A. Sugimoto, M. Ohira, K. Lehti, Crosstalk between cancer associated fibroblasts and cancer cells in scirrhous type gastric cancer, *Front. Oncol.* 10 (2020), 568557, <https://doi.org/10.3389/fonc.2020.568557>.
- [29] K. Nakazawa, M. Yashiro, K. Hirakawa, Keratinocyte growth factor produced by gastric fibroblasts specifically stimulates proliferation of cancer cells from scirrhous gastric carcinoma, *Cancer Res.* 63 (2003) 8848–8852.
- [30] C. Sun, H. Fukui, K. Hara, X. Zhang, Y. Kitayama, H. Eda, T. Tomita, T. Oshima, S. Kikuchi, J. Watari, M. Sasako, H. Miwa, FGF9 from cancer-associated fibroblasts is a possible mediator of invasion and anti-apoptosis of gastric cancer cells, *BMC Cancer* 15 (2015) 333, <https://doi.org/10.1186/s12885-015-1353-3>.
- [31] M. Fiorentino, H. Ding, T.G. Blanchard, S.J. Czinn, M.B. Szein, A. Fasano, *Helicobacter pylori*-induced disruption of monolayer permeability and proinflammatory cytokine secretion in polarized human gastric epithelial cells, *Infect. Immun.* 81 (2013) 876–883, <https://doi.org/10.1128/IAI.01406-12>.
- [32] K. Schweitzer, O. Sokolova, P.M. Bozko, M. Naumann, *Helicobacter pylori* induces NF-kappaB independent of CagA, *EMBO Rep.* 11 (2010) 10–11, <https://doi.org/10.1038/embor.2009.263>, author reply 11–12.
- [33] O. Sokolova, G. Maubach, M. Naumann, MEK3 and TAK1 synergize to activate IKK complex in *Helicobacter pylori* infection, *Biochim. Biophys. Acta* 2014 (1843) 715–724, <https://doi.org/10.1016/j.bbamer.2014.01.006>.
- [34] G. Maubach, M.C.C. Lim, O. Sokolova, S. Backert, T.F. Meyer, M. Naumann, TIFA has dual functions in *Helicobacter pylori*-induced classical and alternative NF-kappaB pathways, *EMBO Rep.* 22 (2021), e52878, <https://doi.org/10.15252/embr.202152878>.
- [35] S. Chaitongyot, P. Jantaree, O. Sokolova, M. Naumann, NF-kappaB in gastric cancer development and therapy, *Biomedicine* 9 (2021) 870, <https://doi.org/10.3390/biomedicine9080870>.
- [36] J. Ferrand, P. Lehours, A. Schmid-Alliana, F. Megraud, C. Varon, *Helicobacter pylori* infection of gastrointestinal epithelial cells in vitro induces mesenchymal stem cell migration through an NF-kappaB-dependent pathway, *PLoS One* 6 (2011), e29007, <https://doi.org/10.1371/journal.pone.0029007>.
- [37] G. Krzysiek-Maczka, A. Targosz, U. Szczyrk, T. Wrobel, M. Strzalka, T. Brzozowski, J. Czyz, A. Ptak-Belowska, Long-term *Helicobacter pylori* infection switches gastric epithelium reprogramming towards cancer stem cell-related differentiation program in Hp-activated gastric fibroblast-TGFbeta dependent manner, *Microorganisms* 8 (2020) 1519, <https://doi.org/10.3390/microorganisms8101519>.
- [38] M.P. Amaral, K.R. Bortoluci, Caspase-8 and FADD: where cell death and inflammation collide, *Immunity* 52 (2020) 890–892, <https://doi.org/10.1016/j.immuni.2020.05.008>.

Chapter 5. Publication III

On-a-chip-based sensitive detection of drug-induced apoptosis in polarized gastric epithelial cells

This study has been published in the journal ACS Biomaterials Science and Engineering on 31st October 2021 and reprinted in this thesis with permission and is cited as follows:

Bakhchova, L.†, Jantaree, P.†, Gupta, A., Isermann, B., Steinmann, U., & Naumann, M. (2021). On-a-chip-based sensitive detection of drug-induced apoptosis in polarized gastric epithelial cells. *ACS Biomater Sci Eng*, 7(12), 5474–5483. <https://doi.org/10.1021/acsbomaterials.1c01094>
Copyright © 2021, American Chemical Society

†Both authors contributed equally to this work

Contribution to the publication

Jantaree, P.	Designed the study Performed experiments Analysed and interpreted data Wrote the manuscript
Bakhchova, L	Designed the study Fabricated microfluidic chips Wrote the manuscript
Gupta, A.	Intellectual supported
Isermann, B.	Intellectual supported
Steinmann, U.	Intellectual supported Edited the manuscript
Naumann, M.	Conceived the study Designed the study Edited the manuscript

On-a-Chip-Based Sensitive Detection of Drug-Induced Apoptosis in Polarized Gastric Epithelial Cells

Liubov Bakhchova,^{*,†} Phatcharida Jantaree,[†] Anubhuti Gupta, Berend Isermann, Ulrike Steinmann, and Michael Naumann



Cite This: *ACS Biomater. Sci. Eng.* 2021, 7, 5474–5483



Read Online

ACCESS |



Metrics & More



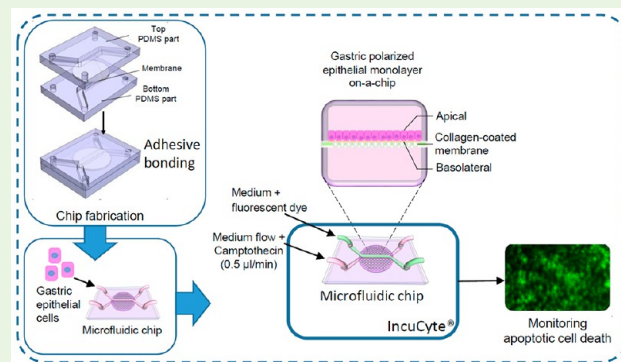
Article Recommendations



Supporting Information

ABSTRACT: Microfluidic devices for culturing cells have been successfully utilized for biomedical applications, including drug screening. Several cell lines could be cultivated in microengineered environments with promising results, but gastric cell lines have not yet been widely used or studied. Therefore, this study focuses on establishing a polarized gastric epithelial monolayer on-a-chip and describes a general-purpose methodology applicable for bonding any porous material to PDMS through an adhesive sublayer. The fully transparent microfluidic chip consists of two microfluidic channels separated by a collagen-coated porous membrane and lined by human polarized gastric epithelial (NCI-N87) cells. We present considerations on how to ensure continuous and stable flow through the channels. The continuous flow rate was achieved using a pressure-driven pump. Media flow at a constant rate ($0.5 \mu\text{L}/\text{min}$) rapidly led the gastric epithelial cells to develop into a polarized monolayer. The barrier integrity was assessed by the FITC-dextran test. The generation of a monolayer was faster than in the static Boyden chamber. Moreover, fluorescence microscopy was used to monitor the apoptotic cell death of gastric epithelial monolayers on-a-chip in response to camptothecin, a therapeutic gastric cancer drug.

KEYWORDS: camptothecin, drug testing, microfluidics, polarized gastric epithelial cell model



INTRODUCTION

Several studies investigated the impact of therapeutic drugs on human cells of different origins using microfluidic technology.¹ However, work about polarized gastric epithelial cells on-a-chip for drug testing is limited.^{2–4} Nevertheless, a significant number of results have already proved the utility of microfluidic devices for cell culture and drug testing experiments.^{5,6} A cell culture chip configuration with two microfluidic channels divided by a porous membrane is optimal for monolayer cell culture as it allows cell growth on the membrane with media flow through the top and bottom channels, which is highly suitable for drug testing.^{5,7,8}

The most common material for chip fabrication is polydimethylsiloxane (PDMS), which is transparent and gas permeable.⁹ Because the microfluidic chip with cultured cells is a dynamic model and continuous pumping is required, the gas permeability fades into the background in importance compared to transparency. The medium's flow supports cells with the gas dissolved in it and delivers the nutrient, which is necessary for cell growth. Proving that cells cover the membrane wholly and homogeneously is essential before starting further experiments, e.g., paracellular permeability measurements and drug testing. Where appropriate, it is best and more cost-efficient to avoid

using fluorescent dye at this stage and instead use an optical microscope. Therefore, not only the “chip body” has to be transparent, but the membrane as well. In several studies, authors used polycarbonate as a translucent membrane material.¹⁰ When using such a membrane, it is necessary to resort to a fluorescent approach to analyze the cell layer's confluency. The membrane can also be fabricated from PDMS,^{11–13} but the process is time consuming and handling of micrometer-thick flexible layers is challenging. Therefore, commercially available transparent polyester membranes are more appropriate. Because of the difference in the material properties, the bonding of PDMS and polyester cannot be done without modifying the surfaces.

In our study, we report a step-by-step technology for PDMS chip fabrication with a $10 \mu\text{m}$ thick polyester membrane bonded with an adhesive liquid PDMS layer. The functional area of the

Received: August 27, 2021

Accepted: October 5, 2021

Published: October 31, 2021



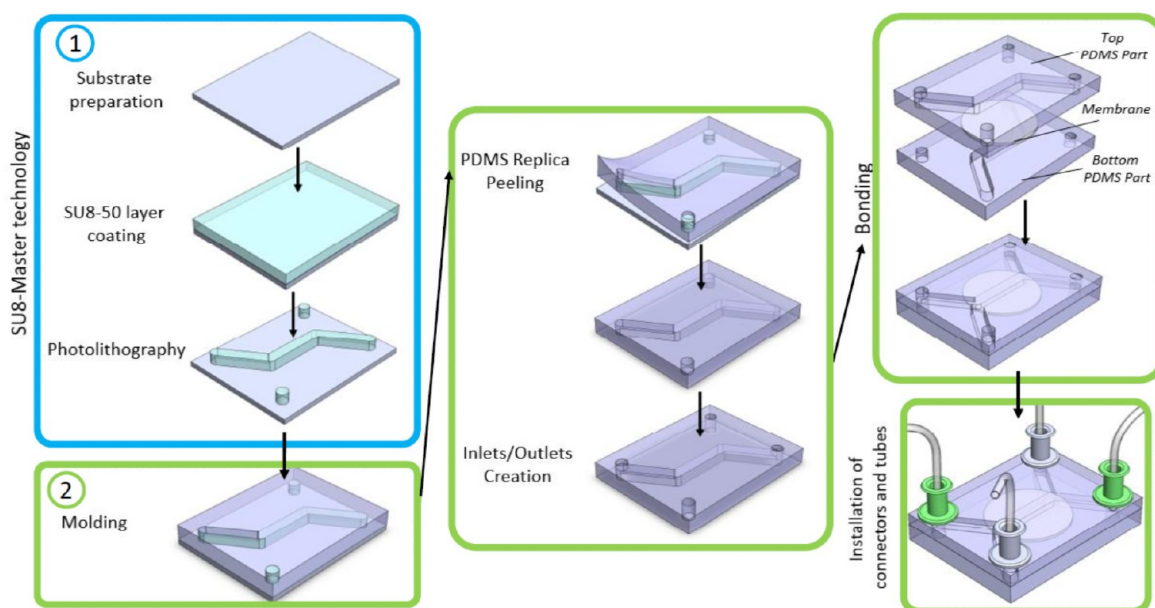


Figure 1. Schematic of the PDMS/polyester microfluidic chip fabrication. The main technological steps are represented by the fabrication of the master wafer, then replicating the master structures in PDMS by molding technology, preparing the cured PDMS layer (cut, outlets creation), and bonding the two equal parts of PDMS to a polyester membrane.

membrane in the channel remains unaffected. We describe the PDMS microfluidic chip fabrication procedure as a micro-engineered environment for a polarized gastric epithelial monolayer on-a-chip culturing. Providing proper media flow to the chip is of paramount importance. This is achieved by a pressure-driven pump with precise, stable flow at even low flow rates.¹⁴ In addition, we used a microfluidic device with a polarized gastric epithelial monolayer to analyze apoptotic cell death in response to a chemotherapeutic drug (CPT) in an IncuCyte automated fluorescent microscope. This provides a robust and adaptive approach for drug testing applications.

■ MICROFLUIDIC CHIP FABRICATION

Materials.

- Reagents and supplies:
 - Silicone 4 in. wafers, single side polished (Wafer Universe GmbH, Elsoff, Germany)
 - Photoresist SU8-100 (MicroChem GmbH, Ulm, Germany)
 - Developer mrDev-600 (MicroChem GmbH, Ulm, Germany)
 - Isopropanol (MicroChem GmbH, Ulm, Germany)
 - Polydimethylsiloxane, PDMS (Sylgard 184, Dow Inc.)
 - Polyester membrane, 10 μm thick, 3 μm pore size, pore density 2×10^6 pores/cm (Sterlitech Inc., Kent, USA)
 - Microfluidic male mini Luer lock connectors (microfluidic ChipShop GmbH, Jena, Germany)
 - DI water with inks (two colors)
- Equipment
 - Spin-coater LabSpin 6 (SüSS MicroTec GmbH, Garching, Germany);
 - Hot plate (SüSS MicroTec GmbH, Garching, Germany)
 - Mask aligner MA/BA (SüSS MicroTec GmbH, Garching, Germany)

- Plasma oven (ThermoFisher Scientific, International);
- Peristaltic pump (Ismatec GmbH, Reglo analog, Wertheim, Germany)

Procedure. The procedure is divided into three steps (Figure 1):

- (1) Master wafer fabrication (for molding) by soft lithography (6 h)
- (2) Molding and PDMS/polyester chip assembly (5 h/10 chips)
- (3) PDMS chip characterization (timing is flexible)

Master Mold Fabrication. Timing 6 h.

- (1) Dehydrate the silicone 4 in. wafer over 5 min at 200 °C and spin-coat photoresist SU8-100 on it at 1250 rpm over 60 s. *Note:* Leave the wafer with spin-coated SU8 on the planar surface for more than 30 min to avoid film thickness inhomogeneity.
- (2) The soft bake step is divided into two parts: Place the wafers with photoresist on the hot plate at 65 °C for 25 min and increase the temperature to 85 °C for 90 min. *Note:* do the soft bake step at reduced temperatures, at 85 °C instead of the recommended 95 °C.
- (3) Expose the wafer in the mask aligner at an exposure dose of 160 mJ/cm² with an appropriate shadow mask and the soft contact setting. *Note:* design the shadow mask without sharp corners to avoid microcracks at the photoresist structures (Supporting Information).
- (4) Postexposure bake the samples on the hot plate (shorter than the soft bake: 10 min at 65 °C followed by 15 min at 85 °C). *Note:* keep the wafer with photoresist SU8 on the hot plate for a slow cooling down.
- (5) Development follows during 60 min in developer mrDev600 and 2 min in isopropanol with constant stirring.

Molding and PDMS/Polyester Chip Assembly. Timing 5 h.

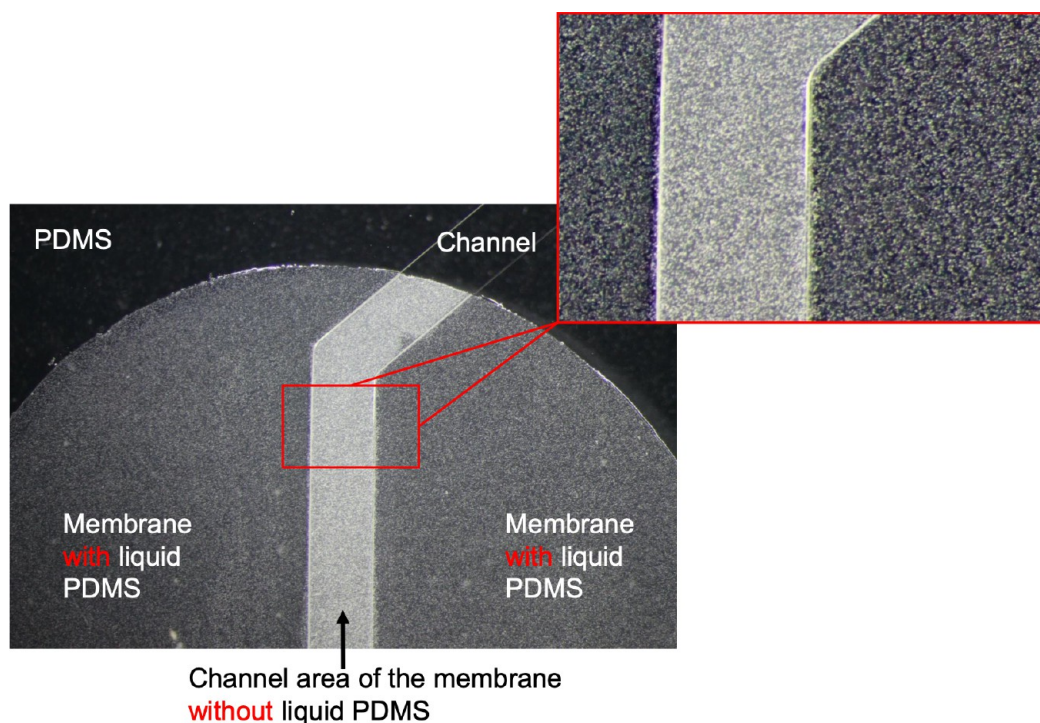


Figure 2. Microphotograph of the “doctor-blade” technique. Porous polyester membrane located on the structured PDMS layer with 1 mm wide microfluidic channel. Liquid PDMS was applied to all areas except for the channel area. The magnification shows that the membrane is clean and the pores are not clogged by liquid PDMS.

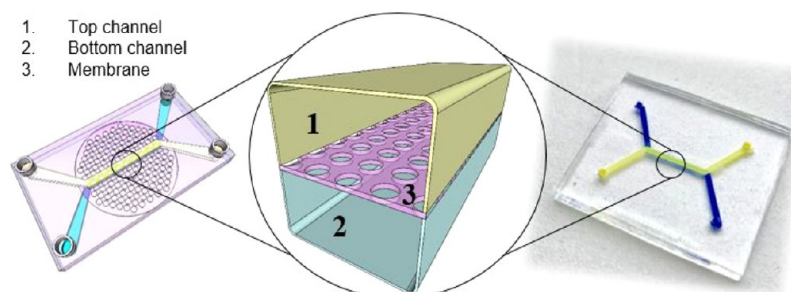


Figure 3. Schematic configuration and photograph of the microfluidic chip for cell culture. Two microfluidic channels (1 and 2) are divided by a porous membrane (3). Dimensions of the channels in the chip are width 1000 μm , height 200 μm . Each channel has an inlet and an outlet.

- (1) Standard PDMS mixing ratio 10:1 (base:curing agent, respectively) is used. Two components have to be mixed with magnetic stirring for 20 min.
- (2) Place 10 mL of pure PDMS on the 4 in. master wafer (mold) and cure it at room temperature for more than 48 h (or at elevated temperatures, 60 $^{\circ}\text{C}$ for 3 h under vacuum).
- (3) As shown in Figure 1: peel the cured PDMS replica off the master mold and cut it; punch holes for the inlets and outlets in the marked spots.
- (4) Next, proceed with the surface treatment with oxygen plasma over 1 min at a pressure of 0.5 mbar and a generator power of 140 W.
- (5) Apply liquid PDMS, prepared at the conditions described before, on the plasma-treated surface of the cured PDMS with the blade in the range of micrometers (doctor-blade technique). Because of this technique, liquid PDMS is distributed only among the desired area. Therefore, the membrane’s area in the channel stays nontouched, liquid PDMS does not clog the pores, and there is no influence on the permeability (Figure 2). *Note:* this step has to be done seconds after the plasma surface treatment.
- (6) Treat one surface of the polyester membrane with oxygen plasma over 20 s, place it on the liquid PDMS layer, and leave it for 10 min.
- (7) Treat the other side of the membrane, which is already on the PDMS chip part, with oxygen plasma over 20 s.
- (8) Apply the next layer of the liquid PDMS by blade screening on the plasma-treated surface of the membrane and leave it for 10 min. *Note:* the 10 min waiting steps are essential for PDMS to fill the pores of the membrane and can be extended.
- (9) Place the prepared half of the chip on the hot plate for 1 h at 110 $^{\circ}\text{C}$.
- (10) Treat the surfaces of the two PDMS replicas (one with membrane and one without) with oxygen plasma over 1 min.
- (11) Align the two halves of the chip in such a way that the channel in one part will face the channel on the other part through the membrane.

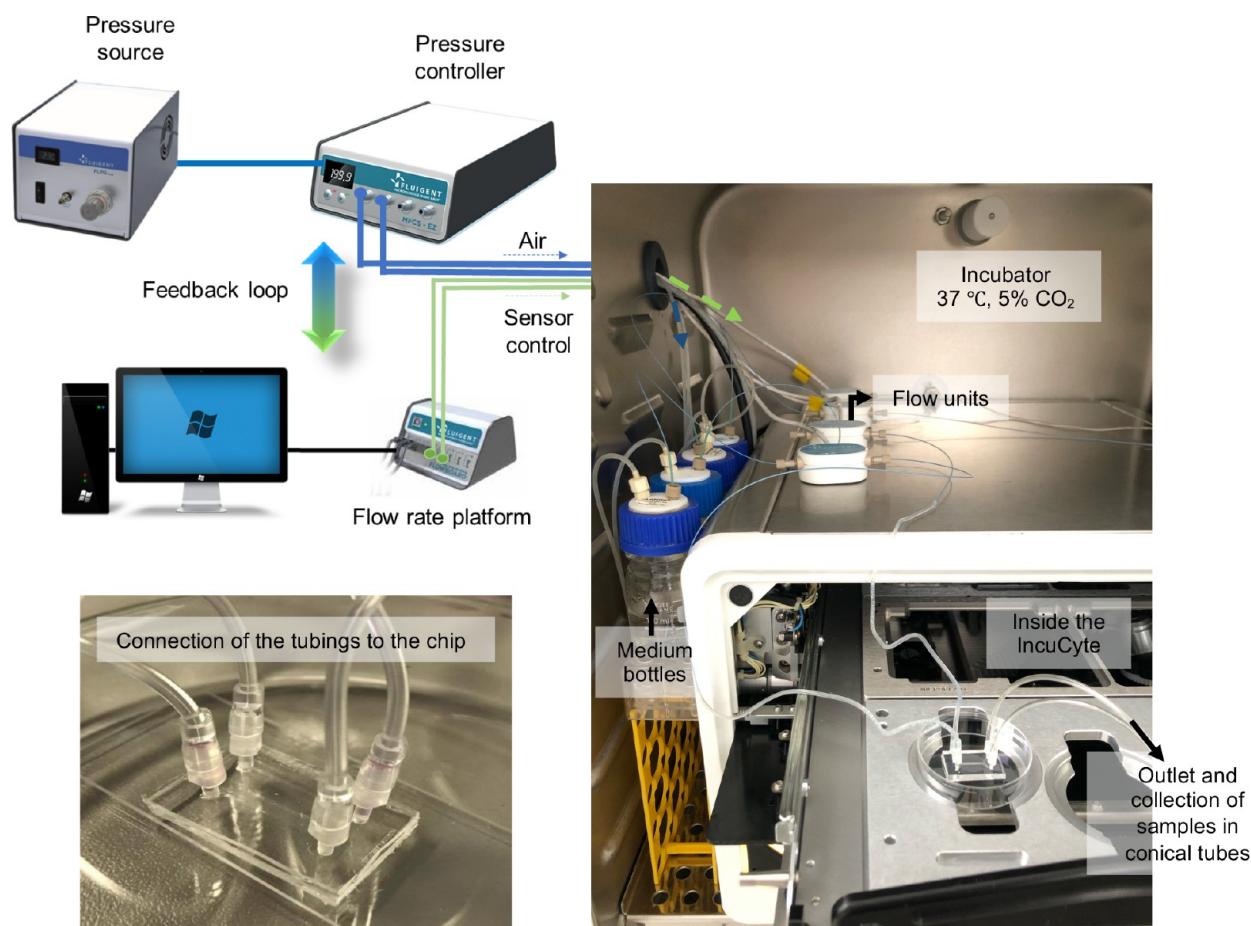


Figure 4. Schematic view of the combination of the pressure-driven pumping system, an IncuCyte automated fluorescent microscope for live-cell analysis, and the microfluidic device for cell culture. In the IncuCyte, the chip is situated on the 35 mm well plate, to which it adheres on the bottom on its own because of the sticky properties of the material itself.

- (12) Bake the chip on the hot plate over 10 min at 80 °C to perform bonding of the layers.
- (13) Chip is then ready and can be characterized to prove the bonding strength, or the membrane can be coated with the collagen to prepare the chip for cell culture (Figure 3).

PDMS Chip Characterization. The most appropriate way to test the microfluidic devices prior to the experiments is a leakage test:

- (1) Connect two inlets of the chip to the tubes that are fed from the peristaltic pump.
- (2) Dip the other end of the tubes into aqueous reservoirs with differently colored liquids. *Note:* use the microscopic inks and choose the colors in a way that will best distinguish the two liquids.
- (3) First option: start pumping with the chosen flow rate (e.g., 0.5 $\mu\text{L}/\text{min}$) and record the time until leakage appears (it will be clearly seen because of the colored liquid). *Note:* in this way, one can realize the time, how long the chip can be pumped. If leakage does not appear over a long time (e.g., a month), the bonding strength can be taken as ideal.
- (4) Second option: start pumping and set the end time of the experiment (e.g., one month) and of the initial flow rate (e.g., 0.5 $\mu\text{L}/\text{min}$). Change the flow rate on the set value (e.g., 0.5 $\mu\text{L}/\text{min}$) after every equal period (e.g., 1 day). Record the value of the flow rate when leakage appears. *Note:* in this way, one will realize the flow rate or its range,

which is the best to use with this chip over the long period of pumping. If there is no leakage until the end of the experiment, the bonding strength can be considered ideal.

CELL CULTURE AND TREATMENTS

Materials.

- Reagents and supplies:
 - Human gastric epithelial cell line NCI-N87 (ATCC)
 - Roswell park memorial institute 1640 medium (RPMI) with L-glutamine (1X) (Gibco)
 - Penicillin-streptomycin (100x) (Gibco)
 - Fetal calf serum (FCS) (Life Technologies)
 - 0.25% Trypsin EDTA (1X) (Gibco)
 - Dulbecco's phosphate-buffered saline (DPBS) (Gibco)
 - Ethanol (J.T.Baker)
 - Camptothecin >90% (HPLC) powder (Sigma)
 - Dimethyl sulfoxide (DMSO) > 99.7% (Sigma)
 - Fluorescein isothiocyanate (FITC)-labeled dextran (3–5 kDa) (Sigma)
 - Caspase-3/7 green reagent (Essen Bioscience)
 - Collagen I, bovine (5 mg/mL) (Gibco)
 - Acetic acid (Sigma)
- Equipment:

- General equipment for cell culture: cell culture flasks/dishes (Greiner bio-one); 1.5 mL tube (Greiner bio-one); 15 mL conical sterile centrifuge tube (Greiner bio-one); 5 and 10 mL sterile pipettes (Corning); micropipettes; incubator (37 °C, 5% CO₂) (Binder); biosafety cabinet (Herasafe KS, Thermo fisher); centrifuge (Eppendorf); cell counter (Invitrogen)
- Cell culture inserts for 12-well multiwell plate (113 mm² culture surface, 1.0 μm pore size membrane) and 12-well multiwell plates (Greiner bio-one)
- Oven 60 °C (Binder)
- Microfluidic flow control system (Fluigent): low-pressure generator (FLPG PLUS), microfluidic flow controller (MFCS-EZ), flowboard, flow-unit sensor, airtight bottle-caps, tubing and fitting kit: Flow Unit LQ connector for 1/32 in. outer diameter (OD) tubing, Green sleeve 1/16 OD 0.033, inner diameter (ID) 1.6, Blue PEEK Tubing 1/32 in. OD and 0.010 ID, Adapter PEEK 1/16 in. to 1/32 in. OD tubing;
- Tubing extension and connectors: Tygon ST R-3607 ID 0.13 mm, OD 1.95 mm tubing from Ismatec Cole-Parmer GmbH, Germany; connectors for the chip, Mini Luer Fluid Connector Fluidic 331 from the “Microfluidic ChipShop”, Germany
- Multimode microplate reader/spectrofluorometer (SpectraMax M5, Molecular devices)
- Fluorescence microscope (Keyence)
- IncuCyte (Essen bioscience)

Procedure. Collagen-Coating of the Membrane in the Chip.

- (1) Sterilization of the microfluidic chip:
 - Wash microfluidic channels with 70% (v/v) ethanol.
 - Dry the entire chip by placing it in a 60 °C oven.
 - Place the chip in a biosafety cabinet and expose it to ultraviolet light for 30 min.
- (2) Prepare collagen solution (50 μg/mL) in 0.02% acetic acid.
- (3) Inject the collagen solution into the top channels of the chip using a micropipette, and then incubate the chip at 37 °C for 1 h.
- (4) Wash the microfluidic channels twice with DPBS and perfuse them with culture medium. *Note:* these processes were performed on the same day before cell seeding and should be done in a biosafety cabinet.

Culturing of NCI-N87 Cells. Human gastric epithelial cells NCI-N87 were grown in RPMI 1640 medium supplemented with 10% FCS and 1% penicillin-streptomycin.

- In the microfluidic chip:
 - (1) Harvest NCI-N87 cells using trypsin and EDTA and adjust the concentration to 9×10^6 cells/mL.
 - (2) Plate the NCI-N87 cells on the collagen-coated membrane by gently filling the cell solution into the top channel (cell density = 1800 cells/mm²).
 - (3) Allow the cells to attach to the collagen-coated membrane for 4–6 h in an incubator at 37 °C.
 - (4) Remove the nonadherent cells by flushing media through the channels.

- (5) Connect the microfluidic chip to the flow system (Figure 4). *Note:* the microfluidic chip, medium bottles and tubes, and flow unit sensors were kept in an incubator at 37 °C; all the flasks and connections in the incubator have to be sealed to avoid evaporation of the medium and thereby contamination of the IncuCyte fluorescence microscope.

- (6) Media flowed through both top and bottom channels at a constant rate of 0.5 μL/min.

- In the Boyden chamber:

- (1) Precoat the cell culture insert membrane with the same collagen solution (100 μL/insert) and incubate and wash as described previously.

- (2) Harvest NCI-N87 cells with trypsin EDTA and prepare them at 2×10^5 cells/mL. *Note:* By this cell number, we get a cell density of 1800 cells/mm² after seeding, the same as on a chip.

- (3) Seed NCI-N87 cells (1 mL) on the top surface of the collagen-coated membrane and add medium (2 mL) to the bottom chamber.

- (4) Refresh the medium every day on both the apical and basolateral sides.

Paracellular Permeability Measurement. The cell monolayer's integrity was determined by measuring the amount of fluorescein isothiocyanate (FITC)-labeled dextran transported from the apical to the basolateral surface of the cell monolayer over time.

- In the microfluidic chip:

- (1) At each time point, perfuse a medium containing FITC-dextran (1 mg/mL) through the top channel at a constant flow rate of 0.5 μL/min. *Note:* the lower channel was perfused with medium without FITC-dextran; while changing the medium bottle, the pumping and flow system should be stopped to avoid the inconstant flow rate and bubble production; a chip without gastric epithelial cells was used as a blank membrane control.

- (2) Collect media from the top and bottom channels for 4 h.

- (3) Replace the medium in the top channel with medium without FITC-dextran. Further culture gastric epithelial cells on-a-chip until the next time point, after which the processes 1–3 should be repeated.

- (4) Measure the fluorescence intensity of the collected media in a spectrofluorometer with an excitation wavelength of 490 nm and an emission wavelength of 520 nm.

- (5) Present the gastric monolayer's permeability as relative permeability, reflecting a percentage of FITC-dextran transported across the gastric monolayer. Calculate relative permeability according to the following equation:

$$P_r = \frac{\frac{FI_{bot}}{FI_{top}}(\text{sample})}{\frac{FI_{bot}}{FI_{top}}(\text{blank})} 100\%$$

where P_r is the relative permeability (% FITC-dextran, normalized to the blank membrane), FI_{bot} is the fluorescence intensity of aliquot from the

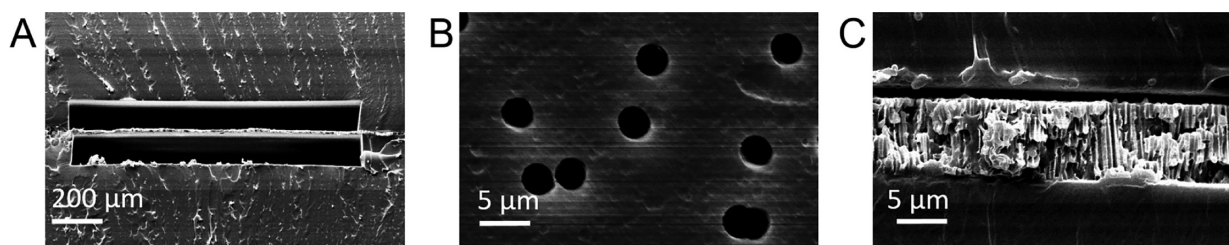


Figure 5. SEM microphotographs of (A) the chip cross-section, (B) membrane surface, and (C) membrane bonded to the two layers of PDMS in a cross-section.

bottom channel, and FI_{top} is the fluorescence intensity of aliquot from the top channel.

- In the Boyden chamber:
 - (1) At each time point, replace the medium in the inset (apical side) with 1 mL of medium containing FITC-dextran (1 mg/mL).
 - (2) Change the medium in the bottom chamber to fresh medium without FITC-dextran (2 mL). *Note:* a Boyden chamber without gastric epithelial cells was used as a blank membrane control.
 - (3) Incubate the chambers at 37 °C for 4 h.
 - (4) Collect aliquots from both the inset and the bottom chamber.
 - (5) Change the medium in the inset without FITC-dextran. Further culture the gastric epithelial cells until the next time point, after which processes 1–5 should be repeated.
 - (6) Measure the fluorescence intensity of the collected samples as described previously.
 - (7) Calculate relative permeability of the gastric monolayer as described previously.

4. Apoptotic Cell Death Assay. The gastric epithelial monolayer on-a-chip was prepared as described previously and maintained under 0.5 $\mu\text{L}/\text{min}$ flow conditions for 3 days to obtain a tight monolayer before starting the apoptotic cell death assay.

- (1) Place the gastric epithelial monolayer on-a-chip inside the IncuCyte and connect it to the flow system. *Note:* store the IncuCyte in an incubator and carry out experiments at 37 °C under 0.5 $\mu\text{L}/\text{min}$ flow conditions.
- (2) Expose the gastric monolayer on-a-chip from the basolateral side with medium containing CPT (20 μM). Simultaneously, provide the medium containing caspase-3/7 green reagent (medium: reagent = 1000:1) through the top channel. *Note:* prepare stock CPT at a concentration of 10 mM in DMSO; use cells exposed to 0.2% DMSO without CPT as a negative control.
- (3) Analyze phase-contrast and fluorescent images by the IncuCyte system according to the time setting, for example, every hour for 24 h. *Note:* analyze the intensity of the fluorescent stained apoptotic cells using the IncuCyte system or *ImageJ* software.

RESULTS AND DISCUSSION

Integrity of Gastric Epithelial Monolayer Is Improved with Continuous Media Flow. For the generation of the microfluidic device, we used liquid PDMS as an adhesive layer and polyester as a porous membrane (Figure 5). The primary strategy of the bonding is to fill the pores with liquid PDMS and cure and bond the membrane (Figure 2). The leakage test¹⁵

shows strong bonding between layers. It is noteworthy that the use of liquid PDMS as an adhesive layer is required for efficient bonding after plasma surface activation and is therefore crucial for a strong bond between the two connected PDMS layers (Figure 2). In contrast, Jang et al.⁷ used only plasma treatment, which is not sufficient for strong bonding of different polymers.

Indeed, Kim et al. showed the development of polarized columnar epithelium by an increase in the height of the cells within 3 days after applying media flow at 0.5 $\mu\text{L}/\text{min}$ across the apical surface of epithelial cells, whereas the cells in the Boyden chamber remained flat.¹⁶ Workman et al. reported that cells exposed to continuous media flow at 0.5 $\mu\text{L}/\text{min}$ for 5 days demonstrated homogeneous and near-complete chip coverage.⁵ Moreover, they also suggested that an increased flow rate to 1 $\mu\text{L}/\text{min}$ did not accelerate the process.^{5,16}

The human gastric epithelial cell line NCI-N87 was cultured in the chip to create a polarized epithelial cell monolayer.² With the applied 0.5 $\mu\text{L}/\text{min}$ flow rate, the chip is stable and reliable for pumping for more than a year. In the presented chip with a channel geometry of 1000 $\mu\text{m} \times 200 \mu\text{m}$ (cross section) at 37 °C, the medium velocity is approximately 0.05 mm/s and the liquid needs about 3 min to pass along a 1 cm channel. These conditions allow for continuous supply of the gastric epithelium monolayer with fresh medium and ensure that cells are not affected by the flow through the channel. Indeed, it was previously shown that the application of physiological fluid flow and shear stress across the apical surface of the epithelium increases the height and polarization of the cells.¹⁶ Gastric epithelial cells (1800 cells/ mm^2) grown under static conditions on-a-chip showed the formation of the cell layer after 1 day. However, the cells failed to develop a continuous confluent monolayer over time (Figure 6A), whereas cells on-a-chip with continuous media flow developed a nearly confluent monolayer after 1 day. Gastric epithelial cells grown in the Boyden chamber showed 70% confluence (Figure 6B). A fully confluent monolayer was observed after 3 days. Interestingly, the growth of cells on-a-chip was significantly faster than in the Boyden chamber (Figure 6B). Thus, the formation of a continuous confluent gastric epithelial monolayer is superior in a microfluidic chip with continuous media flow. Notably, the cells require optimal time for attachment to the collagen-coated membrane surface. Therefore, directly after seeding, the gastric epithelial cells were left in the incubator without media flow for at least 4 h. This period could be different for other cell types and must be found experimentally.

The gastric epithelium represents a barrier in the gastric mucosa and is composed of intercellular contact that seals the paracellular space between epithelial cells. Therefore, the paracellular permeability of the gastric epithelial monolayer was used as an indicator to assess the barrier integrity. The use of FITC-dextran showed that the paracellular permeability of the

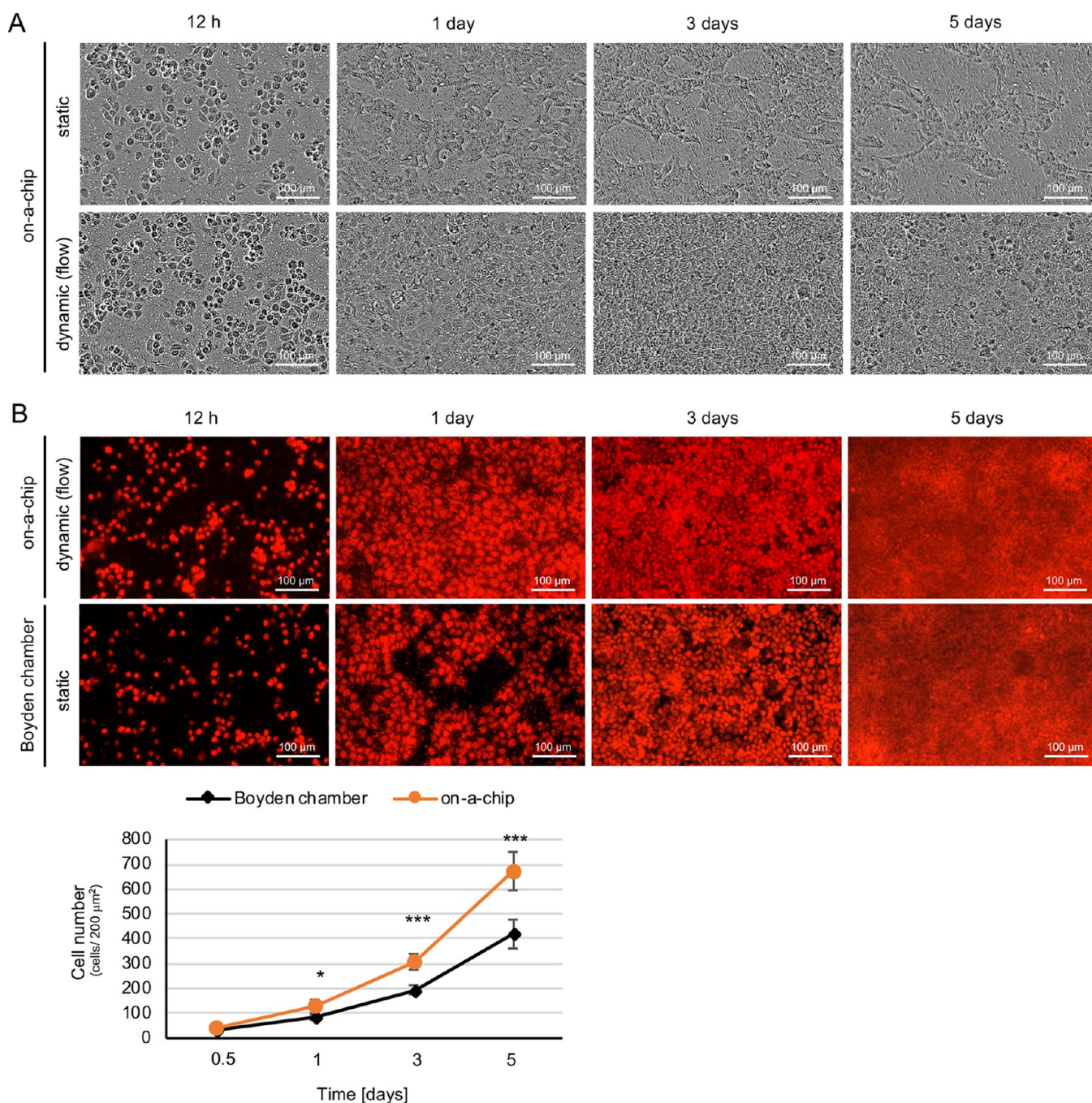


Figure 6. Formation of a continuous gastric epithelial monolayer on-a-chip. (A) Representative phase-contrast images of gastric epithelial cells on-a-chip. NCI-N87 cells were seeded at a density of 1800 cells/mm², and cells were analyzed with a continuous media flow at 0.5 μL/min after 0.5, 1, 3, and 5 days. Tayshe cells in the static chip were cultured without media flow. (B) Red fluorescent stained live cells on-a-chip or cells in the Boyden chamber. Cells were cultured in the media containing IncuCyte NuLight Rapid Red Dye and analyzed after the indicated time. The average numbers of cells from five fields were calculated and the comparison between cells on-a-chip and those in the Boyden chamber at each time point is presented (* $p < 0.05$, *** $p < 0.001$).

gastric epithelial monolayer on-a-chip was significantly decreased over time (Figure 7C), suggesting the formation of continuous intercellular contact. Further, the barrier integrity of cells cultured in the static Boyden chamber was assessed.

We observed that 1 day after seeding, the permeability of the gastric epithelial monolayer on-a-chip was much lower than in the Boyden chamber (Figure 7C). This finding suggested that the gastric epithelial monolayer formed more quickly under dynamic flow conditions in the microfluidic device. Immunofluorescence (IF) staining of E-cadherin within cell monolayer

after 5 days culturing on-a-chip or in the Boyden chamber confirmed the intercellular contact of the continuous cell monolayer (Figure 7D).

Microfluidic Device Is Suitable for Apoptotic Cell Death Analysis in IncuCyte. To demonstrate that the gastric epithelial monolayer on-a-chip was responsive to exogenous stimuli, we analyzed apoptotic cell death after treatment with CPT, a gastric anticancer drug in clinical use. CPT stabilizes the topo I-DNA covalent complex and blocks subsequent DNA relegation step that ultimately leads to DNA damage and

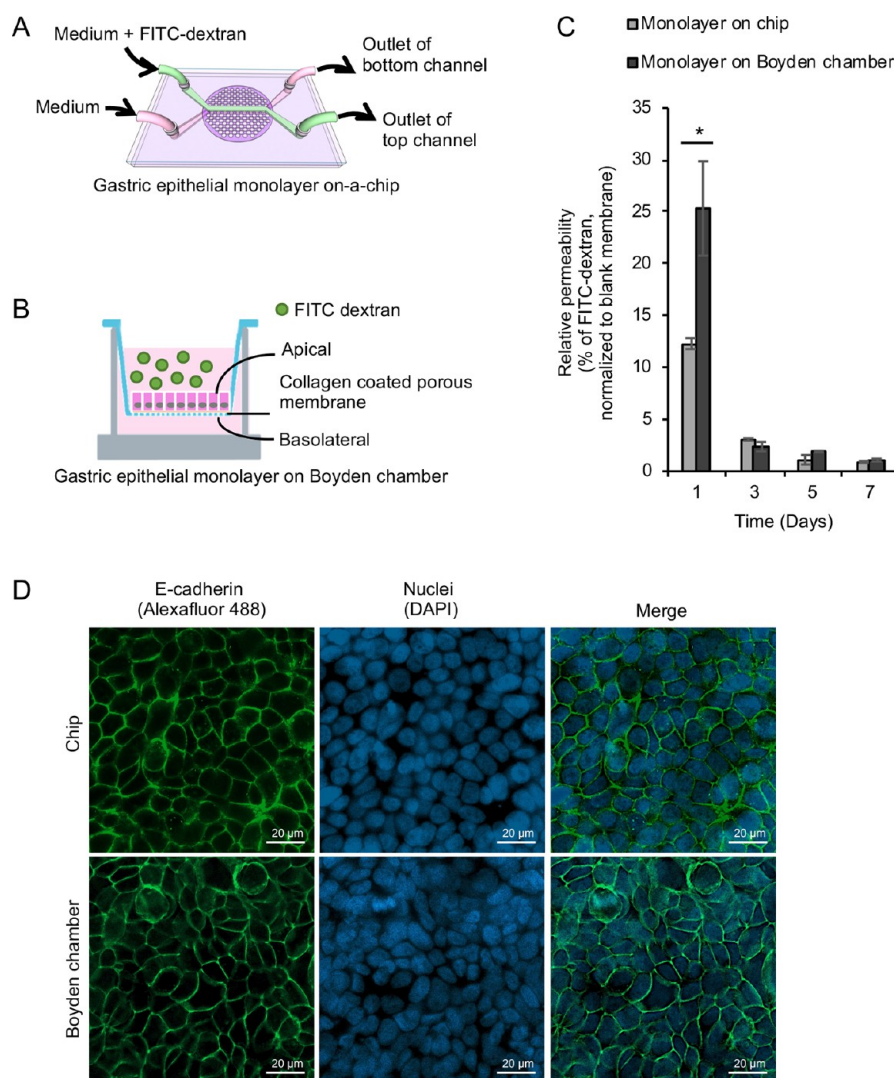


Figure 7. Gastric epithelial monolayer on-a-chip preserved the epithelial barrier integrity. (A) Schematic picture of the permeability measurement of the gastric epithelial monolayer on-a-chip. Medium containing FITC-dextran flowed through the top channel. The media from the top and bottom channels were collected after 4 h and measured for fluorescence intensity of FITC-dextran. (B) Schematic picture of permeability measurement of the gastric epithelial monolayer in Boyden chamber. At each time point, a medium containing FITC-dextran was added to the apical side. After incubation for 4 h, aliquots were collected from both apical and basolateral sides and measured for fluorescence intensity of FITC-dextran. (C) Relative permeability of gastric epithelial monolayer on-a-chip compared with the Boyden chamber, presented as percentages of FITC-dextran transported across the gastric epithelial monolayer (* $p < 0.05$). (D) Immunofluorescent images of E-cadherin (green) in the gastric epithelial monolayer grown for 5 days on-a-chip or in the Boyden chamber.

apoptosis.¹⁷ The gastric epithelial monolayer's basolateral side faces media flow from the bottom channel, which imitates cellular uptake from the bloodstream, for example, of nutrients and other compounds, including therapeutic drugs. Therefore, CPT was applied to the bottom channel in which the cells were exposed to CPT only from the basolateral side. The top channel's media flow contained caspase-3/7 green reagent, a couple of the activated caspase-3/7 recognition motifs (DEVD), and a DNA intercalating green fluorescent dye (Figure 8A) to quantify CPT-induced apoptotic cell death of the gastric epithelial monolayer over time.

In an apoptotic cell, activated caspase-3/7 cleaves the reagent at the DEVD recognition motif and releases a DNA binding dye that fluorescently labels the nuclear DNA of apoptotic cells. The microfluidic chips were placed inside the InCuCyte and connected to the flow system, allowing real-time monitoring of apoptotic cell death of gastric epithelial monolayer on-a-chip.

It was found that apoptotic cell death was induced after exposure to CPT within 8 h and increased in a time-dependent manner (Figure 8B, C). There was no apoptotic cell death in nontreated gastric epithelial monolayer. The stitched image of the gastric monolayer on-a-chip exposed to continuous media flow containing CPT for 24 h demonstrated cell death over all of the growth areas on a chip (Figure 8D). This study suggested that the gastric epithelial monolayer on-a-chip provide a suitable platform for studying drug responses. Of note, the two-channel chip setup allows us to detect not only apoptotic cell death, as shown here, but also other end points triggered by chemotherapeutics, such as inflammasome activation.

CONCLUSIONS AND FUTURE PERSPECTIVE

The presented microfluidic chip is flexible and transparent and allows a continuous laminar medium flow over months. Gastric polarized epithelial cells on-a-chip could provide broad utility to

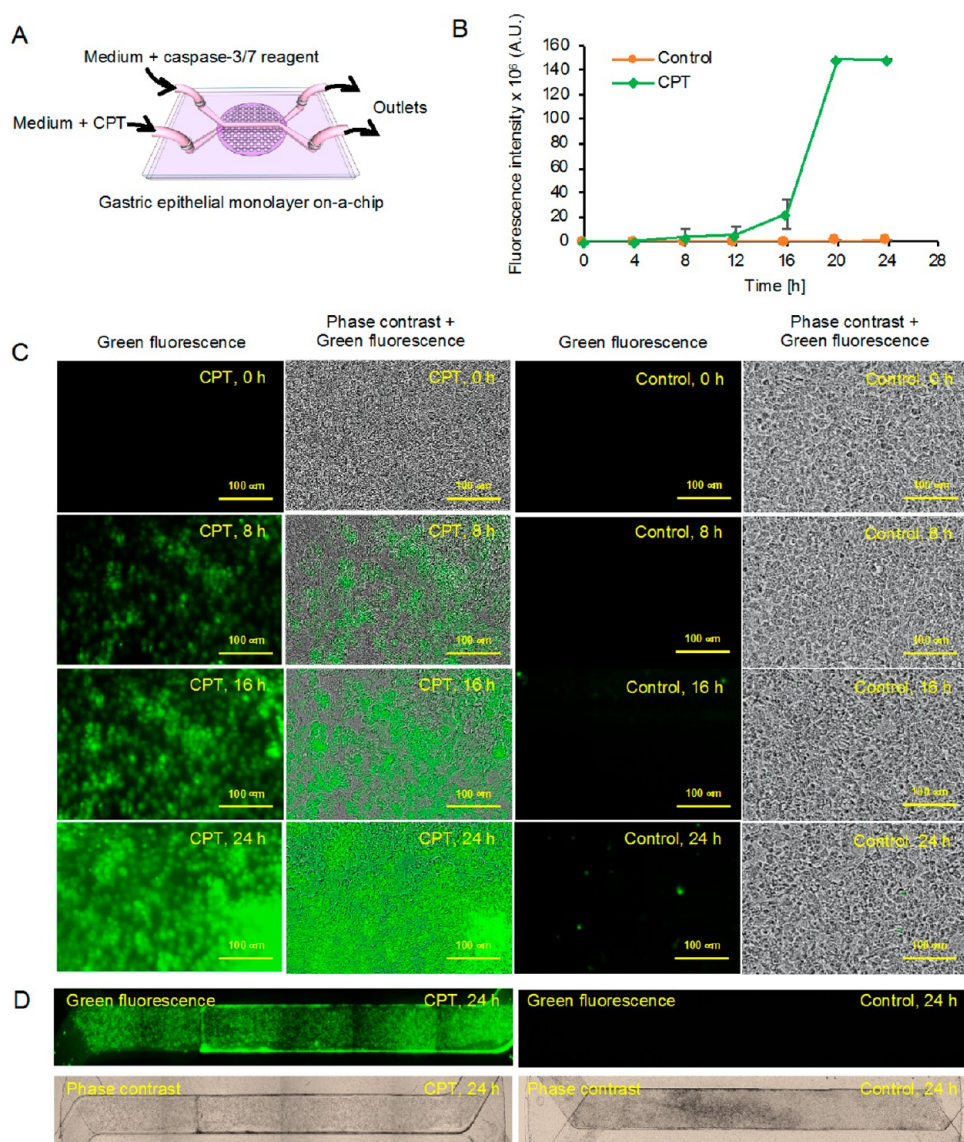


Figure 8. Real-time monitoring of the apoptotic cell death of the gastric epithelial monolayer on-a-chip using the IncuCyte live-cell analysis system. (A) Apoptotic cell death assay performed on-a-chip. Cells were exposed to CPT in the media flow of the bottom channel. At the same time, the medium containing caspase-3/7 reagent flowed through the top channel. The chip was placed in the IncuCyte for real-time monitoring of fluorescent stained apoptotic cells. (B) Fluorescence intensity of CPT-treated cells compared to control (0.2% DMSO treatment). (C) Representative fluorescent and phase-contrast images of gastric epithelial monolayer on-a-chip, automated capturing by the IncuCyte. (D) Stacked fluorescence and phase-contrast images of the gastric epithelial monolayer on-a-chip after 24 h of exposure to continuous media flow containing CPT or 0.2% DMSO (control).

study drug responses. However, other polarized cell types could be also used for drug testing including primary cells. Moreover, as drug efficacies and toxicities often rely on the individual,¹⁸ an engineered gastric epithelium monolayer on-a-chip with organoid-derived cells from an individual patient could reflect patient-specific features and support in identifying optimal treatment strategies. Moreover, microfluidic devices containing gastric monolayer organoids in a coculture of cells from the micromilieu can soon provide an even more near in vivo situation.¹⁹ Overall, the gastric epithelial monolayer on-a-chip promises to be a powerful tool for biomedical applications, including drug testing in preclinical studies.

■ ASSOCIATED CONTENT

Supporting Information

The Supporting Information is available free of charge at <https://pubs.acs.org/doi/10.1021/acsbomaterials.1c01094>.

AutoCAD file - master wafer design, which can be used to fabricate a shadow mask for soft lithography process (ZIP)

■ AUTHOR INFORMATION

Corresponding Author

Liubov Bakhchova – *Institute for Automation Technology, Otto von Guericke University, Magdeburg 39106, Germany; Institute of Experimental Internal Medicine, Medical Faculty, Otto von Guericke University, Magdeburg 39120, Germany;*
 orcid.org/0000-0003-0629-8357;
 Email: liubov.bakhchova@ovgu.de

Authors

Phatcharida Jantaree – *Institute of Experimental Internal Medicine, Medical Faculty, Otto von Guericke University, Magdeburg 39120, Germany*

Anubhuti Gupta – Institute of Experimental Internal Medicine, Medical Faculty, Otto von Guericke University, Magdeburg 39120, Germany; Institute for Laboratory Medicine, Clinical Chemistry and Molecular Diagnostic, Universitätsklinikum Leipzig, Leipzig 04103, Germany

Berend Isermann – Institute for Laboratory Medicine, Clinical Chemistry and Molecular Diagnostic, Universitätsklinikum Leipzig, Leipzig 04103, Germany

Ulrike Steinmann – Institute for Automation Technology, Otto von Guericke University, Magdeburg 39106, Germany

Michael Naumann – Institute of Experimental Internal Medicine, Medical Faculty, Otto von Guericke University, Magdeburg 39120, Germany

Complete contact information is available at:

<https://pubs.acs.org/10.1021/acsbiomaterials.1c01094>

Author Contributions

[†]L.B. and P.J. contributed equally to this work.

Notes

The authors declare no competing financial interest.

ACKNOWLEDGMENTS

The authors thank Dr. L. Deckert (Otto von Guericke University, Magdeburg) for CAD design and representation of the schematic view on the technological steps (Figure 1). This work was supported in part by Grant ZS/2016/04/78155 from the European Union Program European Regional Development Fund of the Ministry of Economy, Science and Digitalisation in Saxony Anhalt within the Center of Dynamic Systems to M.N. and U.S., and by grant 361210922/RTG 2408 (P1) of the German Research Foundation to M.N.

REFERENCES

- (1) Jodat, Y. A.; Kang, M. G.; Kiaee, K.; Kim, G. J.; Martinez, A. F. H.; Rosenkranz, A.; Bae, H.; Shin, S. R. Human-Derived Organ-on-a-Chip for Personalized Drug Development. *Curr. Pharm. Des.* **2019**, *24*, 5471–5486.
- (2) Fiorentino, M.; Ding, H.; Blanchard, T. G.; Czinn, S. J.; Szein, M. B.; Fasano, A. Helicobacter pylori-induced disruption of monolayer permeability and proinflammatory cytokine secretion in polarized human gastric epithelial cells. *Infect. Immun.* **2013**, *81*, 876–883.
- (3) Tegtmeyer, N.; Wessler, S.; Necchi, V.; Rohde, M.; Harrer, A.; Rau, T. T.; Asche, C. I.; Boehm, M.; Loessner, H.; Figueiredo, C.; Naumann, M.; Palmisano, R.; Solcia, E.; Ricci, V.; Backert, S. Helicobacter pylori Employs a Unique Basolateral Type IV Secretion Mechanism for CagA Delivery. *Cell Host Microbe* **2017**, *22*, 552–560.
- (4) Maubach, G.; Sokolova, O.; Täger, C.; Naumann, M. CEACAMs interaction with Helicobacter pylori HopQ supports the type 4 secretion system-dependent activation of non-canonical NF- κ B. *Int. J. Med. Microbiol.* **2020**, *310*, 151444.
- (5) Workman, M. J.; Gleeson, J. P.; Troisi, E. J.; Estrada, H. Q.; Kerns, S. J.; Hinojosa, C. D.; Hamilton, G. A.; Targan, S. R.; Svendsen, C. N.; Barrett, R. J. Enhanced Utilization of Induced Pluripotent Stem Cell-Derived Human Intestinal Organoids Using Microengineered Chips. *CMGH* **2018**, *5*, 669–677.
- (6) Kulthong, K.; Duivenvoorde, L.; Sun, H.; Confederat, S.; Wu, J.; Spengelink, B.; de Haan, L.; Marin, V.; van der Zande, M.; Bouwmeester, H. Microfluidic chip for culturing intestinal epithelial cell layers: Characterization and comparison of drug transport between dynamic and static models. *Toxicol. In Vitro* **2020**, *65*, 104815.
- (7) Jang, K. J.; Mehr, A. P.; Hamilton, G. A.; McPartlin, L. A.; Chung, S.; Suh, K. Y.; Ingber, D. E. Human kidney proximal tubule-on-a-chip for drug transport and nephrotoxicity assessment. *Integr. Biol.* **2013**, *5*, 1119–29.
- (8) Jalili-Firoozinezhad, S.; Prantil-Baun, R.; Jiang, A.; Potla, R.; Mammoto, T.; Weaver, J. C.; Ferrante, T. C.; Kim, H. J.; Cabral, J. M. S.; Levy, O.; Ingber, D. E. Modeling radiation injury-induced cell death and countermeasure drug responses in a human Gut-on-a-Chip. *Cell Death Dis.* **2018**, *9*, 223.
- (9) Kimura, H.; Sakai, Y.; Fujii, T. Organ/body-on-a-chip based on microfluidic technology for drug discovery. *Drug Metab. Pharmacokinet.* **2018**, *33*, 43–48.
- (10) Zhou, C.; Wang, K. Spatiotemporal Divergence of the Warming Hiatus over Land Based on Different Definitions of Mean Temperature. *Sci. Rep.* **2016**, *6*, 31789.
- (11) Zakharova, M.; Palma do Carmo, M. A.; van der Helm, M. W.; Le-The, H.; de Graaf, M. N. S.; Orlova, V.; van den Berg, A.; van der Meer, A. D.; Broersen, K.; Segerink, L. I. Multiplexed blood-brain barrier organ-on-chip. *Lab Chip* **2020**, *20*, 3132–3143.
- (12) Lamberti, A.; Marasso, S. L.; Cocuzza, M. PDMS membranes with tunable gas permeability for microfluidic applications. *RSC Adv.* **2014**, *4*, 61415–61419.
- (13) Huh, D.; Kim, H. J.; Fraser, J. P.; Shea, D. E.; Khan, M.; Bahinski, A.; Hamilton, G. A.; Ingber, D. E. Microfabrication of human organ-on-chips. *Nat. Protoc.* **2013**, *8*, 2135–2157.
- (14) Shen, F.; Li, Z.; Xue, S.; Li, M.; Liu, Z. Particle recirculating orbits within microvortices using microfluidics. *J. Phys. D: Appl. Phys.* **2021**, *54*, No. 025401.
- (15) Abidin, U.; Daud, N. A. S. M.; Le Brun, V. Replication and leakage test of polydimethylsiloxane (PDMS) microfluidics channel. *AIP Conf. Proc.* **2018**, *2062*, No. 020064.
- (16) Kim, H. J.; Huh, D.; Hamilton, G.; Ingber, D. E. Human gut-on-a-chip inhabited by microbial flora that experiences intestinal peristalsis-like motions and flow. *Lab Chip* **2012**, *12*, 2165–74.
- (17) Li, F.; Jiang, T.; Li, Q.; Ling, X. Camptothecin (CPT) and its derivatives are known to target topoisomerase I (Top1) as their mechanism of action: did we miss something in CPT analogue molecular targets for treating human disease such as cancer? *Am. J. Cancer Res.* **2017**, *7*, 2350–2394.
- (18) Pirmohamed, M. Pharmacogenetics: past, present and future. *Drug Discovery Today* **2011**, *16*, 852–861.
- (19) Jantaree, P.; Bakhchova, L.; Steinmann, U.; Naumann, M. From 3D Back to 2D Monolayer Stomach Organoids-on-a-Chip. *Trends Biotechnol.* **2021**, *39*, 745–748.

Chapter 6. Discussion

The human pathogen *H. pylori* colonises in the gastric epithelium and initiates different responses in the infected gastric epithelial cells, including NF- κ B activation, which is a trailblazer of gastric pathophysiology (Maubach et al., 2022). Notably, NF- κ B pathway, in addition to their function in innate immunity and inflammation, regulates crucial physiological processes, including apoptosis (Liu et al., 2017; Sokolova & Naumann, 2017). Furthermore, *H. pylori* infection is associated with significant gastric epithelial cell damages involving apoptotic cell death (Ashktorab et al., 2008; Cover et al., 2003; Jain et al., 2011; Jones et al., 1999; Kim et al., 2007; Maeda et al., 2002; Martin et al., 2004; Ricci et al., 2014; Shibayama et al., 2001). Consequently, dysregulated apoptotic cell death by the infection might lead to an accumulation of DNA damage, mutation, and malignant transformation of gastric epithelial cells. DUBs counteract ubiquitin modification and thereby contribute to the control of NF- κ B and cell survival. Therefore, this thesis addressed the role of the DUBs, USP48 and A20, in the regulation of NF- κ B and apoptotic cell death of *H. pylori*-infected gastric epithelium, as well as the impact from the micromilieu (gastric mucosal fibroblasts). Furthermore, a model of gastric epithelial cells on-a-chip was established as a tool for the study of drug- or *H. pylori*-induced apoptotic cell death in fluid-flow conditions.

6.1 USP48 counteracts UPS-dependent degradation of nuclear NF- κ B/RelA in gastric epithelial cells during *H. pylori* infection.

First, I studied classical NF- κ B activation and its regulation upon *H. pylori* infection (*chapter 3*). I observed fast activation of NF- κ B, which subsequently upregulated NF- κ B target genes, including *NFKBIA* (*publication 1, figure 1*). Activation of NF- κ B is controlled through the termination of NF- κ B/RelA by ubiquitylation and proteasomal degradation (Sacconi et al., 2004). Here, I found that *H. pylori* induced RelA ubiquitylation in the subnuclear fraction, reflecting a decreased nuclear RelA abundance within 6 h of infection. This result suggests that *H. pylori*-induced nuclear RelA is controlled by ubiquitylation. I further demonstrated that *H. pylori*-induced RelA ubiquitylation was abolished in the cells with depletion of elongin B, an adaptor protein of the CRL ECS^{SOCS1}. This result indicates that ECS^{SOCS1} is the predominant E3 ligase for RelA degradation in *H. pylori* infection, which is consistent with a previous study showing regulation of RelA ubiquitylation by ECS^{SOCS1} during TNF stimulation (Maine et al., 2007).

Ubiquitin ligation by the CRLs is inhibited by the protein complex CSN, which removes NEDD8 modifications from the cullin subunits and suppresses the ubiquitylation process (Dubiel et al., 2020). Interestingly, CSN has been reported to associate with DUBs including USP15 (Schweitzer et al., 2007), CYLD (Huang et al., 2021), STAMBPL1 (Chaithongyot & Naumann, 2022) and USP48 (Schweitzer & Naumann, 2015), which regulate different target proteins. In this study, the role of CSN-associated nuclear DUB USP48 in the regulation of NF- κ B was investigated in the context of *H. pylori* infection. Studying USP48-depleted gastric epithelial cells and the *in vitro* DUB assay, I demonstrated that USP48 deubiquitylated nuclear RelA through the

cleavage of poly-ubiquitin chains of nuclear RelA (*publication 1, figure 2*). As a result of nuclear RelA stabilisation, USP48 promoted sustained transcriptional activity of NF- κ B. This finding is consistent with the role of USP48 in the stabilisation of diverse target proteins, including Gli1, TRAF2, BRCA1, Mdm2, SIRT6, and Aurora B (*discussed in publication 1*). Additionally, I identified, using an *in vitro* binding assay, the CSN subunit 1 (CSN1) as a direct physical interaction partner of USP48. The role of CSN in nuclear RelA degradation was further investigated in CSN2 knockdown cells, which impairs the integrity and activity of the CSN complex. I found an increased accumulation of ubiquitinated RelA and a decrease of nuclear RelA abundance in the CSN2 depleted cells, suggesting that stabilisation of nuclear RelA in *H. pylori* infection is CSN-dependent. It was suggested that CSN could function as a platform for USP48-RelA interaction (Schweitzer & Naumann, 2015). However, physical interaction of the catalytic USP domain of USP48 and the N-terminal region of Rel homology domain (RHD) of RelA was demonstrated using an *in vitro* binding assay (Ghanem et al., 2019). Future investigation of CSN1-USP48 interacting domain would provide a better understanding of the structural interaction between the CSN, USP48 and RelA.

6.2 USP48 restrains apoptotic cell death of *H. pylori*-infected gastric epithelial cells in an A20-dependent mechanism.

Our previous data showed the NF- κ B dependent upregulation of A20 in the *H. pylori*-infected gastric epithelial cells. Furthermore, the A20 suppresses apoptotic cell death by removing K63-linked ubiquitin chains stamped onto caspase-8, interfering with caspase-8 activation (Lim et al., 2017). Regarding the finding that USP48 stabilises NF- κ B/RelA and prolongs its transcriptional activity during *H. pylori* infection, the hypothesis was raised that stabilization of NF- κ B/RelA mediated by USP48 might sustain A20 *de novo* synthesis and thereby suppress apoptotic cell death in *H. pylori* infection. In chapter 3, I demonstrated, using USP48 knockdown cells, that USP48 upregulated NF- κ B-induced A20 expression (*publication 1, figure 3*). Using FACS analysis of annexin V/PI staining and Incucyte® live-cell imaging analysis of caspase-3/7 staining, I found an increase of *H. pylori*-induced apoptotic cell death in USP48 depleted cells, indicating the protective effect of USP48 on *H. pylori*-induced apoptotic cell death. Moreover, USP48 suppressed K63-linked ubiquitinylation and activation of caspase-8, prompting to propose a mechanism in which USP48 deubiquitinylates caspase-8 and suppresses caspase cleavages and apoptotic cell death in a A20-dependent manner. I further examined this proposed mechanism by (1) transfecting recombinant USP48 protein into A20-depleted cells which showed that USP48 could not rescue *H. pylori*-induced caspase cleavages and apoptotic cell death in A20-depleted cells, and (2) transfecting recombinant A20 protein into USP48-depleted cells which showed that A20 rescued *H. pylori*-induced caspase cleavages in USP48-depleted cells (*publication 1, figure 4*). The results suggest that A20 is indispensable for the suppressing effect of USP48 on *H. pylori*-induced apoptotic cell death. These findings suggest the possibility of USP48 as a target for future therapeutic strategies. Future studies on how the USP48 is regulated during *H. pylori* infection would provide insights into the molecular pathogenesis of gastric disease.

6.3 Human gastric fibroblasts ameliorate *H. pylori*-induced A20 expression and suppress apoptotic cell death of gastric epithelial cells.

Several reports revealed that fibroblasts possess significant functions involving the control of proliferation, regeneration, differentiation, and apoptosis of epithelial cells via secreted factors (Boccellato et al., 2019; Gomes et al., 2021; Koh et al., 2019; Sigal et al., 2019). Thus, fibroblasts are essential for the homeodynamics of cells in the gastric mucosa, including the adjacent epithelial cells (Liu & Mak, 2022). In the other hand, infection of *H. pylori* in gastric epithelial cells might disturb a response of the gastric fibroblasts, which consequently affects cell inflammation and survival. However, the impact of gastric fibroblasts on the cell survival of gastric epithelial cells during *H. pylori* infection is not characterised. Due to the strong impact of DUBs and NF- κ B on cell survival in *H. pylori* infection, I further hypothesised that DUBs could affect apoptotic cell death within the crosstalk of epithelial cells and fibroblasts.

In chapter 4, the co-culture system of human gastric carcinoma epithelial NCI-N87 cells and human gastric fibroblasts was performed using the Boyden chamber (*publication II, figure 1C*). This system allowed NCI-N87 cells to grow as polarised cell monolayer on the porous membrane and acquire epithelial barrier integrity. By the epithelial's barrier function, *H. pylori* colonised at the NCI-N87 cells, but not fibroblasts that grew at the bottom of the chamber. Moreover, in this indirect-contact co-culture system, the cells communicated via secreted factors in the medium. I demonstrated that *H. pylori*-induced apoptotic cell death of polarised NCI-N87 cells was suppressed in the presence of co-cultured fibroblasts, but not with co-cultured NCI-N87 cells (*publication II, figure 2*), indicating the specific protective role of fibroblasts on apoptotic cell death of the polarised NCI-N87 cells. I further determined the impact of fibroblasts' conditioned media on *H. pylori*-induced cell death in polarised NCI-N87 cells. Results showed that the conditioned medium of fibroblasts after co-culture with *H. pylori*-infected polarised NCI-N87 cells possessed a protective effect against apoptotic cell death (*publication II, figure 3*). The results suggest that the fibroblasts could respond to factor(s) secreted basolaterally by *H. pylori*-infected polarised NCI-N87 cells and then secrete factors that suppress apoptosis in NCI-N87 cells. Multiple cytokines secreted by *H. pylori*-infected epithelial cells were reported, which may trigger the fibroblasts in this regard. For example, Fiorentino et al. (2013) showed that *H. pylori*-infected NCI-N87 cell monolayer secreted pro-inflammatory cytokines (IL-8, IL-6, TNF α , IFN γ , IL-12p70, IL-1 β) and anti-inflammatory cytokine (IL-10) from the basolateral site. Additionally, Ferrand et al. (2011) reported that several cytokines (primarily TNF), were secreted by *H. pylori*-infected gastrointestinal epithelial cells mainly via the NF- κ B-dependent pathway to recruit stromal cells to the site of infection. Moreover, it has been shown that factors secreted by fibroblasts promote the growth and survival of the epithelial cells, such as keratinocyte growth factor (Nakazawa et al., 2003) and fibroblast growth factor 9 (Sun et al., 2015).

Furthermore, I showed that the crosstalk between the gastric epithelial cells and fibroblasts is accompanied by a transient increase in phospho-I κ B α and a substantial increase in the expression of the NF- κ B-regulated A20 in *H. pylori*-infected NCI-N87 cells, when co-cultured with fibroblasts (*publication II, figure 4A*). Interestingly, co-

culture with fibroblasts also suppressed the extent of caspase-8 and -3 cleavages in NCI-N87 cells during *H. pylori* infection. Therefore, the contribution of A20 expression on fibroblasts' suppressive effect was further examined. Depletion of A20 increased cleavage of caspase-8 and -3 when compared with the scrambled control in polarised NCI-N87 cells co-cultured with fibroblasts, indicating that enhanced expression of A20 contributes to the fibroblasts' suppressive effect. Additionally, caspase-8 inhibitor (Z-IETD-FMK) suppressed caspase-8-dependent apoptotic cell death induced by *H. pylori* infection to the same extent as the fibroblast co-culture (*publication II, figure 5*), suggesting that fibroblasts could suppress caspase-8-dependent apoptotic cell death in NCI-N87 cells. In addition, the co-culture of patient-derived gastric mucosoids and fibroblasts, mimicking *in vivo* gastric epithelium-stroma communication, showed a protective effect of fibroblasts on apoptotic cell death of gastric mucosoids during *H. pylori* infection (*publication II, figure 6*). Therefore, I suggest that factor(s) secreted from *H. pylori*-infected gastric epithelial cells trigger fibroblasts' responses, including secretion of survival-promoting factor(s). Fibroblasts' factor(s) then intensify the NF- κ B activation and A20 expression in the gastric epithelial cells and subsequently suppress apoptotic cell death. Future research should be directed to the identification of the secreted factor(s) implicated in this crosstalk.

6.4 Analysis of drug-induced apoptotic cell death in polarised gastric epithelial cells on-a-chip

Cells-on-a-chip are the emerging tools for the *ex vivo* recapitulation of organ systems which show great potential in revolutionising the drug development pipeline (Ma et al., 2021). Several microfluidic chip models from different organs were suggested for applications in precision medicine and biological defence strategies (Wu et al., 2020). However, there are limited studies on the microfluidic chip system and the gastric epithelium. Therefore, in chapter 5, the polarised gastric epithelial monolayer on-a-chip was established. The chamber of the cell culture chip was made from PDMS, which is transparent, flexible and gas permeable. The chip was configured with two microfluidic channels divided by a porous polyester membrane (*publication III, figure 3*) and connected with the pressure-driven pumping system to give a constant media flow (0.5 μ l/min) (*publication III, figure 4*). Here, Ms Liubov Bakchova fabricated the microfluidic chip and set up of pumping system. Notably, the chip was integrated in the analytical detection tool - Incucyte® live-cell analysis system, allowing for automated real-time measurements and identification of biological processes, including proliferation and apoptotic cell death. Herein, the NCI-N87 cells were seeded (1800 cells/ mm^2) on top of the porous membrane on a chip which allowed the cell growth to a confluent polarised cell monolayer within 3 days. I found that membrane coating with collagen type I mixed with Matrigel™ is obligatory for cell attachment on the membrane inside the chip. Furthermore, continuous media flow is necessary for developing of cell monolayer inside the chip and enhancing cell growth (*publication III, figure 6*).

The intercellular contact between epithelial cells seals paracellular space and provides a barrier function of the epithelial cell layer. Therefore, I examined the utility of the polarised NCI-N87 cells on-a-chip to imitate the gastric epithelial barrier function by measuring FITC-dextran permeability. A significant decrease in paracellular permeability over time indicates the formation of intercellular contact of the cell

monolayer (*publication III, figure 7*). Furthermore, the immunofluorescent staining showed E-cadherin, one of the adherent junction proteins essential for barrier function by regulating tight junctions (Tunggal et al., 2005), in all junctions of the cells on-a-chip, similar to in the Boyden chamber, confirming the intercellular contact and development of barrier integrity of the polarised NCI-N87 cells on-a-chip. Different dynamic cell culture systems that imitate the epithelial barrier have been established for compound permeability tests in pharmacological and toxicological studies, using a similar chip design of sandwich structure containing cells of different human origin (Bein et al., 2018; Gao et al., 2013; Imura et al., 2009; Kim et al., 2012; Kulthong et al., 2018; Kulthong et al., 2020; Villenave et al., 2017).

Moreover, the drug response of polarised NCI-N87 cells on-a-chip was determined. Treatment of apoptosis-inducing drug camptothecin (CPT) from the bottom channel, mimicking cellular uptake from the bloodstream, showed an increase in apoptotic cell death (caspase-3/7 stained cells) over time (*publication III, figure 7*). Therefore, the polarised NCI-N87 cells on-a-chip is considered an adequate model for *in vitro* analysis of cell death in response to stimuli. Furthermore, this system could also use for analysing other biological processes, including proliferation and inflammation.

Regarding the recent established patient-derived gastric mucosoids using a transient air-liquid interface in the Boyden chamber, in which the mucosoids encompass various gastric antral cell types and secrete mucus at the apical surface (Boccellato et al., 2019), I further developed gastric mucosoid on-a-chip to better mimic *in vivo* situations with dynamic conditions (unpublished work). The cells from patient-derived gastric mucosoids were implemented on a chip by using a protocol of NCI-N87 cells on-a-chip with modification of culture medium components. I found that gastric mucosoids on-a-chip preserved epithelial barrier integrity (unpublished data). Furthermore, the impact of *H. pylori* infection on apoptotic cell death was determined. I found that the gastric mucosoid on-a-chip was responsive to *H. pylori*-induced apoptotic cell death in a time-dependent manner. This work provides a platform for culturing the patient-derived primary gastric cells in a controlled environment which mimics *in vivo* situations, reflecting patient-specific responses and benefits for the study of apoptotic cell death and disease processes, as well as for personalised medicine. Due to the variety of cells in the gastric mucosa, future development of microfluidic devices containing co-culture of different gastric mucosal cell types will closely mimic *in vivo* conditions and provide a better understanding of the pathophysiology of gastric diseases (Jantaree et al., 2021).

6.5 Conclusions

The studies revealed a novel mechanism in which the DUBs, USP48 and A20, synergistically regulate NF- κ B/RelA and apoptotic cell death of the gastric epithelial cells during *H. pylori* infection. Mechanically, the CSN-associated nuclear DUB USP48 stabilises RelA by deubiquitinylation and thereby promotes the transcriptional activity of RelA to prolong *de novo* synthesis of A20 in *H. pylori* infection. Sustained A20 expression by USP48 suppresses caspase-8 activation and apoptotic cell death in the gastric epithelial cells. Moreover, I found a protective role of human gastric fibroblasts on apoptotic cell death of gastric epithelial cells. The co-cultured gastric fibroblasts

Chapter 6: Discussion

induce an enhanced NF- κ B activity and A20 expression in the gastric epithelial cells, which contributes to the suppression of caspase-8-dependent apoptotic cell death. Finally, I established the gastric epithelial monolayer on-a-chip that resembles the fluid-flow conditions of the *in vivo* situation of the gastric epithelium and provides a powerful approach for biomedical applications, including studying the epithelial cell response to drug treatment and pathogen infections.

List of abbreviation

ADP-heptose	ADP-L-glycero- β -D-manno-heptose
ALPK1	Alpha-protein kinase 1 (ALPK1)
BCL2A1	B-cell lymphoma 2-related protein A1
BIRC	Baculoviral IAP repeat containing
CagA	Cytotoxin-associated gene A
clAP1	Cellular inhibitor of apoptosis 1
CRLs	Cullin-RING ligases
CSN	COP9 signalosome
DUBs	Deubiquitinylases
ECS ^{SOCS1}	Elongin-cullin-suppressor of cytokine signaling 1
EGF	Epidermal growth factor
FGF	Fibroblast growth factor
GGT	γ -glutamyl transpeptidase
GSK β	Glycogen synthase kinase 3 β
HER2	Human epidermal growth factor receptor 2
HGF	Hepatocyte growth factor
IKK	I κ B kinase
LPS	lipopolysaccharide
MMPs	Matrix metalloproteinases
MPN	Mov34-and-Pad1p N-terminal
NEDD8	Neural precursor cell expressed developmentally downregulated gene8
NEMO	NF- κ B essential modulator
NF- κ B	Nuclear factor kappa-light-chain-enhancer of activated B cells
NIK	NF- κ B-inducing kinase
OipA	Outer inflammatory protein A
OTUs	Ovarian tumour proteases
PCI	Proteasome-COP9-initiation factor 3
PDMS	Polydimethylsiloxane
PML	Promyelocytic leukemia
PSCs	Pluripotent stem cells
ROS	Reactive oxygen species
T4SS	Type IV secretion system
TABs	TAK1-binding proteins
TAK1	Transforming growth factor β -activated kinase 1
TGF β	Transforming growth factor β
TIFA	TRAF-interacting protein with forkhead-associated domain
TRAF	Tumour necrosis factor receptor-associated factor
UCHs	Ubiquitin carboxy-terminal hydrolases
UPS	Ubiquitin-proteasome system
UreA	Urease subunit A
USPs	Ubiquitin-specific proteases
VacA	Vacuolating cytotoxin A
VEGFR	Vascular endothelial growth factor receptor

References

- Abdul Rehman, S. A., Kristariyanto, Y. A., Choi, S. Y., Nkosi, P. J., Weidlich, S., Labib, K., Hofmann, K., & Kulathu, Y. (2016). MINDY-1 is a member of an evolutionarily conserved and structurally distinct new family of deubiquitinating enzymes. *Mol Cell*, *63*(1), 146–155. <https://doi.org/10.1016/j.molcel.2016.05.009>
- Ahn, H. J., & Lee, D. S. (2015). *Helicobacter pylori* in gastric carcinogenesis. *World J Gastrointest Oncol*, *7*(12), 455–465. <https://doi.org/10.4251/wjgo.v7.i12.455>
- Ailloud, F., Didelot, X., Woltemate, S., Pfaffinger, G., Overmann, J., Bader, R. C., Schulz, C., Malfertheiner, P., & Suerbaum, S. (2019). Within-host evolution of *Helicobacter pylori* shaped by niche-specific adaptation, intragastric migrations and selective sweeps. *Nat Commun*, *10*(1), 2273. <https://doi.org/10.1038/s41467-019-10050-1>
- Akazawa, Y., Isomoto, H., Matsushima, K., Kanda, T., Minami, H., Yamaguchi, N., Taura, N., Shiozawa, K., Ohnita, K., Takeshima, F., Nakano, M., Moss, J., Hirayama, T., & Nakao, K. (2013). Endoplasmic reticulum stress contributes to *Helicobacter pylori* VacA-induced apoptosis. *PLoS One*, *8*(12), e82322. <https://doi.org/10.1371/journal.pone.0082322>
- Amedei, A., Munari, F., Bella, C. D., Niccolai, E., Benagiano, M., Bencini, L., Cianchi, F., Farsi, M., Emmi, G., Zanotti, G., de Bernard, M., Kundu, M., & D'Elia, M. M. (2014). *Helicobacter pylori* secreted peptidyl prolyl cis, trans-isomerase drives Th17 inflammation in gastric adenocarcinoma. *Intern Emerg Med*, *9*(3), 303–309. <https://doi.org/10.1007/s11739-012-0867-9>
- Ansari, S., & Yamaoka, Y. (2017). Survival of *Helicobacter pylori* in gastric acidic territory. *Helicobacter*, *22*(4). <https://doi.org/10.1111/hel.12386>
- Ashktorab, H., Dashwood, R. H., Dashwood, M. M., Zaidi, S. I., Hewitt, S. M., Green, W. R., Lee, E. L., Darempouran, M., Nouraie, M., Malekzadeh, R., & Smoot, D. T. (2008). *H. pylori*-induced apoptosis in human gastric cancer cells mediated via the release of apoptosis-inducing factor from mitochondria. *Helicobacter*, *13*(6), 506–517. <https://doi.org/10.1111/j.1523-5378.2008.00646.x>
- Bakhti, S. Z., Latifi-Navid, S., & Safaralizadeh, R. (2020). *Helicobacter pylori*-related risk predictors of gastric cancer: The latest models, challenges, and future prospects. *Cancer Med*, *9*(13), 4808–4822. <https://doi.org/10.1002/cam4.3068>
- Bartfeld, S. (2016). Modeling infectious diseases and host-microbe interactions in gastrointestinal organoids. *Dev Biol*, *420*(2), 262–270. <https://doi.org/10.1016/j.ydbio.2016.09.014>
- Bartfeld, S., & Clevers, H. (2015). Organoids as model for infectious diseases: culture of human and murine stomach organoids and microinjection of *Helicobacter pylori*. *J Vis Exp*, (105), 53399. <https://doi.org/10.3791/53359>
- Bartfeld, S., Bayram, T., van de Wetering, M., Huch, M., Begthel, H., Kujala, P., Vries, R., Peters, P. J., & Clevers, H. (2015). *In vitro* expansion of human gastric epithelial stem cells and their responses to bacterial infection. *Gastroenterology*, *148*(1), 126–136 e126. <https://doi.org/10.1053/j.gastro.2014.09.042>

- Bein, A., Shin, W., Jalili-Firoozinezhad, S., Park, M. H., Sontheimer-Phelps, A., Tovagliari, A., Chalkiadaki, A., Kim, H. J., & Ingber, D. E. (2018). Microfluidic organ-on-a-chip models of human intestine. *Cell Mol Gastroenterol Hepatol*, 5(4), 659-668. <https://doi.org/10.1016/j.jcmgh.2017.12.010>
- Boccellato, F., Woelffling, S., Imai-Matsushima, A., Sanchez, G., Goosmann, C., Schmid, M., Berger, H., Morey, P., Denecke, C., Ordemann, J., & Meyer, T. F. (2019). Polarised epithelial monolayers of the gastric mucosa reveal insights into mucosal homeostasis and defence against infection. *Gut*, 68(3), 400-413. <https://doi.org/10.1136/gutjnl-2017-314540>
- Boquet, P., Ricci, V., Galmiche, A., & Gauthier, N. C. (2003). Gastric cell apoptosis and *H. pylori*: has the main function of VacA finally been identified? *Trends Microbiol*, 11(9), 410-413. [https://doi.org/10.1016/s0966-842x\(03\)00211-7](https://doi.org/10.1016/s0966-842x(03)00211-7)
- Bosanac, I., Wertz, I. E., Pan, B., Yu, C., Kusam, S., Lam, C., Phu, L., Phung, Q., Maurer, B., Arnott, D., Kirkpatrick, D. S., Dixit, V. M., & Hymowitz, S. G. (2010). Ubiquitin binding to A20 ZnF4 is required for modulation of NF- κ B signaling. *Mol Cell*, 40(4), 548-557. <https://doi.org/10.1016/j.molcel.2010.10.009>
- Broda, T. R., McCracken, K. W., & Wells, J. M. (2019). Generation of human antral and fundic gastric organoids from pluripotent stem cells. *Nat Protoc*, 14(1), 28-50. <https://doi.org/10.1038/s41596-018-0080-z>
- Calvino Fernandez, M., & Parra Cid, T. (2010). *H. pylori* and mitochondrial changes in epithelial cells. The role of oxidative stress. *Rev Esp Enferm Dig*, 102(1), 41-50. <https://doi.org/10.4321/s1130-01082010000100006>
- Chaithongyot, S., & Naumann, M. (2022). *Helicobacter pylori*-induced reactive oxygen species direct turnover of CSN-associated STAMBPL1 and augment apoptotic cell death. *Cell Mol Life Sci*, 79(2), 86. <https://doi.org/10.1007/s00018-022-04135-2>
- Chaithongyot, S., Jantaree, P., Sokolova, O., & Naumann, M. (2021). NF- κ B in gastric cancer development and therapy. *Biomedicines*, 9(8), 870. <https://doi.org/10.3390/biomedicines9080870>
- Chen, J., & Chen, Z. J. (2013). Regulation of NF- κ B by ubiquitination. *Curr Opin Immunol*, 25(1), 4-12. <https://doi.org/10.1016/j.coi.2012.12.005>
- Cho, S. J., Kang, N. S., Park, S. Y., Kim, B. O., Rhee, D. K., & Pyo, S. (2003). Induction of apoptosis and expression of apoptosis related genes in human epithelial carcinoma cells by *Helicobacter pylori* VacA toxin. *Toxicon*, 42(6), 601-611. <https://doi.org/10.1016/j.toxicon.2003.08.003>
- Cover, T. L., Krishna, U. S., Israel, D. A., & Peek, R. M., Jr. (2003). Induction of gastric epithelial cell apoptosis by *Helicobacter pylori* vacuolating cytotoxin. *Cancer Res*, 63(5), 951-957. <https://www.ncbi.nlm.nih.gov/pubmed/12615708>
- Diaz, P., Valenzuela Valderrama, M., Bravo, J., & Quest, A. F. G. (2018). *Helicobacter pylori* and gastric cancer: adaptive cellular mechanisms involved in disease progression. *Front Microbiol*, 9, 5. <https://doi.org/10.3389/fmicb.2018.00005>

- Domhan, S., Stremmel, W., & Rudi, J. (2004). Role of apoptosis and CD95-receptor/ligand system in aspirin- and *Helicobacter pylori*-induced cell death. *Eur J Clin Invest*, 34(6), 422-428. <https://doi.org/10.1111/j.1365-2362.2004.01358.x>
- Du, L., Li, Y., Kang, M., Feng, M., Ren, Y., Dai, H., Wang, Y., Wang, Y., & Tang, B. (2021). USP48 Is upregulated by Mettl14 to attenuate hepatocellular carcinoma via regulating SIRT6 stabilization. *Cancer Res*, 81(14), 3822–3834. <https://doi.org/10.1158/0008-5472.CAN-20-4163>
- Dubiel, W., Chaithongyot, S., Dubiel, D., & Naumann, M. (2020). The COP9 signalosome: a multi-DUB complex. *Biomolecules*, 10(7), 1082. <https://doi.org/10.3390/biom10071082>
- Echalier, A., Pan, Y., Birol, M., Tavernier, N., Pintard, L., Hoh, F., Ebel, C., Galophe, N., Claret, F. X., & Dumas, C. (2013) Insights into the regulation of the human COP9 signalosome catalytic subunit, CSN5/Jab1. *Proc Natl Acad Sci U S A*, 110(4), 1273-1278. <http://doi.org/10.1073/pnas.1209345110>
- Every, A. L., Ng, G. Z., Skene, C. D., Harbour, S. N., Walduck, A. K., McGuckin, M. A., & Sutton, P. (2011). Localized suppression of inflammation at sites of *Helicobacter pylori* colonization. *Infect Immun*, 79(10), 4186–4192. <https://doi.org/10.1128/IAI.05602-11>
- Ferrand, J., Lehours, P., Schmid-Alliana, A., Megraud, F., & Varon, C. (2011). *Helicobacter pylori* infection of gastrointestinal epithelial cells *in vitro* induces mesenchymal stem cell migration through an NF- κ B-dependent pathway. *PLoS One*, 6(12), e29007. <https://doi.org/10.1371/journal.pone.0029007>
- Fiorentino, M., Ding, H., Blanchard, T. G., Czinn, S. J., Sztejn, M. B., & Fasano, A. (2013). *Helicobacter pylori*-induced disruption of monolayer permeability and proinflammatory cytokine secretion in polarized human gastric epithelial cells. *Infect Immun*, 81(3), 876-883. <https://doi.org/10.1128/IAI.01406-12>
- Gao, D., Liu, H., Lin, J. M., Wang, Y., & Jiang, Y. (2013). Characterization of drug permeability in Caco-2 monolayers by mass spectrometry on a membrane-based microfluidic device. *Lab Chip*, 13(5), 978-985. <https://doi.org/10.1039/c2lc41215b>
- Ghanem, A., Schweitzer, K., & Naumann, M. (2019). Catalytic domain of deubiquitylase USP48 directs interaction with Rel homology domain of nuclear factor κ B transcription factor RelA. *Mol Biol Rep*, 46(1), 1369-1375. <https://doi.org/10.1007/s11033-019-04587-z>
- Gomes, R. N., Manuel, F., & Nascimento, D. S. (2021). The bright side of fibroblasts: molecular signature and regenerative cues in major organs. *NPJ Regen Med*, 6(1), 43. <https://doi.org/10.1038/s41536-021-00153-z>
- Gonciarz, W., Krupa, A., Hinc, K., Obuchowski, M., Moran, A. P., Gajewski, A., & Chmiela, M. (2019). The effect of *Helicobacter pylori* infection and different *H. pylori* components on the proliferation and apoptosis of gastric epithelial cells and fibroblasts. *PLoS One*, 14(8), e0220636. <https://doi.org/10.1371/journal.pone.0220636>

- Gong, M., Ling, S. S., Lui, S. Y., Yeoh, K. G., & Ho, B. (2010). *Helicobacter pylori* gamma-glutamyl transpeptidase is a pathogenic factor in the development of peptic ulcer disease. *Gastroenterology*, *139*(2), 564-573. <https://doi.org/10.1053/j.gastro.2010.03.050>
- Goodwin, C. S., & Worsley, B. W. (1993). Microbiology of *Helicobacter pylori*. *Gastroenterol Clin North Am*, *22*(1), 5-19. <https://www.ncbi.nlm.nih.gov/pubmed/8449570>
- Hooi, J. K. Y., Lai, W. Y., Ng, W. K., Suen, M. M. Y., Underwood, F. E., Tanyingoh, D., Malfertheiner, P., Graham, D. Y., Wong, V. W. S., Wu, J. C. Y., Chan, F. K. L., Sung, J. J. Y., Kaplan, G. G., & Ng, S. C. (2017). Global prevalence of *Helicobacter pylori* infection: systematic review and meta-analysis. *Gastroenterology*, *153*(2), 420-429. <https://doi.org/10.1053/j.gastro.2017.04.022>
- Huang, X., Dubiel, D., & Dubiel, W. (2021). The COP9 signalosome variant CSN^{CSN7A} stabilizes the deubiquitylating enzyme CYLD impeding hepatic steatosis. *Livers*, *1*(3), 116-131. <https://www.mdpi.com/2673-4389/1/3/11>
- Hunt, R. H., Camilleri, M., Crowe, S. E., El-Omar, E. M., Fox, J. G., Kuipers, E. J., Malfertheiner, P., McColl, K. E., Pritchard, D. M., Rugge, M., Sonnenberg, A., Sugano, K., & Tack, J. (2015). The stomach in health and disease. *Gut*, *64*(10), 1650-1668. <https://doi.org/10.1136/gutjnl-2014-307595>
- Imura, Y., Asano, Y., Sato, K., & Yoshimura, E. (2009). A microfluidic system to evaluate intestinal absorption. *Anal Sci*, *25*(12), 1403-1407. <https://doi.org/10.2116/analsci.25.1403>
- Jain, P., Luo, Z. Q., & Blanke, S. R. (2011). *Helicobacter pylori* vacuolating cytotoxin A (VacA) engages the mitochondrial fission machinery to induce host cell death. *Proc Natl Acad Sci U S A*, *108*(38), 16032-16037. <https://doi.org/10.1073/pnas.1105175108>
- Jantaree, P., Bakhchova, L., Steinmann, U., & Naumann, M. (2021). From 3D back to 2D monolayer stomach organoids-on-a-chip. *Trends Biotechnol*, *39*(8), 745-748. <https://doi.org/10.1016/j.tibtech.2020.11.013>
- Jeong, H.-J., Park, J.-H., Kang, J. H., Kong, S.-H., & Park, T.-E. (2022). Organoid-based human stomach micro-physiological system to recapitulate the dynamic mucosal defense mechanism. *bioRxiv*, 2022.2003.2002.482603. <https://doi.org/10.1101/2022.03.02.482603>
- Jodat, Y. A., Kang, M. G., Kiaee, K., Kim, G. J., Martinez, A. F. H., Rosenkranz, A., Bae, H., & Shin, S. R. (2018). Human-derived organ-on-a-chip for personalized drug development. *Curr Pharm Des*, *24*(45), 5471-5486. <https://doi.org/10.2174/1381612825666190308150055>
- Jones, N. L., Day, A. S., Jennings, H. A., & Sherman, P. M. (1999). *Helicobacter pylori* induces gastric epithelial cell apoptosis in association with increased Fas receptor expression. *Infect Immun*, *67*(8), 4237-4242. <https://doi.org/10.1128/IAI.67.8.4237-4242.1999>
- Joshi, S. S., & Badgwell, B. D. (2021). Current treatment and recent progress in gastric cancer. *CA Cancer J Clin*, *71*(3), 264-279. <https://doi.org/10.3322/caac.21657>

- Kalluri, R. (2016). The biology and function of fibroblasts in cancer. *Nat Rev Cancer*, 16(9), 582-598. <https://doi.org/10.1038/nrc.2016.73>
- Katano, T., Ootani, A., Mizoshita, T., Tanida, S., Tsukamoto, H., Ozeki, K., Kataoka, H., & Joh, T. (2015). Gastric mesenchymal myofibroblasts maintain stem cell activity and proliferation of murine gastric epithelium *in vitro*. *Am J Pathol*, 185(3), 798-807. <https://doi.org/10.1016/j.ajpath.2014.11.007>
- Kayali, S., Manfredi, M., Gaiani, F., Bianchi, L., Bizzarri, B., Leandro, G., Di Mario, F., & De' Angelis, G. L. (2018). *Helicobacter pylori*, transmission routes and recurrence of infection: state of the art. *Acta Biomed*, 89(8-S), 72-76. <https://doi.org/10.23750/abm.v89i8-S.7947>
- Ki, M. R., Lee, H. R., Goo, M. J., Hong, I. H., Do, S. H., Jeong, D. H., Yang, H. J., Yuan, D. W., Park, J. K., & Jeong, K. S. (2008). Differential regulation of ERK1/2 and p38 MAP kinases in VacA-induced apoptosis of gastric epithelial cells. *Am J Physiol Gastrointest Liver Physiol*, 294(3), G635-647. <https://doi.org/10.1152/ajpgi.00281.2007>
- Kim, H. J., Huh, D., Hamilton, G., & Ingber, D. E. (2012). Human gut-on-a-chip inhabited by microbial flora that experiences intestinal peristalsis-like motions and flow. *Lab Chip*, 12(12), 2165-2174. <https://doi.org/10.1039/c2lc40074j>
- Kim, H. J., & Ingber, D. E. (2013). Gut-on-a-chip microenvironment induces human intestinal cells to undergo villus differentiation. *Integr Biol (Camb)*, 5(9), 1130-1140. <https://doi.org/10.1039/c3ib40126j>
- Kim, K. M., Lee, S. G., Park, M. G., Song, J. Y., Kang, H. L., Lee, W. K., Cho, M. J., Rhee, K. H., Youn, H. S., & Baik, S. C. (2007). Gamma-glutamyltranspeptidase of *Helicobacter pylori* induces mitochondria-mediated apoptosis in AGS cells. *Biochem Biophys Res Commun*, 355(2), 562-567. <https://doi.org/10.1016/j.bbrc.2007.02.021>
- Koh, B., Jeon, H., Kim, D., Kang, D., & Kim, K. R. (2019). Effect of fibroblast co-culture on the proliferation, viability and drug response of colon cancer cells. *Oncol Lett*, 17(2), 2409-2417. <https://doi.org/10.3892/ol.2018.9836>
- Kuck, D., Kolmerer, B., Iking-Konert, C., Krammer, P. H., Stremmel, W., & Rudi, J. (2001). Vacuolating cytotoxin of *Helicobacter pylori* induces apoptosis in the human gastric epithelial cell line AGS. *Infect Immun*, 69(8), 5080-5087. <https://doi.org/10.1128/IAI.69.8.5080-5087.2001>
- Kulthong, K., Duivenvoorde, L., Mizera, B. Z., Rijkers, D., Dam, G. T., Oegema, G., Puzyn, T., Bouwmeester, H., & van der Zande, M. (2018). Implementation of a dynamic intestinal gut-on-a-chip barrier model for transport studies of lipophilic dioxin congeners. *RSC Adv*, 8(57), 32440-32453. <https://doi.org/10.1039/c8ra05430d>
- Kulthong, K., Duivenvoorde, L., Sun, H., Confederat, S., Wu, J., Spenkelink, B., de Haan, L., Marin, V., van der Zande, M., & Bouwmeester, H. (2020). Microfluidic chip for culturing intestinal epithelial cell layers: Characterization and comparison of drug transport between dynamic and static models. *Toxicol In Vitro*, 65, 104815. <https://doi.org/10.1016/j.tiv.2020.104815>

- Kusters, J. G., van Vliet, A. H., & Kuipers, E. J. (2006). Pathogenesis of *Helicobacter pylori* infection. *Clin Microbiol Rev*, *19*(3), 449-490. <https://doi.org/10.1128/CMR.00054-05>
- Lan, C. H., Sheng, J. Q., Fang, D. C., Meng, Q. Z., Fan, L. L., & Huang, Z. R. (2010). Involvement of VDAC1 and Bcl-2 family of proteins in VacA-induced cytochrome c release and apoptosis of gastric epithelial carcinoma cells. *J Dig Dis*, *11*(1), 43-49. <https://doi.org/10.1111/j.1751-2980.2009.00412.x>
- Lee, K. K., McCauley, H. A., Broda, T. R., Kofron, M. J., Wells, J. M., & Hong, C. I. (2018). Human stomach-on-a-chip with luminal flow and peristaltic-like motility. *Lab Chip*, *18*(20), 3079-3085. <https://doi.org/10.1039/c8lc00910d>
- Li, S., Wang, D., Zhao, J., Weathington, N. M., Shang, D., & Zhao, Y. (2018). The deubiquitinating enzyme USP48 stabilizes TRAF2 and reduces E-cadherin-mediated adherens junctions. *FASEB J*, *32*(1), 230-242. <https://doi.org/10.1096/fj.201700415RR>
- Lingaraju, G.M., Bunker, R.D., Cavadini, S., Hess, D., Hassiepen, U., Renatus, M., Fischer, E.S., & Thoma, N.H. (2014) Crystal structure of the human COP9 signalosome. *Nature*, *512*(7513), 161-165. <http://doi.org/10.1038/nature13566>
- Lim, M. C. C., Maubach, G., Birkl-Toegelhofer, A. M., Haybaeck, J., Vieth, M., & Naumann, M. (2022). A20 undermines alternative NF- κ B activity and expression of anti-apoptotic genes in *Helicobacter pylori* infection. *Cell Mol Life Sci*, *79*(2), 102. <https://doi.org/10.1007/s00018-022-04139-y>
- Lim, M. C. C., Maubach, G., Sokolova, O., Feige, M. H., Diezko, R., Buchbinder, J., Backert, S., Schluter, D., Lavrik, I. N., & Naumann, M. (2017). Pathogen-induced ubiquitin-editing enzyme A20 bifunctionally shuts off NF- κ B and caspase-8-dependent apoptotic cell death. *Cell Death Differ*, *24*(9), 1621-1631. <https://doi.org/10.1038/cdd.2017.89>
- Liu, C., & Mak, M. (2022). Fibroblast-mediated uncaging of cancer cells and dynamic evolution of the physical microenvironment. *Sci Rep*, *12*(1), 791. <https://doi.org/10.1038/s41598-021-03134-w>
- Liu, T., Zhang, L., Joo, D., & Sun, S. C. (2017). NF- κ B signaling in inflammation. *Signal Transduct Target Ther*, *2*, 17023. <https://doi.org/10.1038/sigtrans.2017.23>
- Liu, Y. L., Yan, J., Zheng, J., & Tian, Q. B. (2018). ⁹³⁸RHRK⁹⁴¹ is responsible for ubiquitin specific protease 48 nuclear translocation which can stabilize NF- κ B (p65) in the nucleus. *Gene*, *669*, 77-81. <https://doi.org/10.1016/j.gene.2018.05.035>
- Ma, C., Peng, Y., Li, H., & Chen, W. (2021). Organ-on-a-chip: a new paradigm for drug development. *Trends Pharmacol Sci*, *42*(2), 119-133. <https://doi.org/10.1016/j.tips.2020.11.009>
- Maeda, S., Yoshida, H., Mitsuno, Y., Hirata, Y., Ogura, K., Shiratori, Y., & Omata, M. (2002). Analysis of apoptotic and antiapoptotic signalling pathways induced by *Helicobacter pylori*. *Gut*, *50*(6), 771-778. <https://doi.org/10.1136/gut.50.6.771>

- Maine, G. N., Mao, X., Komarck, C. M., & Burstein, E. (2007). COMMD1 promotes the ubiquitination of NF- κ B subunits through a cullin-containing ubiquitin ligase. *EMBO J*, 26(2), 436-447. <https://doi.org/10.1038/sj.emboj.7601489>
- Malvezzi, M., Bonifazi, M., Bertuccio, P., Levi, F., La Vecchia, C., Decarli, A., & Negri, E. (2010). An age-period-cohort analysis of gastric cancer mortality from 1950 to 2007 in Europe. *Ann Epidemiol*, 20(12), 898-905. <https://doi.org/10.1016/j.annepidem.2010.08.013>
- Marshall, B. J., & Warren, J. R. (1984). Unidentified curved bacilli in the stomach of patients with gastritis and peptic ulceration. *Lancet*, 1(8390), 1311-1315. [https://doi.org/10.1016/s0140-6736\(84\)91816-6](https://doi.org/10.1016/s0140-6736(84)91816-6)
- Martens, A., & van Loo, G. (2020). A20 at the crossroads of cell death, inflammation, and autoimmunity. *Cold Spring Harb Perspect Biol*, 12(1), a036418. <https://doi.org/10.1101/cshperspect.a036418>
- Martin, J. H., Potthoff, A., Ledig, S., Cornberg, M., Jandl, O., Manns, M. P., Kubicka, S., Flemming, P., Athmann, C., Beil, W., & Wagner, S. (2004). Effect of *H. pylori* on the expression of TRAIL, FasL and their receptor subtypes in human gastric epithelial cells and their role in apoptosis. *Helicobacter*, 9(5), 371-386. <https://doi.org/10.1111/j.1083-4389.2004.00269.x>
- Maubach, G., Lim, M. C. C., Sokolova, O., Backert, S., Meyer, T. F., & Naumann, M. (2021). TIFA has dual functions in *Helicobacter pylori*-induced classical and alternative NF- κ B pathways. *EMBO Rep*, 22(9), e52878. <https://doi.org/10.15252/embr.202152878>
- Maubach, G., Vieth, M., Boccellato, F., & Naumann, M. (2022). *Helicobacter pylori*-induced NF- κ B: trailblazer for gastric pathophysiology. *Trends Mol Med*, 28(3), 210-222. <https://doi.org/10.1016/j.molmed.2021.12.005>
- Milivojevic, M., Dangeard, A. S., Kasper, C. A., Tschon, T., Emmenlauer, M., Pique, C., Schnupf, P., Guignot, J., & Arriemerlou, C. (2017). ALPK1 controls TIFA/TRAF6-dependent innate immunity against heptose-1,7-bisphosphate of gram-negative bacteria. *PLoS Pathog*, 13(2), e1006224. <https://doi.org/10.1371/journal.ppat.1006224>
- Naghavi, L., Schwalbe, M., Ghanem, A., & Naumann, M. (2018). Deubiquitinylase USP47 promotes RelA phosphorylation and survival in gastric cancer cells. *Biomedicines*, 6(2), 62. <https://doi.org/10.3390/biomedicines6020062>
- Nakazawa, K., Yashiro, M., & Hirakawa, K. (2003). Keratinocyte growth factor produced by gastric fibroblasts specifically stimulates proliferation of cancer cells from scirrhous gastric carcinoma. *Cancer Res*, 63(24), 8848-8852. <https://www.ncbi.nlm.nih.gov/pubmed/14695201>
- Neumann, M., & Naumann, M. (2007). Beyond I κ Bs: alternative regulation of NF- κ B activity. *FASEB J*, 21(11), 2642-2654. <https://doi.org/10.1096/fj.06-7615rev>
- Noto, J. M., & Peek, R. M., Jr. (2012). *Helicobacter pylori*: an overview. *Methods Mol Biol*, 921, 7-10. https://doi.org/10.1007/978-1-62703-005-2_2

- O'Toole, P. W., Lane, M. C., & Porwollik, S. (2000). *Helicobacter pylori* motility. *Microbes Infect*, 2(10), 1207-1214. [https://doi.org/10.1016/s1286-4579\(00\)01274-0](https://doi.org/10.1016/s1286-4579(00)01274-0)
- Pang, M. J., Burclaff, J. R., Jin, R., Adkins-Threats, M., Osaki, L. H., Han, Y., Mills, J. C., Miao, Z. F., & Wang, Z. N. (2022). Gastric organoids: progress and remaining challenges. *Cell Mol Gastroenterol Hepatol*, 13(1), 19-33. <https://doi.org/10.1016/j.jcmgh.2021.09.005>
- Parkin, D. M. (2006). The global health burden of infection-associated cancers in the year 2002. *Int J Cancer*, 118(12), 3030-3044. <https://doi.org/10.1002/ijc.21731>
- Pfannkuch, L., Hurwitz, R., Traulsen, J., Sigulla, J., Poeschke, M., Matzner, L., Kosma, P., Schmid, M., & Meyer, T. F. (2019). ADP heptose, a novel pathogen-associated molecular pattern identified in *Helicobacter pylori*. *FASEB J*, 33(8), 9087-9099. <https://doi.org/10.1096/fj.201802555R>
- Pfoh, R., Lacdao, I. K., & Saridakis, V. (2015). Deubiquitinases and the new therapeutic opportunities offered to cancer. *Endocr Relat Cancer*, 22(1), T35-54. <https://doi.org/10.1530/ERC-14-0516>
- Polk, D. B., & Peek, R. M., Jr (2010). *Helicobacter pylori*: gastric cancer and beyond. *Nat Rev Cancer*, 10(6), 403-414. <https://doi.org/10.1038/nrc2857>
- Razani, B., Reichardt, A. D., & Cheng, G. (2011). Non-canonical NF- κ B signaling activation and regulation: principles and perspectives. *Immunol Rev*, 244(1), 44-54. <https://doi.org/10.1111/j.1600-065X.2011.01059.x>
- Reshetnyak, V. I., Burmistrov, A. I., & Maev, I. V. (2021). *Helicobacter pylori*: commensal, symbiont or pathogen?. *World J Gastroenterol*, 27(7), 545-560. <https://doi.org/10.3748/wjg.v27.i7.545>
- Ricci, V., Giannouli, M., Romano, M., & Zarrilli, R. (2014). *Helicobacter pylori* gamma-glutamyl transpeptidase and its pathogenic role. *World J Gastroenterol*, 20(3), 630-638. <https://doi.org/10.3748/wjg.v20.i3.630>
- Rolig, A. S., Shanks, J., Carter, J. E., & Ottemann, K. M. (2012). *Helicobacter pylori* requires TlpD-driven chemotaxis to proliferate in the antrum. *Infect Immun*, 80(10), 3713-3720. <https://doi.org/10.1128/IAI.00407-12>
- Saccani, S., Marazzi, I., Beg, A. A., & Natoli, G. (2004). Degradation of promoter-bound p65/RelA is essential for the prompt termination of the nuclear factor κ B response. *J Exp Med*, 200(1), 107-113. <https://doi.org/10.1084/jem.20040196>
- Schlaermann, P., Toelle, B., Berger, H., Schmidt, S. C., Glanemann, M., Ordemann, J., Bartfeld, S., Mollenkopf, H. J., & Meyer, T. F. (2016). A novel human gastric primary cell culture system for modelling *Helicobacter pylori* infection in vitro. *Gut*, 65(2), 202-213. <https://doi.org/10.1136/gutjnl-2014-307949>
- Schweitzer, K., Bozko, P. M., Dubiel, W., & Naumann, M. (2007). CSN controls NF- κ B by deubiquitylation of I κ B α . *EMBO J*, 26(6), 1532-1541. <https://doi.org/10.1038/sj.emboj.7601600>

- Schweitzer, K., & Naumann, M. (2010). Control of NF- κ B activation by the COP9 signalosome. *Biochem Soc Trans*, 38(Pt 1), 156-161. <https://doi.org/10.1042/BST0380156>
- Schweitzer, K., & Naumann, M. (2015). CSN-associated USP48 confers stability to nuclear NF- κ B/RelA by trimming K48-linked Ub-chains. *Biochim Biophys Acta*, 1853(2), 453-469. <https://doi.org/10.1016/j.bbamcr.2014.11.028>
- Senft, D., Qi J., & Ronai ZA (2018) Ubiquitin ligases in oncogenic transformation and cancer therapy. *Nat Rev Cancer*, 18(2), 69-88. <http://doi.org/10.1038/nrc.2017.105>
- Shibayama, K., Doi, Y., Shibata, N., Yagi, T., Nada, T., Iinuma, Y., & Arakawa, Y. (2001). Apoptotic signaling pathway activated by *Helicobacter pylori* infection and increase of apoptosis-inducing activity under serum-starved conditions. *Infect Immun*, 69(5), 3181-3189. <https://doi.org/10.1128/IAI.69.5.3181-3189.2001>
- Sigal, M., Logan, C. Y., Kapalczyńska, M., Mollenkopf, H. J., Berger, H., Wiedenmann, B., Nusse, R., Amieva, M. R., & Meyer, T. F. (2017). Stromal R-spondin orchestrates gastric epithelial stem cells and gland homeostasis. *Nature*, 548(7668), 451-455. <https://doi.org/10.1038/nature23642>
- Sigal, M., Reines, M. D. M., Mullerke, S., Fischer, C., Kapalczyńska, M., Berger, H., Bakker, E. R. M., Mollenkopf, H. J., Rothenberg, M. E., Wiedenmann, B., Sauer, S., & Meyer, T. F. (2019). R-spondin-3 induces secretory, antimicrobial Lgr5(+) cells in the stomach. *Nat Cell Biol*, 21(7), 812-823. <https://doi.org/10.1038/s41556-019-0339-9>
- Skaug, B., Chen, J., Du, F., He, J., Ma, A., & Chen, Z. J. (2011). Direct, noncatalytic mechanism of IKK inhibition by A20. *Mol Cell*, 44(4), 559-571. <https://doi.org/10.1016/j.molcel.2011.09.015>
- Sokolova, O., Borgmann, M., Rieke, C., Schweitzer, K., Rothkotter, H. J., & Naumann, M. (2013). *Helicobacter pylori* induces type 4 secretion system-dependent, but CagA-independent activation of I κ Bs and NF- κ B/RelA at early time points. *Int J Med Microbiol*, 303(8), 548-552. <https://doi.org/10.1016/j.ijmm.2013.07.008>
- Sokolova, O., Kahne, T., Bryan, K., & Naumann, M. (2018). Interactome analysis of transforming growth factor-beta-activated kinase 1 in *Helicobacter pylori*-infected cells revealed novel regulators tripartite motif 28 and CDC37. *Oncotarget*, 9(18), 14366-14381. <https://doi.org/10.18632/oncotarget.24544>
- Sokolova, O., Maubach, G., & Naumann, M. (2014). MEKK3 and TAK1 synergize to activate IKK complex in *Helicobacter pylori* infection. *Biochim Biophys Acta*, 1843(4), 715-724. <https://doi.org/10.1016/j.bbamcr.2014.01.006>
- Sokolova, O., & Naumann, M. (2017). NF- κ B signaling in gastric cancer. *Toxins (Basel)*, 9(4), 119. <https://doi.org/10.3390/toxins9040119>
- Sun, C., Fukui, H., Hara, K., Zhang, X., Kitayama, Y., Eda, H., Tomita, T., Oshima, T., Kikuchi, S., Watari, J., Sasako, M., & Miwa, H. (2015). FGF9 from cancer-associated fibroblasts is a possible mediator of invasion and anti-apoptosis of gastric cancer cells. *BMC Cancer*, 15, 333. <https://doi.org/10.1186/s12885-015-1353-3>

- Sung, H., Ferlay, J., Siegel, R. L., Laversanne, M., Soerjomataram, I., Jemal, A., & Bray, F. (2021). Global cancer statistics 2020: GLOBOCAN estimates of incidence and mortality worldwide for 36 cancers in 185 countries. *CA Cancer J Clin*, *71*(3), 209-249. <https://doi.org/10.3322/caac.21660>
- Tanaka, T., Grusby, M. J., & Kaisho T (2007) PDLIM2-mediated termination of transcription factor NF- κ B activation by intranuclear sequestration and degradation of the p65 subunit. *Nat Immunol*, *8*(6), 584-591. <http://doi.org/10.1038/ni1464>
- Taniguchi, K., & Karin, M. (2018). NF- κ B, inflammation, immunity and cancer: coming of age. *Nat Rev Immunol*, *18*(5), 309-324. <https://doi.org/10.1038/nri.2017.142>
- Teymournejad, O., Mobarez, A. M., Hassan, Z. M., & Talebi Bezmin Abadi, A. (2017). Binding of the *Helicobacter pylori* OipA causes apoptosis of host cells via modulation of Bax/Bcl-2 levels. *Sci Rep*, *7*(1), 8036. <https://doi.org/10.1038/s41598-017-08176-7>
- Tokunaga, F., Nishimasu, H., Ishitani, R., Goto, E., Noguchi, T., Mio, K., Kamei, K., Ma, A., Iwai, K., & Nureki, O. (2012). Specific recognition of linear polyubiquitin by A20 zinc finger 7 is involved in NF- κ B regulation. *EMBO J*, *31*(19), 3856-3870. <https://doi.org/10.1038/emboj.2012.241>
- Traulsen, J., Zagami, C., Daddi, A. A., & Boccellato, F. (2021). Molecular modelling of the gastric barrier response, from infection to carcinogenesis. *Best Pract Res Clin Gastroenterol*, *50-51*, 101737. <https://doi.org/10.1016/j.bpg.2021.101737>
- Tsai, H. F., & Hsu, P. N. (2017). Modulation of tumor necrosis factor-related apoptosis-inducing ligand (TRAIL)-mediated apoptosis by *Helicobacter pylori* in immune pathogenesis of gastric mucosal damage. *J Microbiol Immunol Infect*, *50*(1), 4-9. <https://doi.org/10.1016/j.jmii.2016.01.002>
- Tunggal, J. A., Helfrich, I., Schmitz, A., Schwarz, H., Gunzel, D., Fromm, M., Kemler, R., Krieg, T., & Niessen, C. M. (2005). E-cadherin is essential for in vivo epidermal barrier function by regulating tight junctions. *EMBO J*, *24*(6), 1146-1156. <https://doi.org/10.1038/sj.emboj.7600605>
- Tzimas, C., Michailidou, G., Arsenakis, M., Kieff, E., Mosialos, G., & Hatzivassiliou, E. G. (2006). Human ubiquitin specific protease 31 is a deubiquitinating enzyme implicated in activation of nuclear factor- κ B. *Cell Signal*, *18*(1), 83-92. <https://doi.org/10.1016/j.cellsig.2005.03.017>
- Uckelmann, M., Densham, R. M., Baas, R., Winterwerp, H., Fish, A., Sixma, T. K., & Morris, J. R. (2018). USP48 restrains resection by site-specific cleavage of the BRCA1 ubiquitin mark from H2A. *Nature commu*, *9*(1), 229. <https://doi.org/10.1038/s41467-017-02653-3>
- Valenzuela, M. A., Canales, J., Corvalán, A. H., & Quest, A. F. (2015). *Helicobacter pylori*-induced inflammation and epigenetic changes during gastric carcinogenesis. *World J Gastroenterol*, *21*(45), 12742-12756. <https://doi.org/10.3748/wjg.v21.i45.12742>
- Valenzuela, M., Perez-Perez, G., Corvalan, A. H., Carrasco, G., Urra, H., Bravo, D., Toledo, H., & Quest, A. F. (2010). *Helicobacter pylori*-induced loss of the

- inhibitor-of-apoptosis protein survivin is linked to gastritis and death of human gastric cells. *J Infect Dis*, 202(7), 1021-1030. <https://doi.org/10.1086/656143>
- van den Berg, A., Mummery, C. L., Passier, R., & van der Meer, A. D. (2019). Personalised organs-on-chips: functional testing for precision medicine. *Lab Chip*, 19(2), 198-205. <https://doi.org/10.1039/c8lc00827b>
- Velimezi, G., Robinson-Garcia, L., Muñoz-Martínez, F., Wiegant, W. W., Ferreira da Silva, J., Owusu, M., Moder, M., Wiedner, M., Rosenthal, S. B., Fisch, K. M., Moffat, J., Menche, J., van Attikum, H., Jackson, S. P., & Loizou, J. I. (2018). Map of synthetic rescue interactions for the Fanconi anemia DNA repair pathway identifies USP48. *Nature commun*, 9(1), 2280. <https://doi.org/10.1038/s41467-018-04649-z>
- Verhelst, K., Carpentier, I., Kreike, M., Meloni, L., Verstrepen, L., Kensche, T., Dikic, I., & Beyaert, R. (2012). A20 inhibits LUBAC-mediated NF- κ B activation by binding linear polyubiquitin chains via its zinc finger 7. *EMBO J*, 31(19), 3845-3855. <https://doi.org/10.1038/emboj.2012.240>
- Villeneuve, R., Wales, S. Q., Hamkins-Indik, T., Papafragkou, E., Weaver, J. C., Ferrante, T. C., Bahinski, A., Elkins, C. A., Kulka, M., & Ingber, D. E. (2017). Human gut-on-a-chip supports polarized infection of coxsackie B1 virus *in vitro*. *PLoS One*, 12(2), e0169412. <https://doi.org/10.1371/journal.pone.0169412>
- Wertz, I. E., Newton, K., Seshasayee, D., Kusam, S., Lam, C., Zhang, J., Popovych, N., Helgason, E., Schoeffler, A., Jeet, S., Ramamoorthi, N., Kategaya, L., Newman, R. J., Horikawa, K., Dugger, D., Sandoval, W., Mukund, S., Zindal, A., Martin, F., Quan, C., Tom, J., Fairbrother, W. J., Townsend, M., Warming, S., DeVoss, J., Liu, J., Dueber, E., Caplazi, P., Lee, W. P., Goodnow, C. C., Balazs, M., Yu, K., Kolumam, G., & Dixit, V. M. (2015). Phosphorylation and linear ubiquitin direct A20 inhibition of inflammation. *Nature*, 528(7582), 370-375. <https://doi.org/10.1038/nature16165>
- Workman, M. J., Gleeson, J. P., Troisi, E. J., Estrada, H. Q., Kerns, S. J., Hinojosa, C. D., Hamilton, G. A., Targan, S. R., Svendsen, C. N., & Barrett, R. J. (2018). Enhanced utilization of induced pluripotent stem cell-derived human intestinal organoids using microengineered chips. *Cell Mol Gastroenterol Hepatol*, 5(4), 669-677 e662. <https://doi.org/10.1016/j.jcmgh.2017.12.008>
- Wroblewski, L. E., & Peek, R. M., Jr. (2011). Targeted disruption of the epithelial-barrier by *Helicobacter pylori*. *Cell Commun Signal*, 9(1), 29. <https://doi.org/10.1186/1478-811X-9-29>
- Wu, J. Y., Lee, Y. C., & Graham, D. Y. (2019). The eradication of *Helicobacter pylori* to prevent gastric cancer: a critical appraisal. *Expert Rev Gastroenterol Hepatol*, 13(1), 17-24. <https://doi.org/10.1080/17474124.2019.1542299>
- Wu, Q., Liu, J., Wang, X., Feng, L., Wu, J., Zhu, X., Wen, W., & Gong, X. (2020). Organ-on-a-chip: recent breakthroughs and future prospects. *Biomed Eng Online*, 19(1), 9. <https://doi.org/10.1186/s12938-020-0752-0>
- Zamani, M., Ebrahimitabar, F., Zamani, V., Miller, W. H., Alizadeh-Navaei, R., Shokri-Shirvani, J., & Derakhshan, M. H. (2018). Systematic review with meta-analysis: the worldwide prevalence of *Helicobacter pylori* infection. *Aliment Pharmacol Ther*, 47(7), 868-876. <https://doi.org/10.1111/apt.14561>

- Zhao, Q., Yin, W., Zhao, R., Wang, Y., Song, C., Wang, H., Rong, J., Wang, F., & Xie, Y. (2020). Outer inflammatory protein of *Helicobacter pylori* impacts IL-8 expression, adherence, cell apoptosis and cell cycle of gastric cells independent of its copy number. *Med Microbiol Immunol*, 209(5), 621–630. <https://doi.org/10.1007/s00430-020-00688-w>
- Zhou, P., She, Y., Dong, N., Li, P., He, H., Borio, A., Wu, Q., Lu, S., Ding, X., Cao, Y., Xu, Y., Gao, W., Dong, M., Ding, J., Wang, D. C., Zamyatina, A., & Shao, F. (2018). Alpha-kinase 1 is a cytosolic innate immune receptor for bacterial ADP-heptose. *Nature*, 561(7721), 122-126. <https://doi.org/10.1038/s41586-018-0433-3>
- Zimmermann, S., Pfannkuch, L., Al-Zeer, M. A., Bartfeld, S., Koch, M., Liu, J., Rechner, C., Soerensen, M., Sokolova, O., Zamyatina, A., Kosma, P., Maurer, A. P., Glowinski, F., Pleissner, K. P., Schmid, M., Brinkmann, V., Karlas, A., Naumann, M., Rother, M., Machuy, N., & Meyer, T. F. (2017). ALPK1- and TIFA-dependent innate immune response triggered by the *Helicobacter pylori* type IV secretion system. *Cell Rep*, 20(10), 2384-2395. <https://doi.org/10.1016/j.celrep.2017.08.039>

Declaration of honour

I hereby declare that I prepared this thesis without the impermissible help of third parties and that none other than the aids indicated have been used; all sources of information are clearly marked, including my own publications.

In particular, I have not consciously:

- fabricated data or rejected undesirable results,
- misused statistical methods with the aim of drawing other conclusions than those warranted by the available data,
- plagiarized external data or publications,
- presented the results of other researchers in a distorted way.

I am aware that violations of copyright may lead to injunction and damage claims by the author and also to prosecution by law enforcement authorities.

I hereby agree that the thesis may be electronically reviewed with the aim of identifying plagiarism.

This work has not been submitted as a doctoral thesis in the same or a similar form in Germany, nor in any other country. It has not yet been published as a whole.

Magdeburg, 18 October 2022

Phatcharida Jantaree